ELECTROCHEMICAL OCHRATOXIN A IMMUNOSENSORS BASED ON POLYANILINE NANOCOMPOSITES TEMPLATED WITH AMINE- AND SULPHATE-FUNCTIONALISED POLYSTYRENE LATEX BEADS

By

MUNKOMBWE MUCHINDU

A thesis Submitted in fulfilment of the requirement for the Degree of

Doctor Philosophiae in Chemistry

University of the Western Cape

Supervisor

Professor Emmanuel I. Iwuoha

Co-supervisor

Dr Nazeem Jahed

DATE SUBMITTED: DECEMBER 2010

ABSTRACT

Polyaniline nanocomposites doped with poly(vinylsulphonate) (PV-SO$_3^-$) and nano-structured polystyrene (PS$_{NP}$) latex beads functionalized with amine (PS$_{NP}$-NH$_2$) and sulphate (PS$_{NP}$-OSO$_3^-$) were prepared and characterised for use as nitrite electro-catalytic chemosensors and ochratoxin A immunosensors. The resultant polyaniline electro-catalytic chemosensors (PANI, PANI|PS$_{NP}$-NH$_2$ or PANI|PS$_{NP}$-OSO$_3^-$) were characterized by cyclic voltammetry (CV), ultraviolet-visible (UV-Vis) spectroscopy and scanning electron microscopy (SEM). Brown-Anson analysis of the multi-scan rate CV responses of the various PANI films gave surface concentrations in the order of 10^{-8} mol/cm. UV-vis spectra of the PANI films dissolved in dimethyl sulphoxide showed typical strong absorbance maxima at 480 and 740 nm associated with benzenoid π-π* transition and quinoid excitons of polyaniline, respectively. The SEM images of the PANI nanocomposite films showed cauliflower-like structures that were <100 nm in diameter. When applied as electrochemical nitrite sensors, sensitivity values of 60, 40 and 30 μA/mM with corresponding limits of detection of 7.4, 9.2 and 38.2 μM NO$_2^-$, were obtained for electrodes, PANI|PS$_{NP}$-NH$_2$, PANI and PANI|PS$_{NP}$-SO$_3^-$, respectively. Immobilisation of ochratoxin A antibody onto PANI|PS$_{NP}$-NH$_2$, PANI and PANI|PS$_{NP}$-SO$_3^-$ resulted in the fabrication of immunosensors. A 2-D gel electrophoresis of ochratoxin A antibody (anti-OTA) gave an isoelectric point (pI) value of 6.2 which made electro-deposition of the antibody by oxidation onto the PANI films possible. Impedimetric immunosensors for ochratoxin A (OTA), PANI|anti-OTA, PANI|PS$_{NP}$-NH$_2$|anti-OTA and PANI|PS$_{NP}$-OSO$_3^-$|anti-OTA, were characterised and their responses to standard OTA solutions calibrated at pH 7.2. The surface morphology of the three

PANI platforms conditioned in buffer was characterised by SEM and atomic force microscopy (AFM). Nanocauliflower aggregates of <100 nm were observed under both surface techniques. Absorbance of ochratoxin A antigen in UV-vis was observed at 330 and 390 nm due to the presence of phenolic species within the ochratoxin A structure. A reduction in absorbance values in the presence of antibody confirmed binding of OTA antigen-antibody. The limit of detection and sensitivity of the OTA immunosensors were calculated to be 7, 10 and 12 pg/kg and 400, 563 and 819 kΩ L/ng, for PANI|PS$_{NP}$-NH$_2$|anti-OTA, PANI|anti-OTA and PANI|PS$_{NP}$-OSO$_3^-$|anti-OTA, respectively. The European Commission limit for OTA in roasted coffee and cereals is 5 µg/kg. Sensitivity of ELISA was 5 pg/kg with the limit of detection at 2 ppt making the use of ELISA appropriate in validating the fabricated PANI ochratoxin A immunosensors. Results of the immunosensors in detecting OTA in certified reference materials were comparably with ELISA results and vendor specification.
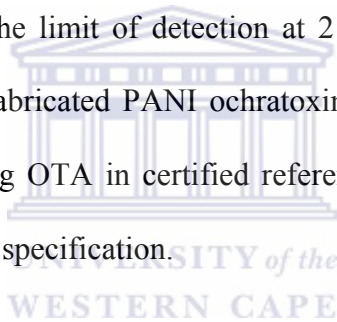
KEYWORDS

Polyaniline

Poly(vinylsulphonate)

Polystyrene

Nanocomposite

Nitrite

Ochratoxin A antigen

Ochratoxin A antibody

n-type semiconductor

Immunosensor

Eelectrochemical impedance spectroscopy

Enzyme-linked immunosorbent assay

Certified reference material

2-D Gel electrophoresis

DECLARATION

I declare that "Electrochemical ochratoxin A immunosensors based on polyaniline nanocomposites templated with amine- and sulphate-functionalised polystyrene latex beads" is my own work, that it has not been submitted for any degree or examination in any other university and that all the resources I have used or quoted have been indicated and acknowledged by means of complete references.

Munkombwe Muchindu

Signed:

ACKNOWLEDGEMENTS

Chemistry Department staff: The Head of Department, Prof Farouk Ameer, Technical and Academic staff for your willingness to assist.

Family: I am grateful to my parents, siblings and the extended family for believing in me and loving me unconditionally throughout my studies. Love you all!

Friends**:** Kevin James, Towela Ng'ambi, Gillian Sibiya, Rosaria Kunda, Refiloe Mofokeng, Dr Sarah Maoela, Edgar Kateshumbwa, Timothy Kyepa, Dr Karen Wallace, Moketsi Mosweu, Gina Wright, Dr Lesego Mmualefe, Dr Joseph Owino and Dr Omotayo Arotiba, thank you for the light moments and for the encouragement.

Sponsorship: I would also like to thank the National Research Foundation (NRF) and Enterprise Ireland for funding my studies and attendance of conferences.

Above all, I thank the Almighty Lord for his never ending blessings.
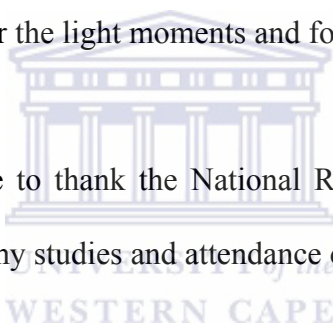
DEDICATION

This work is dedicated to my parents**,** Mercy Mudenda Mwanakasale Muchindu and Lawrence Moono Muchindu, siblings**,** Mungaila Micheal Muchindu and Mwanakasale Dominic Muchindu, my dear Aunt, Maltidah Mwanakasale, cousin, Mwape Kasonde-Makayi and niece, Kenga Robyn Makayi.

LIST OF PUBLICATIONS

Munkombwe Muchindu, Emmanuel Iwuoha, Edmund Pool, Natasha West, Nazeem Jahed, Priscilla Baker, Tesfaye Waryo, Avril Williams (2011), Electrochemical ochratoxin A immunosensor system developed on sulphonated polyaniline, *Electroanalysis 23 (1), Pages 122-128.*

Munkombwe Muchindu, Tesfaye Waryo, Omotayo Arotiba, Ewa Kazimierska, Aoife Morrin, Anthony J. Killard, Malcolm R. Smyth, Nazeem Jahed, Boitumelo Kgarebe, Priscilla G.L. Baker, Emmanuel I. Iwuoha (2010). Electrochemical nitrite nanosensor developed with amine- and sulphate-functionalised polystyrene latex beads self-assembled on polyaniline, *Electrochimica Acta 55 (14), Pages 4274-4280.*

Peter M. Ndangili, Tesfaye T. Waryo, **Munkombwe Muchindu**, Priscilla G.L. Baker, Catherine J. Ngila, Emmanuel I. Iwuoha (2010). Ferrocenium hexafluorophosphate-induced nanofibrillarity of polyaniline-polyvinyl sulfonate electropolymer and application in an amperometric enzyme biosensor, *Electrochimica Acta 55 (14), Pages 4267-4273.*

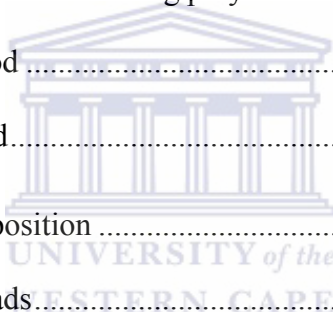Ewa Kazimierska, **Munkombwe Muchindu**, Aoife Morrin, Emmanuel Iwuoha, Malcolm R. Smyth, Anthony J. Killard, (2009), The Fabrication of Structurally Multiordered Polyaniline Films and Their Application in Electrochemical Sensing and Biosensing, *Electroanalysis 21 (3-5), Pages 595-603.*

TABLE OF CONTENTS

LIST OF FIGURES

LIST OF TABLES

UNIVERSITY *of the*
WESTERN CAPE

LIST OF SCHEMES

CHAPTER 1

INTRODUCTION

This chapter gives a brief background on sensors, project's rationale and motivation, aim and specific objectives and also the thesis outline.

1.1 Background

Sensors are devices that measure physical quantities and convert them into signals which can be read by an observer or instrument. These sensor devices include the control and processing electronics, software and inter-connection networks. In living organisms, biological sensors in the form of specialized cells have functions similar to those of mechanical devices applied in machines, cars, aerospace and robotics. Sensors can therefore provide information on the physical, chemical and biological environment. The physical sensors measure parameters such as distance, mass, temperature and pressure. Chemical sensors measure chemical substances by chemical or physical responses and the final type of sensors are biosensors. These measure chemical substances by using a biological sensing element. (Bio)chemical sensors are used to improve point-of-care diagnostics in medical applications, monitor environmental pollution. These sensors provide compact, fast, low power, and sensitive tools for quality and process control in industrial applications, as well as improve or implement warfare threat detection and security[1]. With the heightened level of awareness for pathogenic organisms and toxin detection in respect to bio-safety and bio-security, the field of pathogen analysis has

expanded tremendously in the last few years with applications not only being confined to medical diagnostics but also to environmental control and food safety[2].

In recent years, research in the field of sensors has expanded exponentially in terms of financial investment, published literature and number of active researchers[3]. Advances in the medical or diagnostic test market and escalating use of sensors in large-scale industrial and environmental applications are driving the market for chemical sensors and biosensors[4-7]. The global market for sensors in consumer electronics was expected to grow from \$10,221 million in 2009 to \$22,190 million in 2015[8]. The number of published literature for sensors between 1995 and 2010 was 83 489 as reported by the ISI Thomson Scientific Web of Knowledge[9]. Of these, chemical sensors were 10 570, while 3 467 were biosensors and the rest comprised physical sensors. The last 5 years has seen a 50% increase in the number of these publications.
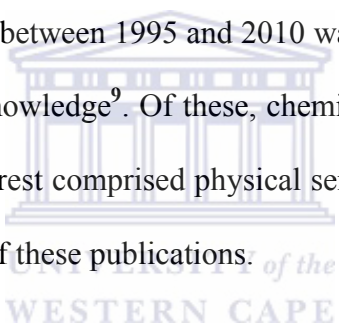
Sensor devices have been made from classical semiconductors, solid electrolytes, insulators, metals and catalytic materials. Since the chemical and physical properties of polymers may be tailored by the chemist for particular needs, polymers have gained importance in the construction of these sensor devices. Better selectivity, fast response and miniaturization have been achieved by replacing classical sensor materials with polymers exploiting either the intrinsic or extrinsic functions of polymers and immobilizing different biological materials on the polymers. This has given polymers tremendous recognition in the field of artificial sensors for mimicking natural sensing organs[4, 6, 10]. Conducting polymers are used as coating materials on electrode surfaces

while non-conducting polymers may be used for immobilization of specific receptor agents on sensor devices. Since the fabrication of the first biosensor by Leland Clark in 1956 for oxygen sensing, the demand and application of sensors has increased tremendously over the years[6]. Due to their chemical and physical properties, polymers may be tailored to display a wide range of characteristics explaining why their use is finding a permanent place in sensor technology. These polymers are used in sensor devices in health care, food industries and environmental monitoring to mention but a few. They can either participate as sensing mechanisms or immobilize the component responsible for sensing an analyte.

Understanding the polymer structure, morphology, adhesion properties and microenvironment is important in the design of a robust and stable sensor as these affect sensor performance[11]. Polymers belonging to polyenes and polyaromatics have been studied extensively in sensing applications[3]. Polyaniline (PANI) is the oldest conductive polymer known and was first prepared in 1862. PANI has generated much interest due to its wide range of conductivity from the insulating to metallic regime, unique redox turn-ability, good environmental stability, low cost and ease of synthesis[12]. Advantages of utilizing polyaniline-coated electrodes in sensors are impressive signal amplification and elimination of electrode fouling[13]. The quest for suitable immobilization materials has become the challenge of electrochemists in designing highly sensitive, biocompatible sensors[14].

1.2 Rationale and motivation

In chemical detection systems, the problem of selectivity, particularly at the low analyte concentrations is of paramount importance and the development of sensors, which are highly selective and easy to handle is a possible solution to this problem. Conducting polymers have enough scope for the development of various sensors. In this project, polyaniline and its nano-composites are explored and applied in development of suitable chemical and biological sensors for nitrite and ochratoxin A, respectively. The determination of nitrite is of significance due to its important role in environmental process and its toxicity and suspected carcinogenicity in human body[15]. Trace levels of Ochratoxin A have shown toxic properties in human beings and animals including sever nephrotoxic, neurotoxic, carcinogenic, immunosuppressive and estrogenic effects[16, 17].
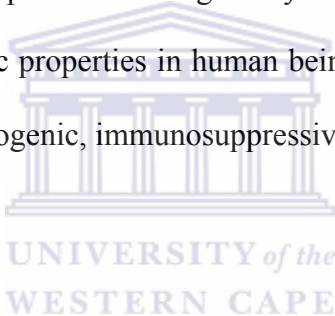
1.3 Aim

To prepare polystyrene template based nanocomposite polyaniline structures on electrodes to be applied as chemosensor and immunosensors in detection of an environmental pollutant and a food contaminant.

1.3.1 Specific objectives

i. To electrochemically polymerise poly(vinylsulphonate) (PV-SO$_3^-$) doped aniline.

ii. To prepare amine- and sulphate-modified polystyrene latex bead template based polyaniline nanocomposites on screen printed carbon and glassy carbon and platinum working electrodes.

iii. To study the morphology of polyaniline, polyaniline-polystyrene nanocomposites on screen-printed carbon paste electrodes using scanning electron microscope (SEM) and atomic force microscope (AFM).

iv. To apply to polyaniline-polystyrene modified glassy carbon electrodes in detection of nitrite ions by amperometry.

v. To immobilise ochratoxin A antibody on the polyaniline amd polyaniline nanocomposite electrodes.

vi. To characterize ochratoxin A immunosensors by electrochemical impendence spectroscopy

vii. To apply of the PANI immunosensors in the analysis of certified food extracts.

1.4 Thesis lay-out
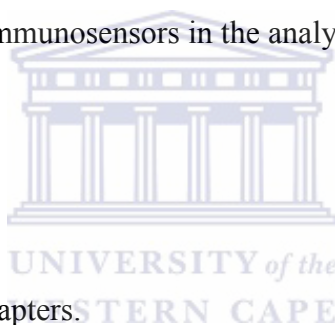
This thesis consists of seven chapters.

Chapter 1 presents a brief background, motivation, thesis statement and research aim and objectives.

Chapter 2 introduces the scope of the literature review.

Chapter 3 is on the experimental. It consists of a general section that explains procedures common to the work in general, and those peculiar to each milestone covered. The chapter also features the list of materials and procedures used.

Chapter 4 and 5 results and discussions of nitrite and ochratoxin A detection on PANI and the PANI|PS$_{NP}$, respectively.

Chapter 6 is the conclusions, recommendations and future work.

References

1. Global Industry Analysts, I. Global Chemical Sensors Market to Reach $17.28 Billion by 2015. http://www.prweb.com/releases/chemical/sensors/prweb3609734.htm. (12/10/2010)

2. Baeumner, A., Biosensors for environmental pollutants and food contaminants. *Analytical and Bioanalytical Chemistry* **2003,** 377, (3), 434-445.

3. Ahuja, T.; Mir, I. A.; Kumar, D.; Rajesh, Biomolecular immobilization on conducting polymers for biosensing applications. *Biomaterials* **2007,** 28, (5), 791-805.

4. Adhikari, B.; Majumdar, S., Polymers in sensor applications. *Progress in Polymer Science* **2004,** 29, (7), 699-766.

5. Dhand, C.; Das, M.; Datta, M.; Malhotra, B. D., Recent Advances in Polyaniline Based Biosensors. *Biosensors and Bioelectronics* In Press, Accepted Manuscript.

6. Gerard, M.; Chaubey, A.; Malhotra, B. D., Application of conducting polymers to biosensors. *Biosensors and Bioelectronics* **2002,** 17, (5), 345-359.

7. Velusamy, V.; Arshak, K.; Korostynska, O.; Oliwa, K.; Adley, C., An overview of food borne pathogen detection: In the perspective of biosensors. *Biotechnology Advances* 28, (2), 232-254.

8. Research and Markets: Global Sensors Market in Consumer Electronics 2010-2015 - The Market to Grow from $10,221 Million in 2009 to $22,190 Million in 2015. http://satellite.tmcnet.com/news/2010/10/13/5064399.htm. (13/10/2010)

9.   ISI of Web Knowledge.

       http://apps.isiknowledge.com/summary.do?qid=18&product=UA&SID=T2L2ime

       BfGnCc4dId8b&search_mode=Refine (13/10/2010)

10.   Xia, L.; Wei, Z.; Wan, M., Conducting polymer nanostructures and their

       application in biosensors. *Journal of Colloid and Interface Science* **2010,** 341, (1),

       1-11.

11.   Sadik, O. A.; Ngundi, M.; Wanekaya, A., Chemical Biological Sensors Based on

       Advances in Conducting Electroactive Polymers. *Microchimica Acta* **2003,** 143,

       (2), 187-194.

12.   Muchindu, M.; Waryo, T.; Arotiba, O.; Kazimierska, E.; Morrin, A.; Killard, A.

       J.; Smyth, M. R.; Jahed, N.; Kgarebe, B.; Baker, P. G. L.; Iwuoha, E. I.,

       Electrochemical nitrite nanosensor developed with amine- and sulphate-

       functionalised polystyrene latex beads self-assembled on polyaniline.

       Electrochimica Acta **2010,** 55, (14), 4274-4280.

13.   Mathebe, N. G. R.; Morrin, A.; Iwuoha, E. I., Electrochemistry and scanning

       electron microscopy of polyaniline/peroxidase-based biosensor. *Talanta* **2004,** 64,

       (1), 115-120.

14.   Arotiba, O. A.; Ignaszak, A.; Malgas, R.; Al-Ahmed, A.; Baker, P. G. L.;

       Mapolie, S. F.; Iwuoha, E. I., An electrochemical DNA biosensor developed on

       novel multinuclear nickel(II) salicylaldimine metallodendrimer platform.

       Electrochimica Acta **2007,** 53, (4), 1689-1696.

15. Guo, M.; Chen, J.; Li, J.; Tao, B.; Yao, S., Fabrication of polyaniline/carbon nanotube composite modified electrode and its electrocatalytic property to the reduction of nitrite. *Analytica Chimica Acta* **2005,** 532, (1), 71-77.

16. Zain, M. E., Impact of mycotoxins on humans and animals. *Journal of Saudi Chemical Society* **2010,** doi:10.1016/j.jscs.2010.06.006.

17. Fernández-Cruz, M. L.; Mansilla, M. L.; Tadeo, J. L., Mycotoxins in fruits and their processed products: Analysis, occurrence and health implications. *Journal of Advanced Research* **2010,** 1, (2), 113-122.

CHAPTER 2

LITERATURE REVIEW

The main focus of this chapter is a review of polyaniline, a conducting polymer, its synthesis in the presence of a dopant, poly(vinylsulphonate) and layer by layer deposition of nano-structured polystyrene (PS_{NP}) latex beads functionalized with amine (PS_{NP}-NH_2) and sulphate (PS_{NP}-OSO_3^-) to form nanocomposites. Occurrence and method of detection of nitrite and ochratoxin A analytes are also presented. The structure of antibody and immobilization techniques will also be investigated.

2.1 Conducting polymers

Polymers form an integral part of our existence. From the basic building blocks of life constituting of proteins, nucleic acids and polysaccharides, to commercial products obtained in automobile and construction industries and households[1]. Most of these materials are a combination of one or more of these materials to form polymer composites. Naturally occurring polymer composites such as bone, teeth and wood, possess a unique combination of material properties and a broad spectrum of applications which the constituents alone cannot offer. Early investigations used conductive filler materials such as carbon black, graphite fibres, or metal particles for preparation of composite materials. Scientists from many disciplines are now combining expertise to study organic solids that exhibit remarkable conducting properties[2]. A large number of

organic compounds which effectively transport charge are roughly divided into three groups, that is, charge transfer complexes or ion radical salts[3-6], organometallic species[7-10] and conjugated organic polymers[2, 11-16]. However, the traditional role of polymers as electric insulators is being discarded as they are now taking charge as conductors with a range of novel applications. They have a wide range of potential applications in areas such as rechargeable batteries, light emitting diodes (LED), electrochromic display devices, gas separation membranes, electromagnetic interference (EMI) shielding, sensors and molecular electronic devices[14] as shown in Figure 2.1.
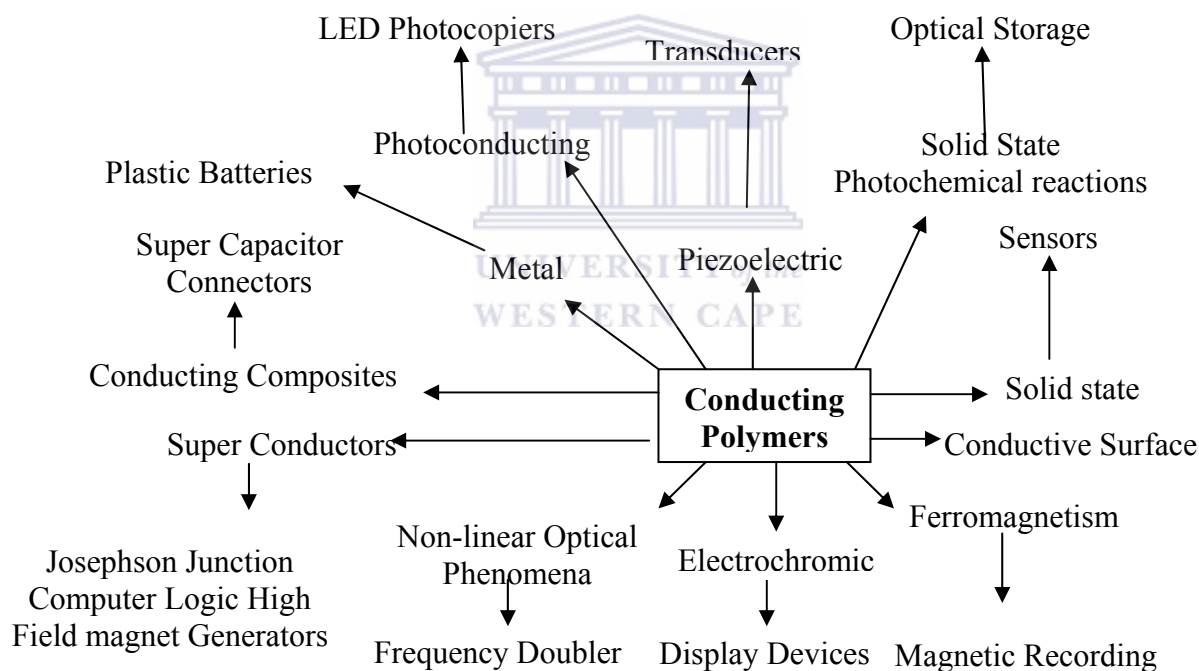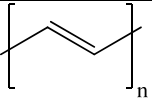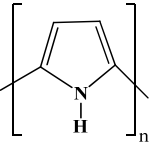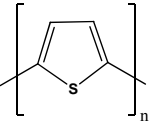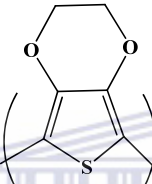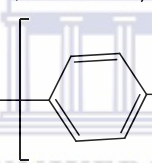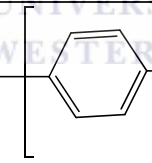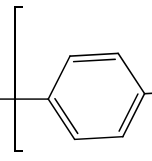
Figure 2.1: Applications of conducting polymers.

Since their discovery in the mid-1970s, research into conducting polymers has supported the industrial development of conducting polymer products and provided the fundamental

understanding of the chemistry, physics and material science of these polymers[17]. Research on polypyrrole dates back to the 1960s, but little was understood about the polymer at the time and this discovery was essentially lost[2]. The impact of conducting polymers on science was recognized in 2000 by the awarding of the Nobel Prize for Chemistry to the three discoverers of conducting polymers: Alan MacDiarmid, Alan Heeger, and Hideki Shirakawa. In 1977, they reported a 10 million-fold increase in the conductivity of polyacetylene doped with iodine[18]. Polyacetylene was therefore the first inherently conductive polymer to be recognized. Although it is a non-cyclic polyene, polyacetylene is still one of the most studied polymers in this field; it has significant limitations, such as, difficulty with processing and high instability in air. However, unlike polyacetylene, polyphenylenes, cyclic polyenes, are known to be thermally stable as a result of their aromaticity. These polymers are conducting due to an extended π-conjugation along the polymer backbone[18, 19]. Their structure contains a one-dimensional organic backbone based on the alternation of single and double bonded sp^2 hybridized atoms which endow the polymer with metal like semi-conductive properties. These enable π-molecular orbitals to be formed for electronic conduction. However, in the neutral (undoped) state these polymers can only be semiconducting. The neutral polymer is converted into an ionic complex consisting of a polymeric cation or anion and a counter-ion which is the reduced form of the oxidizing agent or the oxidized form of the reducing agent, respectively[20]. Doping, *p*- or *n*-type, in conducting polymers refers to the oxidation or reduction of π-electronic systems, respectively[13]. This doping can be effected chemically or electrochemically. In order to maintain electro-neutrality, doping requires incorporation of a counter-ion. The doped and undoped states have different

electronic, optical, physical, chemical and electrochemical aspects. Therefore, reversible interchange between the redox states in conducting polymers gives rise to the changes in its properties including polymer conformation, doping level, conductivity and colour. Electrons of π-character can be easily removed or added to form a polymeric ion without much disruption of the σ-bonds which are primarily responsible for holding the polymer together. Unsaturated π-bonded polymers also have small ionization potentials and large electron affinities. The electronic conductivity, a measure of electrical conduction and thus a measure of the ability of a material to pass a current, appears when the material is doped. Conductivity in conducting polymers is influenced by a variety of factors including polaron length, the conjugation length and overall chain length and by the charge transfer to adjacent molecules. Presented in Table 2.1 are structures, conductivities and type of doping of conducting polymers for polyaniline, polyacetylene, polypyrole, polythiophene and poly(*para*-phenylene) and their derivatives that have been studied extensively[2, 17, 18, 20]. Studies have demonstrated that planar conformation of the alternating double-bond system, which maximizes sideways overlap between the π molecular orbitals, is critical for conductivity[18]. This π-bonded system is further described in terms of electronic wave-functions that are delocalized over the entire chain. This delocalization allows charge mobility along the polymer backbone and between adjacent chains, but delocalization is limited by both disorder and Coulombic interactions between electrons and holes. Generally, materials with conductivities less than 10^{-8} S/cm are considered insulators, while those between 10^{-8} and 10^3 S/cm are semiconductors and those with conductivities greater than 10^3 S/cm are considered conductors.

Table 2.1: Conducting polymer structures

Name	Structure	Conductivity (S/cm)	Type of doping
Polyacetylene		200-10 000	n,p
Polypyrole		40-7500	p
Polythiophene		10-1000	p
Poly(ethylenedioxythiophene)		10-600	n, p
Poly(para-phenylene)		1000	n,p
Poly(para-phenylene sulfide)		3-500	p
Polyaniline		5-200	n,p

The mechanism of conduction in conducting polymers is very complex because such materials exhibit conductivity across a range of about fifteen orders of magnitude and many involve different mechanisms within different regimes[2]. Conducting polymers show enhanced electrical conductivity by several orders of magnitude of doping. The concept of solitons, polarons and bipolarons has been used to explain the electronic phenomena in these systems[20].

2.2 Synthesis of conducting polymers
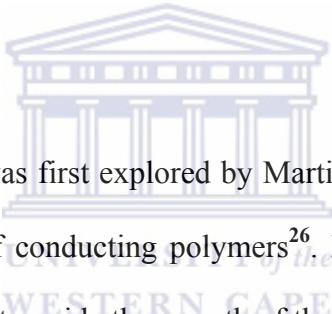
Various methods are available for the synthesis of conducting polymers[2]. However, the most widely used technique for the synthesis of conducting polymers is the oxidative coupling involving the oxidation of monomers to form a cation radical followed by the coupling to form di-cations and this repetition finally leads to formation of the polymer. Electrochemical synthesis is rapidly becoming the preferred general method of synthesizing conducting polymers because of its simplicity and reproducibility[21]. Other advantages of electrochemical polymerization reactions are that it can be carried out at room temperature and by varying either potential or current with time, the thickness of the film can be controlled. Electrochemical synthesis can be used to prepare free standing, homogenous and self doped films[2]. The electrochemical synthesis of conducting polymer is an electro-organic process rather than an organic electrochemical one. Emphasis is on the electrochemical process rather than organic synthesis. Electrochemical techniques employed in the polymerization of conducting polymers on the electrode surface are; pulse, galvanostatic, potentiostatic or sweeping techniques[22]. However, potentiodynamic techniques are preferred because of the homogenous film produced and strong adherence of the film to the electrode surface[21].

2.3 Synthesis of nanostructured conducting polymer

Functionalized conducting polymer nanomaterials have been receiving great attention in nanoscience and nanotechnology because of their large surface area further increasing the merit of conducting polymers in designing and making novel sensors[16]. The specific

surface area of conducting polymers plays a key role in determining the sensitivity of a sensor. When a bulk polymer is used to construct a sensor, the response time is relatively long due to slow penetration of the target molecules into the conducting polymer often with an accompanying hysteretic effect[23]. In contrast, for a sensor constructed of conducting polymer nanostructures, the response time is expected to be significantly faster due to the porous structure of the nanomaterial. Hard- and soft-template methods have been widely used to synthesize conducting polymer nanostructures[12, 24, 25]. Basic concepts, advantages, and limitations are discussed as follows.

2.3.1 Hard-template method

A template-synthesis method was first explored by Martin's group to prepare nanofibers or nanotubes and nanowires of conducting polymers[26]. In the hard-template method, a template membrane is required to guide the growth of the nanostructures within the pores or channels of the membrane as a hard-template, leading to completely controlled nanostructures in morphology and diameter, dominated by the pores or channels[16]. The advantages of the hard-template method include the fact that it is a general tool to prepare nanostructured materials that can be synthesized either chemically or electrochemically. The diameter of the nanostructure is controlled by the size of the pores or channels in the membrane, whereas the length and thickness of the nanostructure is usually adjusted by changing polymerization time. For these reasons, the hard-template method is the most commonly used and efficient approach for preparing well controlled and highly oriented nanostructures. However, one the disadvantages of the hard-template method include

complications in the removal of the membrane that can often destroy or disorder the formed nanostructures. Another disadvantage is that the quantity of the nanostructures produced by this method is limited by the size of the template membrane, therefore, limiting its applications in large-scale nanostructure production.

The preparation of conducting polymer nanostructures by a hard-template method is carried out by either chemical or electrochemical polymerization. Chemical hard-template synthesis is accomplished by simply immersing a membrane in a solution of the desired mixture of monomer, dopant, and oxidant, and then allowing monomer polymerization within the pores[27, 28]. By controlling the polymerization time, different types of nanostructures can be produced[29]. Short polymerization time periods lead to tubules with thin walls, while longer polymerizations can produce thick walled tubules or fibres. Compared to chemical hard-template method, the electrochemical hard-template method is more complex and expensive, but it is more controllable through changing current density, applied potential and polymerization time. On the other hand, large mass synthesis by the electrochemical hard-template method is impossible because of the limiting size of the membrane used as the template. The porous membrane is the basic and most important part of the hard-template method. Although alumina and polycarbonate membranes are commercially available, only a limited number of pore diameters are available. Martin's group has synthesized polypyrrole (PPy), polyaniline (PANI) and polythiophene (PTh) nanostructures using alumina and polycarbonate as templates[26, 28, 30]. Other type of membranes, such as colloidal particles[31-33], porous silicate[34], mesoporous zeolites[35] and carbon nanotubes[36] have also been employed as the templates to prepare conducting polymer nanostructures.

2.3.2 Soft-template method

Soft-template method also called template-free or self-assembly method, is a relatively simple, cheap, and powerful approach for fabricating conducting polymer nanostructures via a self-assembly process. Self-assembly is based on selective control of non-covalent interactions, such as hydrogen bonds, van der Waal forces, π-π stacking interaction, metal coordination and dispersive forces as the driving forces of self-assembly[37]. To date, surfactants, colloidal particles, structure-directing molecules, oligomers and colloids as soft-templates, as well as interfacial polymerization, have been employed to synthesize conducting polymer nanostructures.
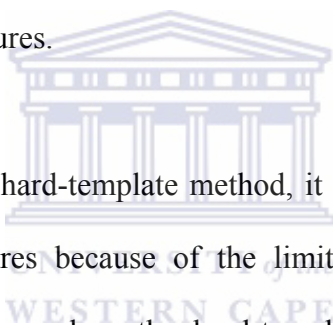
It must be noted that with the hard-template method, it is almost impossible to prepare complex micro-or nanostructures because of the limitations imposed by the porous morphology of the membrane used as the hard-template[16]. Three-dimensional (3-D) structures assembled from one-dimensional (1-D) conducting polymer nanostructures are required to provide high functionality and performance for technological applications. For a template-free method, formation, size and morphology are affected by the nature of the polymeric chain, the dopant and the oxidant, as well as the polymerization conditions. Therefore, with a combination of soft-templates and the molecular interactions as the driving forces 3-D nanostructures constructed via a self-assembly process have been prepared[38-40]. Based on this idea, the formation of perfectly ordered 3D polystyrene (PS) templates using the layer by layer deposition technique has been developed.

2.4 Layer-by-layer (LbL) deposition

In order to prepare 3-D ordered macroporous PANI structures, close-packed assemblies of polystyrene latex beads as templates are used[31]. Layer-by-layer deposition is a technique based on the consecutive electrostatic adsorption of oppositely charged polyelectrolytes on a surface-charged particle[41]. LbL deposition is recognized as a low cost and environmentally friendly technology for surface functionalization of conducting polymers. The driving force of LbL deposition is mainly electrostatic in nature, thus, the resulting polymeric nanostructure are usually composed of polyelectrolytes. The dimensions of resulting polymeric nanostructures including, size, composition, thickness and uniformity, can therefore be easily controlled. Sodium salt of poly(styrene sulfonate) (PSS) is a widely used polyanion for LbL deposition[38, 39, 42, 43]. Using PSS as polyanions and poly(diallyldimethylammonium chloride) (PDDA) as polycations, sulphate- or amine-modified polystyrene (PS) core shell templates on bulk polyaniline, PANI|PS nanocomposites have been fabricated by alternating LbL deposition of PS-SO$_3^-$ and PDDA[38-40]. The thickness of polyelectrolyte shell in the nano-meter range can be precisely adjusted by controlling the adsorption time.

2.4.1 Polystyrene latex beads

Polystyrene (PS) latex beads are spherical amorphous polymer particles in the colloidal size range[31, 44]. The average molecular weight of the polymer chains in the particle is about 1×10^6 g for particles with diameter <100 nm and drops of about 2.4×10^5 g for larger

particles. A polystyrene chain is a linear hydrocarbon chain with a benzene ring attached to every second carbon atom. The aromatic rings control the way the chains coil, entangle and dominate the space. When a model of the particle surface is viewed, randomly stacked benzene rings are highly visible with an occasional chain end sticking out. Hence, the surface is very hydrophobic in character and provides for strong physical adsorption of molecular species with hydrophobic regions. Surfactants and protein molecules stick strongly by simple passive adsorption. Models of sulphate- and amine-modified beads are shown in Figures 2.2 and 2.3.
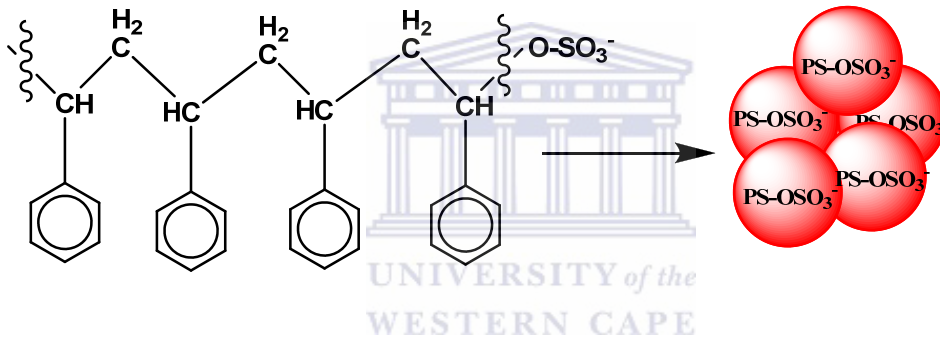
Figure 2.2: Structure of sulphate-modified polystyrene latex beads (PS_{NP}-OSO_3^-).

Well-separated monovalent sulphate and amine groups occupy 5-10% of the bead, while the remaining 90-95% of the surface is hydrophobic and is made up of stacked benzene rings of the polystyrene.
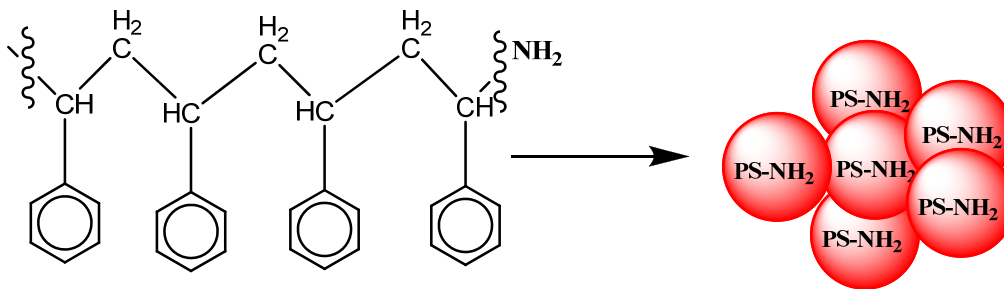
Figure 2.3: Chemical structure of amine-modified polystyrene latex beads (PS$_{NP}$-NH$_2$).

2.5 Electrocatalysis at conducting polymer electrodes
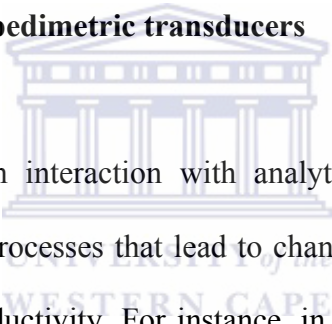
During electrocatalytic conversion of solution species on conducting polymer modified electrodes, three processes can be considered[45]. The first process is a heterogeneous electron transfer between the electrode and a conducting polymer layer. This process is accompanied by the movement of charge compensating anions and solvent molecules within the conducting polymer film and possible conformational changes of polymer structure. The rate of this process is determined by many factors including, electric conductivity of a polymer layer, electron self-exchange rate between the chains and/or clusters of polymer and anion movement within polymer. The second process is the diffusion of solution species to the reaction zone, where the electro-catalytic conversion occurs. This process is more complicated in cases where electro-catalytic conversion occurs within the polymer film as compared to simple electrode reactions. In the diffusion process, the diffusion of species within the film, as well as the possible electrostatic interaction of the species with the polymer film should be taken into account. Finally, the third process is a chemical heterogeneous reaction that takes place between

solution species and conducting polymer. As a result of these complex processes, the kinetic behaviour and voltammetric responses are difficult to interpret and a great deal of attention has been paid to consider some simplified models. From both theoretical and practical points of view, the question on the location of electro-catalytic process is of primary interest. If the charge transfer within the layer of conducting polymer proceeds much faster than the mass transfer of reacting species and their electrochemical conversion, the electro-catalytic process should proceed at the outer conducting polymer|solution interface. However, if the opposite is the case, where mass transfer and electrochemical reaction proceed faster than the electron transfer in the conducting polymer, an electrocatalytic process occurs at the inner substrate electrode|conducting polymer interface. This is assuming permeability of a porous conducting polymer layer is sufficiently high enough to penetrate the reacting species and solution ions. In cases were both of above processes are occurring at a comparable rate, the electro-catalytic process is then located within the conducting polymer layer. The depth of the reaction zone within the conducting polymer layer will be determined by the balance between charge and mass transfer and also the rate of electro-catalytic conversion. It must be noted that the setback on the location of the electro-catalytic process is often considered as a question on whether the metal-like electro-catalysis is at a conducting polymer solution interface, or semiconductor-like electro-catalysis is either within the polymer layer, or at inner substrate electrode conducting polymer interface behaviour. Due to these electro-catalytic properties, conducting polymers are used as transducers or as components of transducers.

2.6 Conducting polymers as transducers

Many conducting polymers (CP) including polyaniline (PANI), polypyrole (PPy), polycarbazole and polyazines posses acidic or/and basic groups which can be protonated or deprotonated[46]. Strong and reversible influence of these oxidation/reduction, protonation/deprotonation and conformational changes on electrical and optical properties of conducting polymers make it possible for their use as transducers or as components of transducers.

2.6.1 Conductometric and impedimetric transducers

The conductivity change upon interaction with analytes is one of the mostly used transducing principles. Many processes that lead to changes in charge carrier density or mobility cause changes in conductivity. For instance, in conductometric gas sensors, an interaction of electron acceptors or donors with conducting polymers causes changes in the doping state of the polymer due to oxidation/reduction or protonation/deprotonation reactions, leading to changes in conductivity. Using this interaction, chemosensors for different gases were developed[12, 46, 47]. The change of charge carrier density due to protonation/deprotonation of CP is used not only in gas sensors for acidic/basic gases, but also in conductometric pH. The main principle in conductive transducers in enzymatic biosensors involve pH changes as well as modification of the redox state of conducting polymers induced by substrates, products or intermediates of enzymatic reactions[48, 49]. However in most cases, a simple two-point conductivity measurement on a chemoresistor

device is used[46]. The less used four-point conductivity measurement technique can provide a higher sensitivity, especially for highly conducting polymers or essential contribution of polymer/contact resistance into the value measured by two-point configuration[50, 51]. This technique was modified by combining the two- and four-point techniques for simultaneous measurements and was named as s24[46, 52].This approach provides new analytical possibilities[46]. In cases were low conductivity of CP, as is typical for bioanalytical applications (neutral pH, modest oxidation potential), transversal resistance measurements between electrode coated by CP and an electrode in the solution are used[53]. Impedance spectroscopy has a number of advantages because of irreversible effects of applied electrical potential on CP[46].

2. 6.2 Potentiometric transducers

In potentiometric transducers, the conducting polymer is deposited directly on the solid surface of metal or graphite. This configuration resembles ion-selective electrodes with polymer membrane without inner solution[46]. However, electrochemical activity of the conducting polymer results in interference of ionic and electronic equilibrium on the interface with electrolyte. This may lead to a strong interference in the presence of redox active compounds.

2.6.3 Voltammetric and amperometric transducers

Voltammetric and amperometric transducers based on conducting polymers are used for detection of current caused by either electro-catalysis or by ion flux into or from conducting polymer during its oxidation or reduction[38, 40, 53]. Differences in redox behavior and specific chemical interactions allow one to get required selectivity for several particular analytes. The advantage of conducting polymer modified electrodes over conventional metal or glassy carbon electrodes is provided by the electro-catalytic ability of some conducting polymers. This often leads to better separation of oxidation or reduction peaks of the different analytes in voltammograms. The compounds are oxidized via electron transfer from the analytes to the oxidized polymer units. This process can be monitored by measuring the current of re-oxidation of the reduced polymer units. High selectivity in electro-catalysis can be achieved by incorporation of enzymes into polymer matrix. Such conducting polymer modified transducers with oxidases or peroxidases are used in amperometric biosensors[46, 54, 55]. The electron transfer from enzyme to electrode is realized by mediators immobilized in the conducting polymer matrix, and in some cases the conducting polymer itself can play the role as a mediator.

2.6.4 Optical transducers

Changes in the redox or protonation state of a conducting polymer can lead to a strong modification of its electronic band structure, therefore an interaction of analytes which oxidize/reduce or protonate/deprotonate conducting polymer can be measured by

ultraviolet-visible spectroscopy. This UV-visible property has been used in chemical sensors[56, 57]. More sensitive detection of optical changes in conducting polymer can be realized by application of surface plasmon resonance (SPR). The measurable parameter is in this case either refractive index or optical absorbance at a particular wavelength. This approach was used to detect changes in ultra-thin films of conducting polymer upon interaction with different analytes[56, 57]. Alternatively, Raman spectroscopy can be used for transducing[58]. Modification of the optical properties of conducting polymer due to analyte binding can be detected also by fluorescence measurements. However detection schemes based on energy transfer are more typical. Intrinsic fluorescence of some polymers caused by backbone units or a fluorescence of fluorophores introduced into the polymer can be used. Fluorescence changes can be induced by modification of self-quenching effects by interaction with analyte or by quenching of polymer fluorescence by analyte[46, 59, 60].
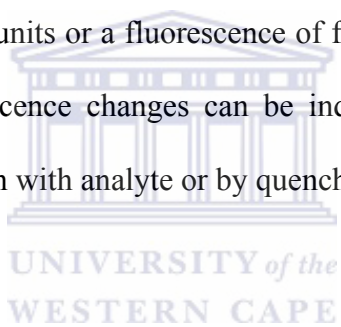
2.7 Polyaniline

Polyaniline is one of the oldest conductive polymers known[21]. The polyaniline family of conjugated polymers is of much interest worldwide because of its unique conduction mechanism and good environmental stability in the presence of oxygen and water[15, 61, 62]. Polyaniline is a dark-green precipitate that is an oxidative polymeric product of aniline under acidic conditions. It was first prepared by Letheby in 1862 by anodic oxidation of aniline in sulphuric acid and described as existing in four different states, each of which was an octamer[14]. It soon became known as aniline black[21]. The polymer is phenylene-

based with imine group in a polymer chain flanked each side by a phenylene ring. The base forms of polyaniline contain only N-C and C-C covalent aromatic bonds as shown in Figure 2.4[63].
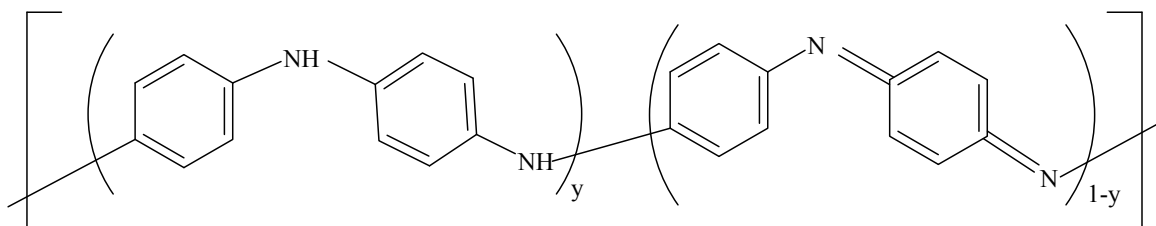
Figure 2.4: Polyaniline base.

The terms "leucoemeraldine", "emeraldine" and "pernigraniline" refer to the different oxidation states of the polyaniline. The base form of polyaniline consists of alternating reduced and oxidized repeated units. The presence of both the reduced and oxidised form, as shown in Figure 2.4 is referred to as the emeraldine base. The leucoemeraldine is the reduced state and the pernigraniline is the oxidised state of polyaniline and these are shown in Figure 2.5.
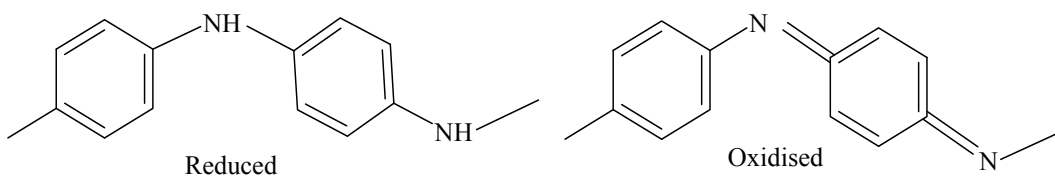
Figure 2.5: The reduced (leucoemeraldine) and oxidized (pernigraniline) forms of emeradine base.

Polyaniline can be prepared by either chemical or electrochemical oxidation of aniline under acidic conditions. The electrochemical method of polymerization is preferred because of its thin films and better-ordered polymers. The best films are reported to be produced in electrochemical techniques that employ the three electrode system in a cell, that is, working, counter and reference electrodes[21]. In principle, the imine nitrogen atoms can be protonated in whole or in part to give the corresponding salts. The degree of protonation of the polymeric base will depend on its oxidation state and on the pH of the aqueous acid. This protonated form of polyaniline is electronically conducting and the magnitude of increase in its conductivity is a function of the level of protonation[21]. The mechanism for the electrochemical polymerisation of aniline into polyaniline is shown in Scheme 2.1.
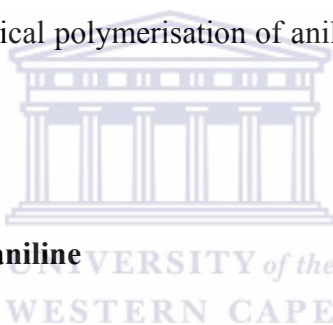
2.8 Electropolymerisation of aniline

The preparation of PANI-modified electrodes with the electropolymerisation method offers the potential to incorporate a wide range of dopants[64]. Desirable conductivity, optical and mechanical properties of the PANI film is controlled by doping the polymer by various chemical agents and blending with conventional polymer matrixes[65, 66]. The concept of doping implies the use of chemical agents that directly interact with the polymer chain. The functional group present in the doping acid, its structure and orientation plays an important role in solubilising a conducting form of polyaniline. The electrochemical oxidation of aniline followed by protonic doping has been reported for obtaining the polymer in conducting form[67, 68].
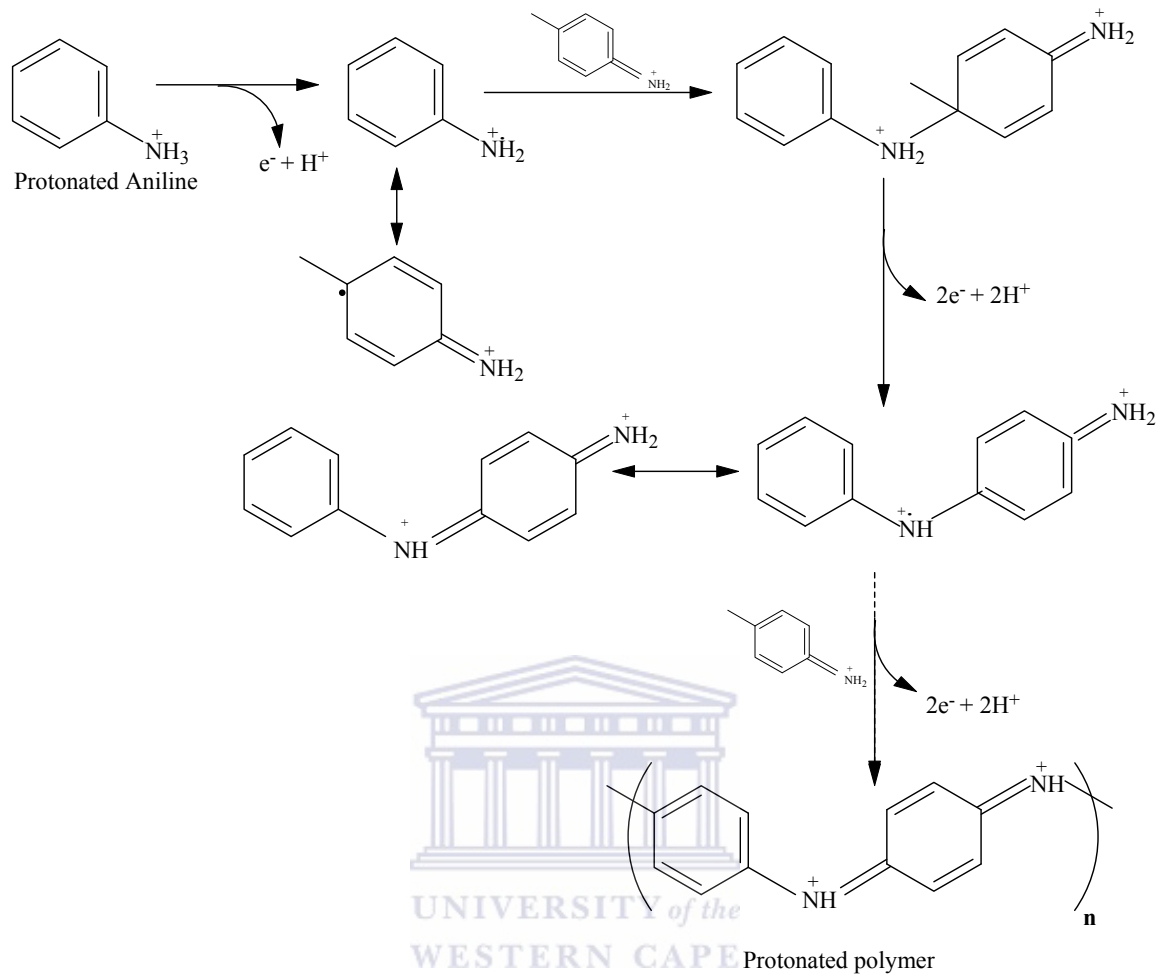
Scheme 2.1: Mechanism for electrochemical polymerisation of aniline in acidic medium.

Non-redox doping of polyaniline by protonic acids is an important aspect as a number of electrons in the polymer chain remain unchanged during the doping process while all the hetero atoms, in this case nitrogen, become protonated[21]. Electrochemical polymerisation is a radical combination reaction and is diffusion controlled. The radicals generated thus diffuse together and react faster than they can diffuse away from the electrode vicinity. An acid's dissociation constant (pK$_a$) is also an important aspect of polyaniline synthesis. The polyaniline protonation equilibrium exclusively involves the quinine diamine

segment having two imine nitrogen with pK_{a1} =1.05 and pK_{a2} =2.55. A suitable acid dopant should have a pK_a value within this range. Anilinium ion has a pK_a of 4.60 and acids with pK_a values around that of anilinium ion would be suitable as solvents if they have liquid or can be used to prevent over-oxidation of polyaniline. The incorporation of polyelectrolytes is interesting in that, it is possible to form structures with high water content or are water soluble. The multifunctional nature of polyelectrolytes such as, poly(vinylsulphoic) acid also facilitates incorporation of electroactive groups into a polymer matrix[69]. However, it has been shown that some compounds that are not primarily dopants for PANI, can substantially improve conductivity of PANI films. These findings have led to the recognition of the fact that high conductivity of PANI films can be reached not only due to chemical doping of the polymer, but also due to suitable conformations of the polymer chains yielding specific morphology of the films[70, 71]. Therefore, both doping and processing of polyaniline films are needed to induce chemical and conformational changes of the polymer and to obtain highly conductive films, respectively. Polymerisation routes involving the use of templates have significantly improved the processability of polyaniline[72]. Initiating the polymerisation by first electrostatically complexing the aniline monomer to a polyelectrolyte template inherently minimizes the parasitic branching and promotes a more *para*-directed, head-to-tail polymerisation of aniline. A polyelectrolyte also helps to emulsify the monomer molecules prior to the polymerisation and provide counter ions for charge compensation in the doped polyaniline.

Doped PANI copolymer nanostructured networks have been electrochemically prepared[73]. However, compared with the template method, these template-free methods cannot precisely control the structure and morphology of the prepared PANI nanomaterial. Hence, template assisted synthesis is more promising in designing nanostructured PANI. The insertion of organic host material by intercalation technique has resulted in the preparation of nanocomposite materials[74]. Polyaniline-coated transducers have been found to be very useful as sensors due to the signal amplification characteristics of PANI and the elimination of electrode fouling[15, 38, 40]. Nanoparticles embedded in polymeric materials have been widely studied[75]. The layer-by-layer assembly (LbL), invented by Decher, as discussed in Section 2.4, is one of the most promising bottom-up assembly methods of thin film deposition[76 77].
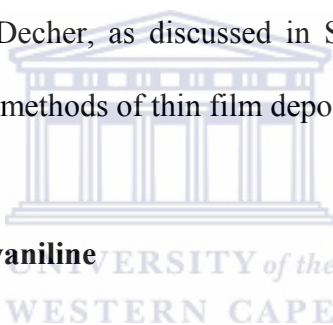
2.9 Template synthesis of polyaniline

One of the most effective and simple techniques of nanostructure formation is template synthesis as discussed in Section 2.3. The template method has been used for both chemical and electrochemical polymerization in order to obtain conducting polymer nanotubes[38-40, 55, 64, 78]. Template-based methods have attracted great attention as a viable technology enabling manipulation of length and diameter of PANI nanowires [28, 79, 80]. One of the interesting and useful features of this method is its effectiveness in the preparation of one-dimensional microstructured or nanostructured PANI with a controllable diameter, length and orientation[81]. However, the disadvantages of the method are that a tedious post-synthesis process is required in order to remove the

templates and the nanostructured PANI may be destroyed or form undesirable aggregates after they are released from the templates[82, 83]. Polystyrene (PS) latex beads are functional polymer materials, which have many admirable properties such as biocompatibility, non-toxicity, high surface area and chemical inertness[84]. Taking into account the advantages of PS and PANI, core-shell nanocomposites have been fabricated and applied as nitrite chemosensors, hydrogen peroxide biosensor[38, 40] and immunosensors[13, 18, 84].

2.10 Nitrite: Occurrence and health effects

Nitrite ion is found in soil, water, food and physiological systems[85], and its determination is very important due to its role in environmental processes and its toxicity in humans[86]. In the environment, nitrites are active intermediate species in the nitrogen cycle (Figure 2.6) in which they are formed during the oxidation of ammonia or reduction of nitrates[87]. One of the principal sources of nitrite is rainwater which can be a scavenger of soluble components from the atmosphere and thus can be a useful index of atmospheric pollution. Unpolluted rainwater is slightly acidic due to the absorption of CO_2. Rainwater chemistry plays an important role in defining the level of acid deposition, anthropogenic activities and the state of biogeochemical cycle. Anthropogenic activities release acidic gases such as SO_2 and NO_x and basic gases like NH_3 into the atmosphere. In the human body, nitrites combine with blood pigments to produce met-haemoglobin[88] which does not transport oxygen to the tissues. It may also combine in the digestive tract with amines and amides to produce highly carcinogenic N-nitrosamine compounds[89].
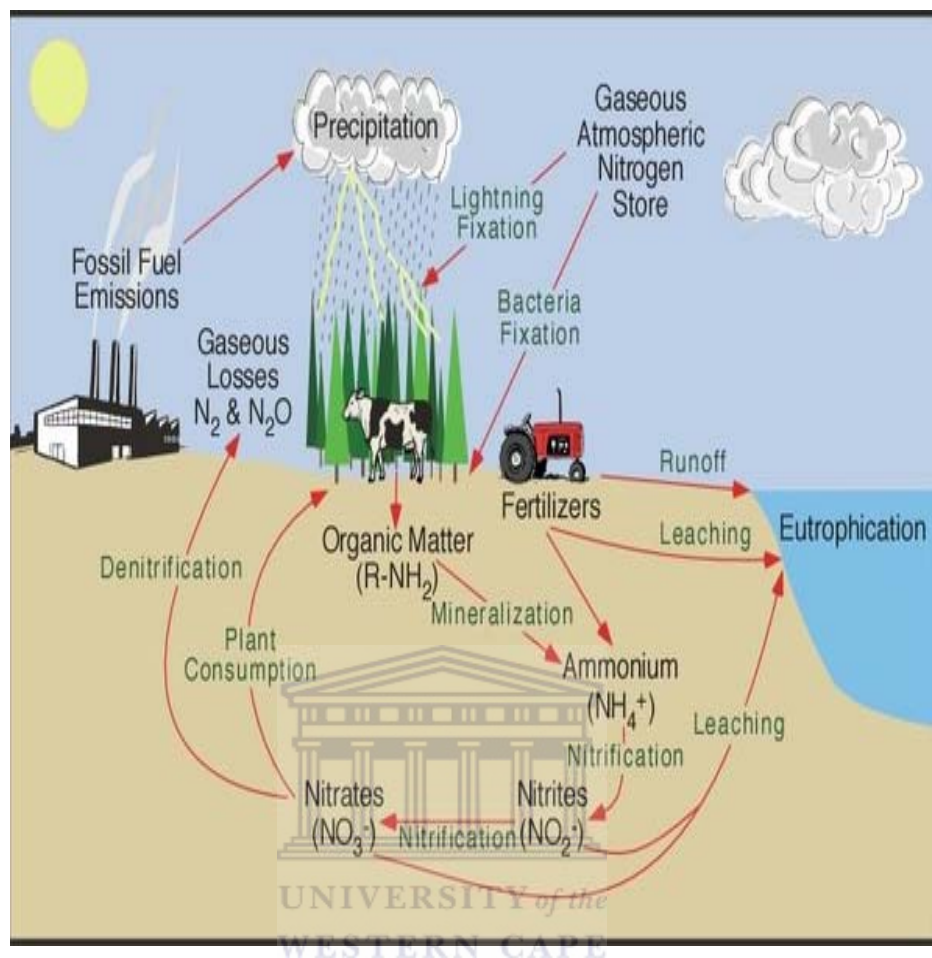
Figure 2.6: Nitrogen cycle[90].

2.10.1 Methods of nitrite detection

Analytical techniques such as, chromatography[91], spectrophotometry[92, 93], capillary electrophoresis[94] and electrochemistry[95, 96] have been used to determine the nitrite content in environmental and physiological samples. Electrochemical sensors have been found very useful in nitrite determination due to their high sensitivity, relatively good selectivity and fast response time[97]. In acidic medium, amperometric techniques for

nitrite detection based on nitrite reduction are favoured more than that involving nitrite oxidation due to the high over-potential necessary for nitrite oxidation[98]. The high over-potential tends to attract interference from co-existing substances. Apart from the fouling of the electrode surface[96], denaturation of enzymes and slow removal of modifiers from the sensors' surface[99] are also some of the drawbacks in using the amperometric oxidative techniques. Nanomaterials have found broad applications in analytical chemistry[64, 83] including the determination of nitrite in environmental samples, due to their high surface area-to-volume ratio and enhanced catalytic activity[100]. Nitrite detection methods have been reviewed by Moorcroft *et al.*[101] Nitrite concentrations of the order of 10^{-4}M have been detected on sulphamic-doped PANI[102]. Determination of nitrite based on the reduction of nitrite on nano-structured polystyrene (PS_{NP}) latex beads functionalized with amine (PS_{NP}-NH_2) and sulphate (PS_{NP}-OSO_3^-) self-assembled on the modified PANI doped with polyvinyl sulphonate PV-SO_3^- have been reported[38, 40]. In Chapter Four of this thesis, electro-catalytic determination of nitrite in standard solutions and in rainwater samples with electrode systems containing PANI, PANI|PS_{NP}-NH_2 and PANI|PS_{NP}-OSO_3^- nanomaterials will be reported[40]. Major cations and anions found in rainwater were also studied as potential interferences in nitrite determination.

2.11 Mycotoxin

Mycotoxins are secondary metabolites mainly produced by various mycelia structures of filamentous fungi growing on a wide range of agricultural commodities. The term "myco" in mycotoxin comes from the Greek word, *mykes* and it refers to fungus[103]. Some

fungi are capable of producing more than one mycotoxin and some mycotoxins are produced by more than one fungal species[104]. These mycotoxin compounds are acutely toxic to humans and animals[105].

2.11.1 Occurrence and health effects of mycotoxins

Evidence of mycotoxicoses, an illness due to mycotoxins can be traced back to the ancient times and the middle ages. During the World War II, many Russians died after having eaten grain poorly stored and highly contaminated grains with mycotoxins[105]. However, it was only after 1960 that mycotoxins were identified as potential health hazards when 100 000 turkeys in the UK, died from an acute necrosis of the liver after consuming mycotoxin infected groundnuts[106]. Toxic properties of mycotoxins in human beings and animals include severe nephrotoxic, neurotoxic, carcinogenic, immunosuppressive and estrogenic effects. Intake of trace amounts of mycotoxins may result in mild conditions of reduced feed intake in animals and diarrhoea in humans. Over two hundred different mycotoxin species have been discovered so far. They exhibit a great structural diversity. Most of them also offer considerable thermal and chemical stability. They cannot or can only be partly removed by food processing or by other suitable decontamination procedures[106]. Mycotoxins of great agro-economic importance include aflatoxins, trichothecenes, zearelenone, ochratoxins, fumonisins, ergot alkaloids, putalin and cyclopiasonic[104, 107].

2.11.2 Ochratoxin A

Ochratoxin represents a group of mycotoxins produced by several *Aspergillus* and *Penicillium* species[106, 108]. The three types of ochratoxin; ochratoxin A, B and C (OTA, OTB and OTC) all have a polyketide-derived dihydroisocoumarin moiety linked via a 7-carboxy group to L-*β*-phenylalanine by an amide bond in common as shown in Scheme 2.2. Ochratoxin A (OTA) is the most important one among the ochratoxins as it is distinctly more toxic and prevalent than OTB due to its chlorine atom and it is rapidly formed in vivo from OTC, an ethyl ester of OTA. OTA has weak acidic properties with pK_a values in the ranges of 4.2-4.4 and 7.0-7.3, respectively, for the carboxyl group of the phenylalanine moiety and phenolic hydroxyl group of the isocoumarin part[109]. Two ionizable moieties of OTA, monoanion (OTA$^-$) and dianion (OTA^{2-}) are present at neutral pH at the pK_as of the carboxyl and phenol groups in OTA. The presence of ochratoxin A depends on climatic and storage conditions[110]. Its diversity in nature is due to the facility of OTA-producing filamentous fungi, *Aspergillus ochraceus* and *Penicillium verrucosum,* to grow on a wide range of substrates under varying climatic and storage conditions[111]. High temperatures, moisture and unseasonal rains during harvest and flash floods lead to fungal proliferation and production of ochatoxin A. Poor harvesting
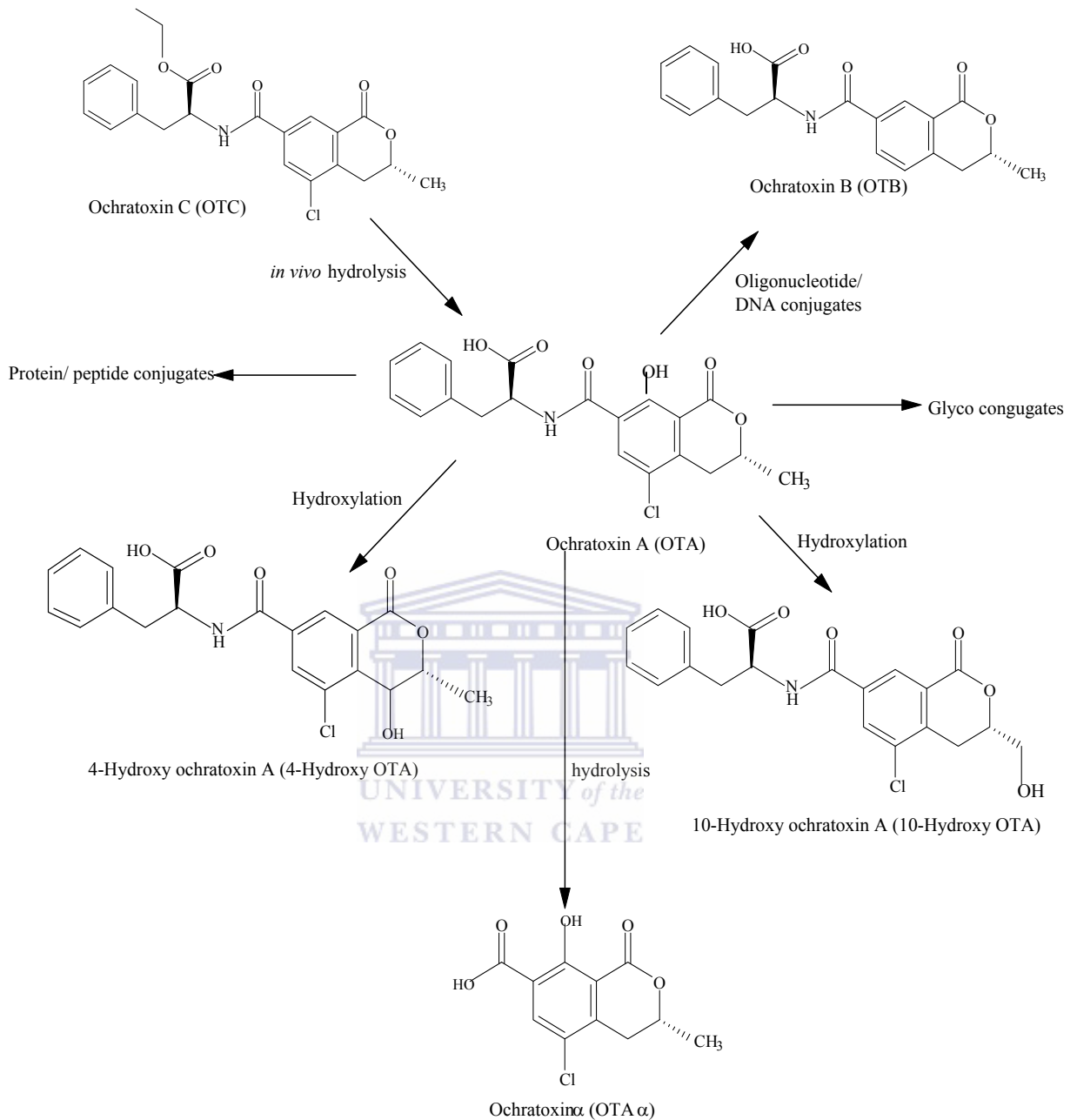
Scheme 2.2: *In vivo* metabolism of ochratoxin A and structures of other ochratoxins.

practice, improper storage and less than optimal conditions during transportation, marketing and processing can also contribute to fungal growth and increase the risk of

mycotoxin production. These climatic conditions and food production chains are characteristic of- most parts of Africa, including South Africa [112, 113].

Ochratoxin A is a stable molecule able to resist most food processing steps[114]. It is a common contaminant in improperly stored foods such as cereals, coffee beans, cocoa, milk, beer, wine, grape juice, spices and dried fruits[108, 110, 115]. The Food and Agricultural Organization (FAO) of the United Nations estimated that up to 25% of the world's food crops are significantly contaminated with mycotoxins [113, 116]. The toxin is potently nephrotoxic, tetratogenic and an immuno-suppressive agent that has been considered by the International Agency for Research on Cancer (IARC) to be a group 2B potential carcinogen for humans[117, 118]. Bioaccumulation due to contaminated food has resulted in the detection of OTA in eggs, porcine liver, kidney, muscle and blood. Ochratoxin A has a 35-day half-life time required for its elimination. It has been found in blood and breast milk of people exposed to contaminated products. Toxicological studies show that upon adsorption from the gastrointestinal tract, OTA can easily reach the bloodstream and completely bind to serum proteins[108]. Re-adsorption of OTA from the intestine back to circulation, as a result of biliary recycling of blood, favours the systematic re-distribution of OTA towards different tissues. Kidney and liver are the most susceptible organs to OTA. Its accumulation in the kidneys can cause both acute and chronic lesions by induction of a defect in the anion transport mechanism[115]. Ochratoxin A is suspected to cause Balkan endemic nephropathy (BEN), a progressive nephritis occurring in populations from south-eastern Europe. Ochratoxin A also affects the immune system of many mammalian species and it is a genotoxic, tetragenic, myelotoxic, carcinogen and

possibly a neurotoxic agent to several animal species. In terms of OTA genotoxicity, the toxin promotes oxidative stress[119, 120], oxidative damage[120] and single strand deoxyribonucleic acid (DNA) cleavage through production of reactive oxygen species[121]. Redox-active transition metals facilitate oxidative DNA strand scission in the presence of copper without the aid of an external reducing agent[122]. The toxicity of OTA is therefore related to its ability to inhibit protein synthesis by competing with phenylalanine in the reaction catalyzed by phenylalanyl-tRNA synthetase and other systems requiring this amino acid[123]. However, ochratoxin A is rapidly metabolised in ruminants to non-toxic ochratoxin α and to a small degree, 4- and 10- hydroxyl OTA[106].

2.11.3 Methods of ochratoxin A detection

Persistence of mycotoxins in the food chain has prompted adoption of regulatory limits in several countries, which in turn require the development of validated official analytical methods for rapid, cost effective, sensitive and accurate screening of mycotoxins in different matrices[124, 125]. In Africa, the presence of mycotoxins in food is often overlooked due to public ignorance about their existence, lack of regulatory mechanisms, dumping of food products and introduction of contaminated commodities into the human food chain during chronic food shortage due to drought, wars, political and economic instability[126-130]. International enquiries on existing mycotoxin legislation in foodstuff and animal feeding stuff have been carried out and details on tolerances, official protocols of analysis and sampling have been published[131-134]. Due to these findings, many countries have set limits on OTA levels in food, typically between 1 and 10 ppb depending on the

type and quality of the food stuff[131]. However, these regulations require accurate and suitable methods of detection and quantification. Research studies have been conducted to develop appropriate methods for the detection of OTA in food and feed samples[114]. Traditional methods include gas chromatography, thin layer chromatography, capillary electrophoresis and high-performance liquid chromatography. Due to the strong native fluorescence activity of ochratoxin, high performance liquid chromatography coupled to a fluorescent detector (HPLC-FL) has been established as the preferred routine analysis technique for OTA, OTB and OTC and their metabolites. It offers better selectivity and sensitivity compared to other detectors. Other analytical methods available for mycotoxins determination include thin-layer chromatography (TLC), gas chromatography (GC) and enzyme-linked immunosorbent assay (ELISA)[124]. TLC is not ideal as a technique due to its comparably low sensitivity towards trace levels (ppb range) of OTA. GC-based methods suffer from a time-consuming and error prone methylation derivatisation protocol needed to achieve sufficient volatility of the analytes. However, more recently, there has been a tendency for the use of less costly techniques and a reduction in use of organic solvents since they result in high ecological costs. Even though ELISA assays have shown to be extremely suitable for rapid screening of large sample numbers, possible cross-reactivities with matrix components make confirmation by other techniques highly desirable to avoid false positive results or inaccurate and overestimated quantitative data[106, 109]. Owing to their high sensitivity, good specificity, and less dependence on sample cleanup, electrochemical sensors have also been developed for fast and effective screening of OTA in foodstuffs. Among these electrochemical sensors, immunological procedures seem most promising due to their

low cost, compatibility with miniaturization and portability, high sensitivity and low endogenous background[135]. Immunosensors also have the added advantage of analysing samples without need for intensive sample pre-treatment.

Electrochemical immunosensors are used extensively for the direct detection of antibody-antigen interactions. Various kinds of immunosensors including optical waveguide lightmode spectroscopy (OWLS)[136], fluorescent biosensor arrays, electrochemical[125] and impedimetric immunosensors[137] have been developed for clinical and environmental purposes as a result of the possibility of generating a large number of antigens for the analysis of numerous chemical species[125, 138]. Their main advantages are that they are non-invasive and require little sample pre-treatment[53]. Electrochemical techniques such as voltammetry and impedance have been successfully used in the detection and determination of various biological compounds due to their high sensitivity. Since, electrochemical immunosensors are concerned with the formation of a recognition complex between the sensing biomaterial and the analyte under investigation in a monolayer or thin-film configuration on an electronic transducer, the formation of a complex on a conductive surface may alter the capacitance and the resistance at the surface-electrolyte interface[139]. This alteration can be exploited to determine concentration of the required analyte. Impedimetric immunosensors were chosen for this project due to their high stability and enhanced orientation[137, 140]. Impedance spectroscopy is a powerful tool for the characterisation of biological thin-films involved in the transduction of biomolecular interactions at electrode surfaces[141]. Kinetics and mechanisms of electron-transfer processes that correspond to the biocatalytic reaction

occurring at modified electrodes can also be derived from Faradaic impedance spectroscopy (FIS). Polyaniline has been successfully used for the immobilization of antibodies within the conducting thin-film at the electrode surface[141-143]. Sensor modification with neutravidin and biotin allowed site-specific coupling of the antibody to the polyaniline matrix. Electrochemical impendence spectroscopy was also used to measure the electro-activity of a TiO_2-chitosan impedimetric immunosensors for ochratoxin A[137]. The matrix had free -NH_2 and -OH groups due to a higher probability of hydrogen and covalent bonding between -OH group in chitosan molecules with Ti-O-Ti which supported immobilisation of rabbit antibodies (IgGs) and proteins.

2.12 Biocomponents

Biocomponents, which function as biochemical transducers can be enzymes, tissues, bacteria, yeast, antibodies or antigens, liposomes, organelles[144, 145]. Most of the biological molecules such as enzymes, receptors, antibodies and cells, have very short lifetimes in solution phase. Thus, they have to be fixed on a suitable matrix. The immobilization of the biological component against the environmental conditions results in decreased enzyme activity[146]. The activity of immobilized molecules depends upon surface area, porosity, hydrophilic character of immobilizing matrix, reaction conditions and the methodology chosen for immobilization. A number of techniques such as physical adsorption, cross-linking, gel entrapment and covalent coupling have been used to immobilize biological molecules in carrier materials[2]. Various matrices have been used for the immobilization of enzymes such as, membranes, gels, carbon, graphite, silica and

polymeric films[147, 148]. There is thus a great need to design electrodes that are compatible with the biological component that can lead to rapid electron transfer at the electrode surface.

2.12.1 Antibodies

Antibodies are ideal bio-recognition elements due to their exquisite specificities and strong affinities for cognate antigens. The antibody molecule has four polypeptide chains, two heavy (H) chains with molecular weights of 50 kDa and two light (L) chains (25 kDa molecular weight) linked by disulphide bonds as shown in Figure 2.7. The chains have both constant (C) and variable (V) regions. The H chain has one variable region (V_H) that is responsible for antigen binding and three constant regions (C_{H1}, C_{H2} and C_{H3}).
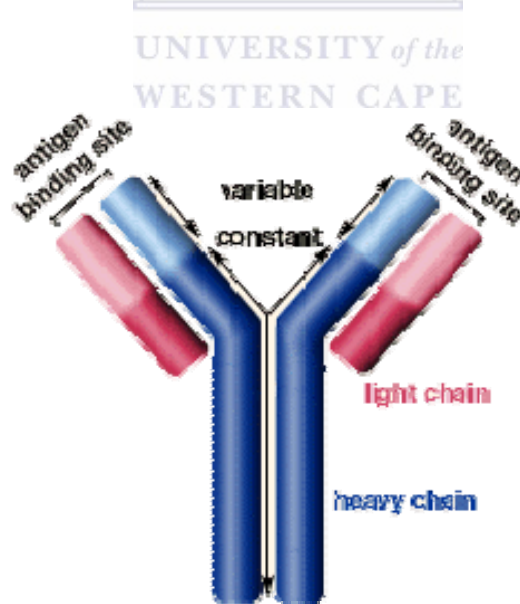
Figure 2.7: General structure of an antibody.

The light chain has one variable region (V_L), which is an important part of the antigen-binding site and one constant region (C_L)[149, 150]. Antigen binding is mediated by the variable light (V_L) and heavy (V_H) domains which bring together the hyper-variable regions of the antibody, known as the complementarily determining regions (CDRs). The antibody constant regions are generally conserved with only small differences in sequence being found in the various antibody classes. In general, antibodies have positively charged amino acid residues on the outside due to a pI of 6.2[151] and at neutral pH of 7, the antibody has a negative charge. Antibodies have numerous successful applications in the area of diagnostics with monoclonal and polyclonal antibodies being successfully exploited in many biosensors[150]. Polyclonal antibodies are derived from multiple plasma cells while monoclonal antibodies are derived from a single clonal hybridoma, all of which are terminally differentiated in response to an antigen. Some key parameters exist for antibodies in biosensor applications. These include sensitivity, selectivity, stability, immobilization, labelling and antibody size. Various chemical reactions have been applied to the immobilization of the antibody onto the solid surfaces[152]. Immobilization of biomolecules can either be by direct adsorption[143] or by their incorporation into the polymer matrix during the growth of the latter[53]. Properly functionalized polymer precursors can create readily reactive polymer films to biomolecules bearing amino or carboxyl groups or to avidin-based conjugates[53, 154]. Linkage between the antibody and the solid phase material by glutaraldehyde, carbodiimide, succinimide ester, maleinimide and chitosan, have been developed. Albumin derivatized with aryldiazirines as a photolinker in photo-immobilization of

antibodies is applicable. Antibodies have to be properly immobilized on different types of immunosensing surfaces so as to improve reaction kinetic parameters[152].

2.13 Electrochemical biosensors

A biosensor is an analytical device, which incorporates a biological recognition element in close proximity or integrated with a signal transducer to provide a sensing system specific to a target analyte[2]. Many different types of biosensors are presently available. However, all of them basically comprise a biological recognition element or bioreceptor, which interacts with the analyte and responds in a manner that can be detected by a transducer. The construction of biological assemblies on various conductive and semi-conductive surfaces forms the basis of most electrochemical-based biosensors[155]. More than half of the biosensors reported in the literature involve the electrochemical detection method, that is, amperometric, potentiometric, capacitive and conductometric[156-158]. A number of investigators have reviewed the application of electrochemical impedance spectroscopy (EIS) in the development of biosensors at conductive and semi-conductive surfaces[159-161]. EIS provides important mechanistic information on adsorption by measuring the changes in the interfacial capacitance and resistance of surfaces[162-165]. Similarly, the immobilization and adsorption behaviour of various biomolecules onto conductive surfaces has also been investigated by impedance spectroscopy[166-168].

2.13.1 Immunosensor

An immunosensor is a biosensor that uses antibodies or antibody fragment as the biological element[169]. The specificity of molecular recognition of antigens by antibodies to form a stable complex is the basis of immunosensors on solid-state interfaces[152]. This fundamental concept of immunosensors as ligand assays is based on the observation of products of the ligand-binding reaction between a target analyte and a highly specific binding reagent. Therefore, the specificity for the measurement of analytes in immunosensor systems is dependent on application of binding molecules. The selectivity of the ligand-binding of antibodies allows immunosensors to be employed in analytical methods that are highly specific and in complex biological matrices, such as blood and urine. The transduction element in the case of immunosensors is largely based on optical, electrochemical, microgravimetric, thermometric and piezoelectric signals[170]. Electrochemical immunosensors are further divided into potentiometric, amperometric, conductometric or capacitative[152]. All immunosensor types can either be run as labelled or non-labelled. The non-labelled, also known as, direct sensors are able to detect the physical changes during the immune complex formation, whereas the labelled or indirect sensors use signal-generating labels which allow more sensitive and versatile detection modes when incorporated into the complex. A variety of labels including enzymes, electroactive compounds and fluorescent labels have been applied in indirect immunosensors.

2.13.1.1 Electrochemical immunosensor

The electrochemical sensors include impedimetric, potentiometric and amperometric immunosensors[169, 171].

2.13.1.1.1 Potentiometric immunosensors

These are based on the change in potential that occurs when an antigen in a sample reacts with the corresponding antibody previously immobilised to an electrode[169]. The potential difference between an antibody-immobilised electrode and a reference electrode is a function of the analyte in the sample.
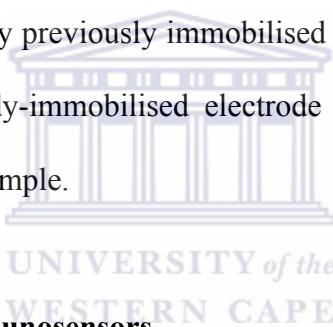
2.13.1.1.2 Amperometric immunosensors

These rely on the measurement of current generated when an electroactive species is either oxidised or reduced at an antibody- (or antigen-) coated electrode to which an analyte binds specifically[169].

2.13.1.1.3 Impedimetric immunosensors

Pioneering works in the late 1980s by Newman *et al.* and Martelet *et al.*, on the concept of capacitive, or impedimetric based immunosensors, has led to a lot of work being done

on electrochemical impedance spectroscopy-based sensors[171, 172]. Impedimetric immunosensors possess a number of attractive characteristics associated with the use of electrochemical transducers, namely; low cost of electrode mass production, cost effective instrumentation, the ability to be miniaturized and integrated into multi-array or microprocessor-controlled diagnostic tools and remote control of implanted sensors[171]. Based on the nature of the measuring signal, impedance immunosensors can be classified as capacitive or faradaic. Capacitive, where the surface of the electrode is completely covered by a dielectric layer and the whole electrode assembly behaves as an insulator. In this type of sensor, no redox probe is present in the measuring solution and the capacitive current is measured under small amplitude sinusoidal voltage signal, at low excitation frequencies (typically 10-1000 Hz). Therefore, Ab-Ag interactions are expected to cause a decrease of the measuring capacitance. On the other hand, Faradaic impedimetric immunosensors are partially or wholly covered by a non insulating layer electrode surfaces. They can also be partially covered by an insulating layer that is able to catalyze a redox probe which exists in the measuring solution. In this case, the measured parameter is the charge transfer resistance (the real component of impedance at low frequency values, typically 0.1-1.0 Hz). Ab-Ag interactions are expected to cause an increase in charge resistance value as the faradic reaction becomes increasingly hindered. In general, faradic impedimetric immunosensors exhibit a higher sensitivity to Ab-Ag interactions. However, the redox species may have an effect on both the stability and activity of the electrode assembly. As the disassociation constant for the antigen-antibody complex is low, the reusability and reproducibility of these immunosensors is difficult to achieve. Regeneration procedures include, the use of low (<3), or high (>9) pH buffer

solutions, detergents, high ionic strength solution or non-polar water soluble solvents that normally have an influence on the activity of bio-recognition.

2.13.1.2 Piezoelectric immunosensor

A piezoelectric immunosensor is a device based on materials such as quartz crystals, which resonate on application of an external alternating electric field[170]. The frequency of the resulting oscillation is a function of the mass of the crystal. Thus, interaction of an analyte in a sample with the corresponding antibody, previously immobilised by passive adsorption or by covalent interaction to a quartz crystal, will increase the overall mass, which is measured as a change in the frequency of oscillation. The two types of piezoelectric immunosensors are bulk acoustic (BA) devices and surface acoustic wave (SAW) devices. In the BA device, the specific adsorption of an analyte with the corresponding antibody-immobilised crystal occurs at the surface, which is connected to an oscillating circuit, but resonance occurs on the entire mass of the crystal. Thus, the increase in mass will result in a decrease in the resonant frequency, which is a function of the analyte concentration. In SAW immunosensors, an acoustic wave travels only over the surface of the crystal that is coated with a specific antibody. A change in the frequency will occur as the analyte in a sample binds to the corresponding immobilised antibody.

2. 13.1.3 Optical immunosensor

Optical immunosensors include the variants fibre optic (FO), surface plasmon resonance (SPR) and evanescent wave (EW) immunosensor[170]. In the FO immunosensor, antibodies are immobilised to the distal end of an optical fibre by a number of mechanisms, including passive adsorption, covalent interaction or immobilisation through a gel matrix. Light is then introduced at the proximal end, which travels to the distal tip by total internal reflection. In most cases, the fluorescence emission of either the analytes intrinsic fluorescence or subsequent binding of a fluorescent-labelled reactant in a competitive or non-competitive immunoassay format is measured. The extent of fluorescence corresponds either directly or inversely to the analyte concentration, depending on the assay format.
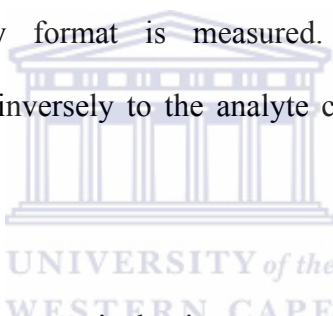
The principle for SPR immunosensors is that it measures the mass concentration changes as a refractive index change caused by binding of an analyte (or antibody) to the corresponding antibody (or antigen) immobilised to the sensor surface. The change in mass concentration gives rise to a shift in the SPR angle. The SPR angle is the angle where the intensity of the reflected light is reduced as a result of resonance with free electrons in the sensor surface.

In the EW immunosensor, light travelling through a waveguide by multiple internal reflections creates an electromagnetic wave called an evanescent wave, which penetrates a distance of approximately 200 nm away from the surface. An analyte bound to the

corresponding antibody immobilized on the surface of a waveguide will interact with the wave by absorption and then emission fluorescence which is measured as a function of the analyte concentration.

Light-addressable potentiometric sensor (LAPS) is combination of an optical and an electrochemical transduction system that has an assay that comprises two stages[173]. The first stage comprises an immuno-ligand assay. The test bacteria are captured (sandwiched) between a biotinylated antibacterial antibody bound to streptavidin-biotinylated bovine serum albumin which in turn is coupled to a nitrocellulose membrane and a fluoresceinated antibacterial antibody. This is subsequently detected with an anti-fluorescein-urease conjugate in the presence of the urea substrate. In the second stage, the membrane containing the immune complex is in close contact with a pH-sensitive insulator coated onto a semiconducting silicon chip. Incident light from a light-emitting diode generates a photocurrent and allows independent measurement of the captured immune complexes. Conversion of the pH change associated with the urease activity to voltage allows fast measurement of the immune complexes.

Evidently, the interface between the sensor surface and the chemical or biological system must be tailored in a way that ensures that the receptor molecules attached to the solid support retain their activity[155]. Consequently, EIS is an ideal tool for observing the dynamics of biomolecular interactions, and it has been used to predict important aspects of biosensor development such as rates of reaction, surface loading, surface reactivity or stability and binding constants.

In a physical adsorption process, the biomolecule gets adsorbed in the polymer/solution interface due to static interactions between the polycationic matrix of the oxidised polymer and the total negative enzyme charge, provided pH is higher than the isoelectric point (pI) of the enzyme[174]. But this process has some known disadvantages like binding forces can change with pH and adsorption is limited to one monolayer on the polymer surface hence amount of enzyme incorporated is very small[175]. Since biomaterial is immobilized on the outer layer of conducting polymer, it may also get leached out into sample solution during measurements. This decreases the lifetime stability of enzyme electrode[176].

2.13.2 Enzyme sensors

Other biosensors include enzyme sensors based primarily on the immobilization of an enzyme onto an electrode. The development of enzyme-based sensors for the detection of glucose in blood represents a major area of biosensor research. Material selection is an important aspect of sensor development as it allows the response characteristics of a sensor to be altered in a way that minimizes non-specific adsorption by other molecules. The fabrication of a long-term amperometric enzyme biosensor for the real-time monitoring of biomolecules in blood demands a device that inhibits the adsorption or reaction of interfering components with the sensor surface[155].

2.13.3 DNA sensors

The use of nucleic acid recognition layers in DNA sensors represents a rapidly growing and an exciting area of biosensor research[177-179]. In most cases, the detection of DNA relies on the immobilization of a single-stranded oligonucleotide onto a transducer surface and exposure of the sensor to a sample containing the target results in a hybridization event. A crucial step in the development of DNA biosensors involves the immobilization of a single-stranded DNA, and a great deal of work has been carried out using EIS to understand this process[180, 181].

2.13.4 Ion channel sensors

Ion channel sensors are chemically modified membranes, which incorporate biomimetic ion channels. They play an important role in the biomedical, pharmaceutical and bioanalytical fields. A unique approach for the development of biomimetic ion channel technology is the use of EIS. In fact, it has been shown that EIS is an ideal tool for investigating the formation of tethered bilayer membrane ion channels[182, 183]. Impedance measurements are made over a range of ionic species, ionic concentrations, reservoir chemistries, tether structures, spacer molecules and potentials. More importantly, changes in capacitance are interpreted in terms of variants which account for the ionic distribution on a metal surface[182]. It is clearly evident from the above studies that EIS is a reliable and sensitive tool for detecting the trans-membrane currents and interfacial changes on various modified surfaces.

References

1.   Nambiar, S.; Yeow, J. T. W., Conductive polymer-based sensors for biomedical applications. *Biosensors and Bioelectronics* **2011,** 26, (5), 1825-1832.

2.   Gerard, M.; Chaubey, A.; Malhotra, B. D., Application of conducting polymers to biosensors. *Biosensors and Bioelectronics* **2002,** 17, (5), 345-359.

3.   Casar, Z.; Leban, I.; Majcen-le Marechal, A.; Piekara-Sady, L.; Lorcy, D., Charge transfer complexes and cation radical salts of azino-diselenadiazafulvalene. *Comptes Rendus Chimie* **2009,** 12, (9), 1057-1065.

4.   Kobayashi, Y.; Yoshioka, M.; Saigo, K.; Hashizume, D.; Ogura, T., Hydrogen-bonding tetrathiafulvalene (TTF) conductors: Carrier generation by self-doping. *Physica B: Condensed Matter* **2010,** 405, (11, Supplement 1), S23-S26.

5.   Demolliens, A.; Muller, C.; Müller, R.; Turquat, C.; Goux, L.; Deleruyelle, D.; Wouters, D. J., Solution growth of metal-organic complex CuTCNQ in small dimension interconnect structures. *Journal of Crystal Growth* **2010,** 312, (22), 3267-3275.

6.   di Lena, F.; Matyjaszewski, K., Transition metal catalysts for controlled radical polymerization. *Progress in Polymer Science* **2010,** 35, (8), 959-1021.

7.   Debuigne, A.; Poli, R.; Jérôme, C.; Jérôme, R.; Detrembleur, C., Overview of cobalt-mediated radical polymerization: Roots, state of the art and future prospects. *Progress in Polymer Science* **2009,** 34, (3), 211-239.

8.   Gligorich, K. M.; Iwai, Y.; Cummings, S. A.; Sigman, M. S., A new approach to carbon-carbon bond formation: development of aerobic Pd-catalyzed reductive

coupling reactions of organometallic reagents and styrenes. *Tetrahedron* **2009,** 65, (26), 5074-5083.

9.   Moreda-Piñeiro, J.; Alonso-Rodríguez, E.; López-Mahía, P.; Muniategui-Lorenzo, S.; Prada-Rodríguez, D.; López-Mahía, P.; Prada-Rodríguez, D.; Romarís-Hortas, V.; Míguez-Framil, M.; Moreda-Piñeiro, A.; Bermejo-Barrera, P., Matrix solid-phase dispersion of organic compounds and its feasibility for extracting inorganic and organometallic compounds. *TrAC Trends in Analytical Chemistry* **2009,** 28, (1), 110-116.

10.   Nakai, H.; Isobe, K., Photochromism of organometallic compounds with structural rearrangement. *Coordination Chemistry Reviews* **2010,** 254, (21-22), 2652-2662.

11.   Snook, G. A.; Kao, P.; Best, A. S., Conducting-polymer-based supercapacitor devices and electrodes. *Journal of Power Sources* **2011,** 196, (1), 1-12.

12.   Adhikari, B.; Majumdar, S., Polymers in sensor applications. *Progress in Polymer Science* **2004,** 29, (7), 699-766.

13.   Dhand, C.; Das, M.; Datta, M.; Malhotra, B. D., Recent Advances in Polyaniline Based Biosensors. *Biosensors and Bioelectronics* In Press, Accepted Manuscript.

14.   Kumar, D.; Sharma, R. C., Advances in conductive polymers. *European Polymer Journal* **1998,** 34, (8), 1053-1060.

15.   Mathebe, N. G. R.; Morrin, A.; Iwuoha, E. I., Electrochemistry and scanning electron microscopy of polyaniline/peroxidase-based biosensor. *Talanta* **2004,** 64, (1), 115-120.

16.   Xia, L.; Wei, Z.; Wan, M., Conducting polymer nanostructures and their application in biosensors. *Journal of Colloid and Interface Science* **2010,** 341, (1), 1-11.

17.   Wallace, G. G., *Conductive electroactive polymers: intelligent polymer systems* **2009**. CRC Press: Boca Raton, 10-27.

18.   Guimard, N. K.; Gomez, N.; Schmidt, C. E., Conducting polymers in biomedical engineering. *Progress in Polymer Science* **2007,** 32, (8-9), 876-921.

19.   Harsányi, G., Polymeric sensing films: new horizons in sensorics? *Materials Chemistry and Physics* **1996,** 43, (3), 199-203.

20.   Bredas, J. L.; Street, G. B., Polarons, bipolarons, and solitons in conducting polymers. *Accounts of Chemical Research* **1985,** 18, (10), 309-315.

21.   Trivedi, D. C., *Handbook of Organic Conductive Molecules and Polymers: Volume 2 Conductive Polymers: Synthesis and Electrical Properties*. John Wiley and Sons Ltd: New York, **1996**; 506–572.

22.   Grennan, K.; Killard, A. J.; Hanson, C. J.; Cafolla, A. A.; Smyth, M. R., Optimisation and characterisation of biosensors based on polyaniline. *Talanta* **2006,** 68, (5), 1591-1600.

23.   Zheng, W.; Min, Y.; MacDiarmid, A. G.; Angelopoulos, M.; Liao, Y. H.; Epstein, A. J., Effect of organic vapors on the molecular conformation of non-doped polyaniline. *Synthetic Metals* **1997,** 84, (1-3), 63-64.

24.   Hatchett, D. W.; Josowicz, M., Composites of intrinsically conducting polymers as sensing nanomaterials. *Chemical Reviews* **2008,** 108, (2), 746-769.

25.   Wang, J., Nanomaterial-based electrochemical biosensors. *Analyst* **2005,** 130, (4), 421-426.

26.   Parthasarathy, R. V.; Martin, C. R., Synthesis of polymeric microcapsule arrays and their use for enzyme immobilization. *Nature* **1994,** 369, (6478), 298-301.

27.   Ozin, G. A., Nanochemistry: Synthesis in diminishing dimensions. *Advanced Materials* **1992,** 4, (10), 612-649.

28.   Parthasarathy, R. V.; Martin, C. R., Template-synthesized polyaniline microtubules. *Chemistry of Materials* **1994,** 6, (10), 1627-1632.

29.   Huang, J.; Virji, S.; Weiller, B. H.; Kaner, R. B., Polyaniline nanofibers: Facile synthesis and chemical sensors. *Journal of the American Chemical Society* **2003,** 125, (2), 314-315.

30.   Martin, C. R.; Parthasarathy, R.; Menon, V., Template synthesis of electronically conductive polymers - a new route for achieving higher electronic conductivities. *Synthetic Metals* **1993,** 55, (2 -3 pt 2), 1165-1170.

31.   Bartlett, P. N.; Birkin, P. R.; Ghanem, M. A.; Toh, C. S., Electrochemical syntheses of highly ordered macroporous conducting polymers grown around self-assembled colloidal templates. *Journal of Materials Chemistry* **2001,** 11, (3), 849-853.

32.   Cassagneau, T.; Caruso, F., Semiconducting polymer inverse opals prepared by electropolymerization. *Advanced Materials* **2002,** 14, (1), 34-38.

33.   Sumida, T.; Wada, Y.; Kitamura, T.; Yanagida, S., Electrochemical preparation of macroporous polypyrrole films with regular arrays of interconnected spherical voids. *Chemical Communications* **2000**, (17), 1613-1614.

34.   Wu, C. G.; Bein, T., Conducting polyaniline filaments in a mesoporous channel host. *Science* **1994,** 264, (5166), 1757-1759.

35.   Beck, J. S.; Vartuli, J. C.; Roth, W. J.; Leonowicz, M. E.; Kresge, C. T.; Schmitt, K. D.; Chu, C. T. W.; Olson, D. H.; Sheppard, E. W.; McCullen, S. B.; Higgins, J. B.; Schlenker, J. L., A new family of mesoporous molecular sieves prepared with liquid crystal templates. *Journal of the American Chemical Society* **1992,** 114, (27), 10834-10843.

36.   Cao, L.; Chen, H. Z.; Zhou, H. B.; Zhu, L.; Sun, J. Z.; Zhang, X. B.; Xu, J. M.; Wang, M., Carbon-nanotube-templated assembly of rare-earth phthalocyanine nanowires. *Advanced Materials* **2003,** 15, (11), 909-913.

37.   Boal, A. K.; Ilhan, F.; Derouchey, J. E.; Thurn-Albrecht, T.; Russell, T. P.; Rotello, V. M., Self-assembly of nanoparticles into structured spherical and network aggregates. *Nature* **2000,** 404, (6779), 746-748.

38.   Kazimierska, E.; Muchindu, M.; Morrin, A.; Iwuoha, E.; Smyth, M. R.; Killard, A. J., The fabrication of structurally multiordered polyaniline films and their application in electrochemical sensing and biosensing. *Electroanalysis* **2009,** 21, (3-5), 595-603.

39.   Luo, X.; Vidal, G.; Killard, A.; Morrin, A.; Smyth, M., Nanocauliflowers: A Nanostructured Polyaniline-Modified Screen-Printed Electrode with a Self-Assembled Polystyrene Template and Its Application in an Amperometric Enzyme Biosensor. *Electroanalysis* **2007,** 19, (7-8), 876-883.

40.   Muchindu, M.; Waryo, T.; Arotiba, O.; Kazimierska, E.; Morrin, A.; Killard, A. J.; Smyth, M. R.; Jahed, N.; Kgarebe, B.; Baker, P. G. L.; Iwuoha, E. I.,

Electrochemical nitrite nanosensor developed with amine- and sulphate-functionalised polystyrene latex beads self-assembled on polyaniline. *Electrochimica Acta* **2010,** 55, (14), 4274-4280.

41.   Fu, G.-D.; Li, G. L.; Neoh, K. G.; Kang, E. T., Hollow polymeric nanostructures--Synthesis, morphology and function. *Progress in Polymer Science* **2011**, 36, (1), 127-167.

42.   Sun, H.; Hu, N., Electroactive layer-by-layer films of heme protein-coated polystyrene latex beads with poly(styrene sulfonate). *Analyst* **2005**, 130, (1),76-84.

43.   Luo, X.; Killard, A. J.; Smyth, M. R., Nanocomposite and Nanoporous Polyaniline Conducting Polymers Exhibit Enhanced Catalysis of Nitrite Reduction. *Chemistry - A European Journal* **2007,** 13, 2138-2143.

44.   Kanungo, M.; Deepa, P. N.; Collinson, M. M., Template-Directed Formation of Hemispherical Cavities of Varying Depth and Diameter in a Silicate Matrix Prepared by the Sol-Gel Process. *Chemistry of Materials* **2004,** 16, (25), 5535-5541.

45.   Malinauskas, A., Electrocatalysis at conducting polymers. *Synthetic Metals* **1999,** 107, (2), 75-83.

46.   Lange, U.; Roznyatovskaya, N. V.; Mirsky, V. M., Conducting polymers in chemical sensors and arrays. *Analytica Chimica Acta* **2008,** 614, (1), 1-26.

47.   von Schickfus, M.; Stanzel, R.; Kammereck, T.; Weiskat, D.; Dittrich, W.; Fuchs, H., Improving the SAW gas sensor: device, electronics and sensor layer. *Sensors and Actuators B: Chemical* **1994,** 19, (1-3), 443-447.

48.   Nishizawa, M.; Matsue, T.; Uchida, I., Penicillin sensor based on a microarray electrode coated with pH-responsive polypyrrole. *Analytical Chemistry* **1992,** 64, (21), 2642-2644.

49.   Myler, S.; Collyer, S. D.; Davis, F.; Gornall, D. D.; Higson, S. P. J., Sonochemically fabricated microelectrode arrays for biosensors: Part III. AC impedimetric study of aerobic and anaerobic response of alcohol oxidase within polyaniline. *Biosensors and Bioelectronics* **2005,** 21, (4), 666-671.

50.   Kulikov, V.; Mirsky, V. M., Equipment for combinatorial electrochemical polymerization and high-throughput investigation of electrical properties of the synthesized polymers. *Measurement Science and Technology* **2004,** 15, (1), 49-54.

51.   Partridge, A. C.; Harris, P.; Andrews, M. K., High sensitivity conducting polymer sensors. *Analyst* **1996,** 121, (9), 1349-1353.

52.   Kulikov, V.; Mirsky, V. M.; Delaney, T. L.; Donoval, D.; Koch, A. W.; Wolfbeis, O. S., High-throughput analysis of bulk and contact conductance of polymer layers on electrodes. *Measurement Science and Technology* **2005,** 16, (1), 95-99.

53.   Grant, S.; Davis, F.; Law, K. A.; Barton, A. C.; Collyer, S. D.; Higson, S. P. J.; Gibson, T. D., Label-free and reversible immunosensor based upon an ac impedance interrogation protocol. *Analytica Chimica Acta* **2005,** 537, (1-2), 163-168.

54.   Gvozdenović, M. M.; Jugović, B. Z.; Bezbradica, D. I.; Antov, M. G.; Knežević-Jugović, Z. D.; Grgur, B. N., Electrochemical determination of glucose using

polyaniline electrode modified by glucose oxidase. *Food Chemistry* **2011,** 124, (1), 396-400.

55.   Ndangili, P. M.; Waryo, T. T.; Muchindu, M.; Baker, P. G. L.; Ngila, C. J.; Iwuoha, E. I., Ferrocenium hexafluorophosphate-induced nanofibrillarity of polyaniline-polyvinyl sulfonate electropolymer and application in an amperometric enzyme biosensor. *Electrochimica Acta* **2010,** 55, (14), 4267-4273.

56.   Ewbank, P. C.; Loewe, R. S.; Zhai, L.; Reddinger, J.; Sauvé, G.; McCullough, R. D., Regioregular poly(thiophene-3-alkanoic acid)s: Water soluble conducting polymers suitable for chromatic chemosensing in solution and solid state. *Tetrahedron* **2004,** 60, (49), 11269-11275.

57.   Christie, S.; Scorsone, E.; Persaud, K.; Kvasnik, F., Remote detection of gaseous ammonia using the near infrared transmission properties of polyaniline. *Sensors and Actuators, B: Chemical* **2003,** 90, (1-3), 163-169.

58.   Lindfors, T.; Ivaska, A., Raman based pH measurements with polyaniline. *Journal of Electroanalytical Chemistry* **2005,** 580, (2), 320-329.

59.   Toal, S. J.; Trogler, W. C., Polymer sensors for nitroaromatic explosives detection. *Journal of Materials Chemistry* **2006,** 16, (28), 2871-2883.

60.   Thomas III, S. W.; Swager, T. M., Trace hydrazine detection with fluorescent conjugated polymers: A turn-on sensory mechanism. *Advanced Materials* **2006,** 18, (8), 1047-1050.

61.   Iwuoha, E. I.; de Villaverde, D. S.; Garcia, N. P.; Smyth, M. R.; Pingarron, J. M., Reactivities of organic phase biosensors. 2. The amperometric behaviour of horseradish peroxidase immobilised on a platinum electrode modified with an

electrosynthetic polyaniline film. *Biosensors and Bioelectronics* **1997,** 12, (8), 749-761.

62.   Iwuoha, E. I.; Mavundla, S. E.; Somerset, V. S.; Petrik, L. F.; Klink, M. J.; Sekota, M.; Bakers, P., Electrochemical and Spectroscopic Properties of Fly Ash–Polyaniline Matrix Nanorod Composites. *Microchimica Acta* **2006,** 155, (3), 453-458.

63.   Venancio, E. C.; Wang, P-C.; MacDiarmid, A. G., The azanes: A class of material incorporating nano/micro self-assembled hollow spheres obtained by aqueous oxidative polymerization of aniline. *Synthetic Metals* **2006,** 156, (5-6), 357-369.

64.   Luo, X.; Morrin, A.; Killard, A.; Smyth, M., Application of Nanoparticles in Electrochemical Sensors and Biosensors. *Electroanalysis* **2006,** 18, (4), 319-326.

65.   Smertenko, P. S.; Dimitriev, O. P.; Schrader, S.; Brehmer, L., Doping of polyaniline by transition metal salts: current-voltage characteristics of the ITO/polymer film/metal heterostructures. *Synthetic Metals* **2004,** 146, (2), 187-196.

66.   Dimitriev, O. P.; Smertenko, P. S.; Stiller, B.; Brehmer, L., Polyaniline-transition metal salt complexes: insight into formation mechanisms. *Synthetic Metals* **2005,** 149, (2-3), 187-192.

67.   Nabid, M. R.; Sedghi, R.; Jamaat, P. R.; Safari, N.; Entezami, A. A., Catalytic oxidative polymerization of aniline by using transition-metal tetrasulfonated phthalocyanine. *Applied Catalysis A: General* **2007,** 328, (1), 52-57.

68.   Nabid, M. R.; Asadi, S.; Shamsianpour, M.; Sedghi, R.; Osati, S.; Safari, N., Oxidative polymerization of 3,4-ethylenedioxythiophene using transition-metal

tetrasulfonated phthalocyanine. *Reactive and Functional Polymers* **2010,** 70, (1), 75-80.

69. Huang, L.-M.; Chen, C.-H.; Wen, T.-C., Development and characterization of flexible electrochromic devices based on polyaniline and poly(3,4-ethylenedioxythiophene)-poly(styrene sulfonic acid). *Electrochimica Acta* **2006,** 51, (26), 5858-5863.

70. Dimitriev, O. P., Doping of polyaniline by transition metal salts: effect of metal cation on the film morphology. *Synthetic Metals* **2004,** 142, (1-3), 299-303.

71. MacDiarmid, A. G.; Epstein, A. J., Secondary doping in polyaniline. *Synthetic Metals* **1995,** 69, (1-3), 85-92.

72. Sun, L.; Liu, H.; Clark, R.; Yang, S. C., Double-strand polyaniline. *Synthetic Metals* **1997,** 84, (1-3), 67-68.

73. Mu, S., Poly(aniline-co-o-aminophenol) nanostructured network: Electrochemical controllable synthesis and electrocatalysis. *Electrochimica Acta* **2006,** 51, (17), 3434-3440.

74. Yang, G.; Hou, W.; Feng, X.; Xu, L.; Liu, Y.; Wang, G.; Ding, W., Nanocomposites of polyaniline and a layered inorganic acid host: Polymerization of aniline in the layers, conformation, and electrochemical studies. *Advanced Functional Materials* **2007,** 17, (3), 401-412.

75. Antoine, O.; Durand, R., In situ electrochemical deposition of Pt nanoparticles on carbon and inside Nafion. *Electrochemical and Solid-State Letters* **2001,** 4, (5) A55-A58.

76.   Decher, G., Fuzzy nanoassemblies: Toward layered polymeric multicomposites. *Science* **1997,** 277, (5330), 1232-1237.

77.   Cong, H.-P.; Yu, S.-H., Self-assembly of functionalized inorganic-organic hybrids. *Current Opinion in Colloid & Interface Science* **2009,** 14, (2), 71-80.

78.   Bhadra, S.; Khastgir, D.; Singha, N. K.; Lee, J. H., Progress in preparation, processing and applications of polyaniline. *Progress in Polymer Science* **2009,** 34, (8), 783-810.

79.   Choi, J.; Sauer, G.; Nielsch, K.; Wehrspohn, R. B.; Gösele, U., Hexagonally arranged monodisperse silver nanowires with adjustable diameter and high aspect ratio. *Chemistry of Materials* **2003,** 15, (3), 776-779.

80.   Sauer, G.; Brehm, G.; Schneider, S.; Nielsch, K.; Wehrspohn, R. B.; Choi, J.; Hofmeister, H.; Gösele, U., Highly ordered monocrystalline silver nanowire arrays. *Journal of Applied Physics* **2002,** 91, (5), 3243-3247.

81.   Wang, C.; Wang, Z.; Li, M.; Li, H., Well-aligned polyaniline nano-fibril array membrane and its field emission property. *Chemical Physics Letters* **2001,** 341, (5-6), 431-434.

82.   Wei, Z.; Zhang, Z.; Wan, M., Formation mechanism of self-assembled polyaniline micro/nanotubes. *Langmuir* **2002,** 18, (3), 917-921.

83.   Zhang, D.; Wang, Y., Synthesis and applications of one-dimensional nano-structured polyaniline: An overview. *Materials Science and Engineering B: Solid-State Materials for Advanced Technology* **2006,** 134, (1), 9-19.

84. Gu, M.; Zhang, J.; Li, Y.; Jiang, L.; Zhu, J.-J., Fabrication of a novel impedance cell sensor based on the polystyrene/polyaniline/Au nanocomposite. *Talanta* **2009,** 80, (1), 246-249.

85. Bryan, N. S., Nitrite in nitric oxide biology: Cause or consequence? A systems-based review. *Free Radical Biology and Medicine* **2006,** 41, (5), 691-701.

86. Guo, M.; Diao, P.; Cai, S., Hydrothermal growth of perpendicularly oriented ZnO nanorod array film and its photoelectrochemical properties. *Applied Surface Science* **2005,** 249, (1-4), 71-75.

87. Santos, W. J. R.; Lima, P. R.; Tanaka, A. A.; Tanaka, S. M. C. N.; Kubota, L. T., Determination of nitrite in food samples by anodic voltammetry using a modified electrode. *Food Chemistry* **2009,** 113, (4), 1206-1211.

88. Okonjo, K. O.; Iwuoha, E. I., Subunit iron spin heterogeneity in human aquomethemoglobin A. *Biochimica et Biophysica Acta (BBA)/Protein Structure and Molecular* **1986,** 873, (2), 304-307.

89. Mirvish, S. S., Role of N-nitroso compounds (NOC) and N-nitrosation in etiology of gastric, esophageal, nasopharyngeal and bladder cancer and contribution to cancer of known exposures to NOC. *Cancer Letters* **1995,** 93, (1), 17-48.

90. Nitrogen Cycle. http://www.physicalgeography.net/fundamentals/9s.html (12/09/2010)

91. Niedzielski, P.; Kurzyca, I.; Siepak, J., A new tool for inorganic nitrogen speciation study: Simultaneous determination of ammonium ion, nitrite and nitrate by ion chromatography with post-column ammonium derivatization by

Nessler reagent and diode-array detection in rain water samples. *Analytica Chimica Acta* **2006,** 577, (2), 220-224.

92.   Kuznetsov, V. V.; Zemyatova, S. V., Flow-injection spectrophotometry of nitrites based on the diazotization reactions of azine dyes. *Journal of Analytical Chemistry* **2007,** 62, (7), 637-644.

93.   Takiguchi, H.; Tsubata, A.; Miyata, M.; Odake, T.; Hotta, H.; Umemura, T.; Tsunoda, K. I., Liquid core waveguide spectrophotometry for the sensitive determination of nitrite in river water samples. *Analytical Sciences* **2006,** 22, (7), 1017-1019.

94.   Miyado, T.; Tanaka, Y.; Nagai, H.; Takeda, S.; Saito, K.; Fukushi, K.; Yoshida, Y.; Wakida, S. I.; Niki, E., Simultaneous determination of nitrate and nitrite in biological fluids by capillary electrophoresis and preliminary study on their determination by microchip capillary electrophoresis. *Journal of Chromatography A* **2004,** 1051, (1-2), 185-191.

95.   Dai, Z.; Liu, S.; Ju, H.; Chen, H., Direct electron transfer and enzymatic activity of hemoglobin in a hexagonal mesoporous silica matrix. *Biosensors and Bioelectronics* **2004,** 19, (8), 861-867.

96.   Larsen, L.H.; Damgaard, L. R.; Kjaer T.; Stenstrom T.; Lynggaard-Jensen A.; Revsbech N.P., Fast responding biosensor for on-line determination of nitrate/nitrite in activated sludge. *Water Research* **2000,** 34, 2463-2468.

97.   Dai, Z.; Bai, H.; Hong, M.; Zhu, Y.; Bao, J.; Shen, J., A novel nitrite biosensor based on the direct electron transfer of hemoglobin immobilized on CdS hollow nanospheres. *Biosensors and Bioelectronics* **2008,** 23, (12), 1869-1873.

98.   Zhao, G.; Jiang, T.; Gao, H.; Han, B.; Huang, J.; Sun, D., Mannich reaction using acidic ionic liquids as catalysts and solvents. *Green Chemistry* **2004,** 6, (2), 75-77.

99.   O'Shea, T. J.; Leech, D.; Smyth, M. R.; Vos, J. G., Determination of nitrite based on mediated oxidation at a carbon paste electrode modified with a ruthenium polymer. *Talanta* **1992,** 39, (4), 443-447.

100. Ko, W. Y.; Chen, W. H.; Cheng, C. Y.; Lin, K. J., Highly electrocatalytic reduction of nitrite ions on a copper nanoparticles thin film. *Sensors and Actuators, B: Chemical* **2009,** 137, (2), 437-441.

101. Moorcroft, M. J.; Davis, J.; Compton, R. G., Detection and determination of nitrate and nitrite: A review. *Talanta* **2001,** 54, (5), 785-803.

102. Dhaoui, W.; Zarrouk, H.; Pron, A., Spectroscopic properties of thin layers of sulfamic acid-doped polyaniline and their application to reagentless determination of nitrite. *Synthetic Metals* **2007,** 157, (13-15), 564-569.

103. Josephs, R. D.; Derbyshire, M.; Stroka, J.; Emons, H.; Anklam, E., Trichothecenes: reference materials and method validation. *Toxicology Letters* **2004,** 153, (1), 123-132.

104. Hussein, H. S.; Brasel, J. M., Toxicity, metabolism, and impact of mycotoxins on humans and animals. *Toxicology* **2001,** 167, (2), 101-134.

105. Papp, E.; H-Otta, K.; Záray, G.; Mincsovics, E., Liquid chromatographic determination of aflatoxins. *Microchemical Journal* **2002,** 73, (1-2), 39-46.

106. Zöllner, P.; Mayer-Helm, B., Trace mycotoxin analysis in complex biological and food matrices by liquid chromatography-atmospheric pressure ionisation mass spectrometry. *Journal of Chromatography A* **2006,** 1136, (2), 123-169.

107. Abbas, H. K.; Cartwright, R. D.; Xie, W.; Thomas Shier, W., Aflatoxin and fumonisin contamination of corn (maize, Zea mays) hybrids in Arkansas. *Crop Protection* **2006,** 25, (1), 1-9.

108. Oliveira, S. C. B.; Diculescu, V. C.; Palleschi, G.; Compagnone, D.; Oliveira-Brett, A. M., Electrochemical oxidation of ochratoxin A at a glassy carbon electrode and in situ evaluation of the interaction with deoxyribonucleic acid using an electrochemical deoxyribonucleic acid-biosensor. *Analytica Chimica Acta* **2007,** 588, (2), 283-291.

109. Valenta, H., Chromatographic methods for the determination of ochratoxin A in animal and human tissues and fluids. *Journal of Chromatography A* **1998,** 815, (1), 75-92.

110. Prieto-Simón, B.; Noguer, T.; Campàs, M., Emerging biotools for assessment of mycotoxins in the past decade. *TrAC Trends in Analytical Chemistry* **2008,** 26, (7), 689-702.

111. Prieto-Simón, B.; Campàs, M.; Marty, J.-L.; Noguer, T., Novel highly-performing immunosensor-based strategy for ochratoxin A detection in wine samples. *Biosensors and Bioelectronics* **2008,** 23, (7), 995-1002.

112. Bhat, R. V.; Vasanthi, S., Mycotoxin food safety risks in developing countries. Food Safety in Food Security and Food Trade. *Vision 2020 for Food, Agriculture and Environment, Focus* **2003,** 10, (brief 3 of 17), 1–2.

113. Wagacha, J. M.; Muthomi, J. W., Mycotoxin problem in Africa: Current status, implications to food safety and health and possible management strategies. *International Journal of Food Microbiology* **2008,** 124, (1), 1-12.

114. Turner, N. W.; Subrahmanyam, S.; Piletsky, S. A., Analytical methods for determination of mycotoxins: A review. *Analytica Chimica Acta* **2009,** 632, (2), 168-180.

115. Ringot, D.; Chango, A.; Schneider, Y. J.; Larondelle, Y., Toxicokinetics and toxicodynamics of ochratoxin A, an update. *Chemico-Biological Interactions* **2006,** 159, (1), 18-46.

116. World Health Organisation (WHO), Mycotoxins in African foods: implications to food safety and health. *AFRO Food Safety Newsletter. World Health Organization Food safety (FOS)* **2003**, (July 2006).

117. International Agency for Research on Cancer (IARC)., Ochratoxin A. *In: IARC Monographs on the Evaluation of Carcinogenic Risks to Humans; WHO, France.* **1993,** 56, 489-521.

118. Radi, A.-E.; Muñoz-Berbel, X.; Lates, V.; Marty, J.-L., Label-free impedimetric immunosensor for sensitive detection of ochratoxin A. *Biosensors and Bioelectronics* **2009,** 24, (7), 1888-1892.

119. Gautier, J.-C.; Holzhaeuser, D.; Markovic, J.; Gremaud, E.; Schilter, B.; Turesky, R. J., Oxidative damage and stress response from ochratoxin a exposure in rats. *Free Radical Biology and Medicine* **2001,** 30, (10), 1089-1098.

120. Schaaf, G. J.; Nijmeijer, S. M.; Maas, R. F. M.; Roestenberg, P.; de Groene, E. M.; Fink-Gremmels, J., The role of oxidative stress in the ochratoxin A-mediated toxicity in proximal tubular cells. *Biochimica et Biophysica Acta (BBA) - Molecular Basis of Disease* **2002,** 1588, (2), 149-158.

121. Creppy, E. E.; Kane, A.; Dirheimer, G., Lafarge-Frayssinet, C.; Mousset, S.; Frayssinet, C., Genotoxicity of ochratoxin a in mice: DNA single-strand break evaluation in spleen, liver and kidney. *Toxicology Letters* **1985,** 28, (1), 29-35.

122. Manderville, R.A.; Calcutt, W. M.; Dai J.; Park G.; Gillman I.G.; Noftle R.E.; Mohammed A.K.; Dizdaroglu M.; Rodriguez H.; Akman S.A., Stoichiometric preference in copper-promoted oxidative DNA damage by ochratoxin A. *Journal of Inorganic Biochemistry* **2003,** 95, 87-96.

123. Cramer, B.; Harrer, H.; Nakamura, K.; Uemura, D.; Humpf, H.-U., Total synthesis and cytotoxicity evaluation of all ochratoxin A stereoisomers. *Bioorganic & Medicinal Chemistry* **2010,** 18, (1), 343-347.

124. Adányi, N.; Levkovets, I. A.; Rodriguez-Gil, S.; Ronald, A.; Váradi, M.; Szendro, I.., Development of immunosensor based on OWLS technique for determining Aflatoxin B1 and Ochratoxin A. *Biosensors and Bioelectronics* **2007,** 22, (6), 797-802.

125. Alarcón, S. H.; Palleschi, G.; Compagnone, D.; Pascale, M.; Visconti, A., Barna-Vetró, I., Monoclonal antibody based electrochemical immunosensor for the determination of ochratoxin A in wheat. *Talanta* **2006,** 69, (4), 1031-1037.

126. Medical Research Council (MRC), Aflatoxin in peanut butter. *Science in Africa* **2006**.

127. Sibanda, L.; Marovatsanga, L. T.; Pestka, J. J., Review of mycotoxin work in sub-Saharan Africa. *Food Control* **1997,** 8, (1), 21-29.

128. Bankole, S. A.; Adenusi, A. A.; Lawal, O. S.; Adesanya, O. O., Occurrence of aflatoxin B1 in food products derivable from 'egusi' melon seeds consumed in southwestern Nigeria. *Food Control* **2010**, 21, (7), 974-976.

129. Dutton, M. F., Mycotoxin Research in South Africa. *Advances in Applied Microbiology* **2003**, 53, 213-241.

130. Muthomi, J. W.; Ndung'u, J. K.; Gathumbi, J. K.; Mutitu, E. W.; Wagacha, J. M., The occurrence of Fusarium species and mycotoxins in Kenyan wheat. *Crop Protection* **2008,** 27, (8), 1215-1219.

131. van Egmond, H.; Schothorst, R.; Jonker, M., Regulations relating to mycotoxins in food. *Analytical and Bioanalytical Chemistry* **2007,** 389, (1), 147-157.

132. Anklam, E.; Stroka, J.; Boenke, A.; Acceptance of analytical methods for implementation of EU legislation with a focus on mycotoxins. *Food Control* **2002,** 13, (3), 173-183.

133. Gilbert, J.; Anklam, E., Validation of analytical methods for determining mycotoxins in foodstuffs. *TrAC Trends in Analytical Chemistry* **2002,** 21, (6-7), 468-486.

134. Kuiper-Goodman, T., Mycotoxins: risk assessment and legislation. *Toxicology Letters* **1995,** 82-83, 853-859.

135. Liu, X.-P.; Deng, Y.-J.; Jin, X.-Y.; Chen, L.-G.; Jiang, J.-H.; Shen, G.-L.; Yu, R.-Q., Ultrasensitive electrochemical immunosensor for ochratoxin A using gold colloid-mediated hapten immobilization. *Analytical Biochemistry* **2009,** 389, (1), 63-68.

136. Chen, W.-C.; Wen, T.-C.; Hu, C.-C.; Gopalan, A., Identification of inductive behavior for polyaniline via electrochemical impedance spectroscopy. *Electrochimica Acta* **2002,** 47, (8), 1305-1315.

137. Khan, R.; Dhayal, M., Nanocrystalline bioactive TiO_2-chitosan impedimetric immunosensor for ochratoxin-A. *Electrochemistry Communications* **2008,** 10, (3), 492-495.

138. Tang, D.; Yuan, R.; Chai, Y.; Fu, Y.; Dai, J.; Liu, Y.; Zhong, X., New amperometric and potentiometric immunosensors based on gold nanoparticles/tris(2,2'-bipyridyl)cobalt (III) multilayer films for hepatitis B surface antigen determinations. *Biosensors and Bioelectronics* **2005,** 21, (4), 539-548.

139. Ouerghi, O.; Touhami, A.; Jaffrezic-Renault, N.; Martelet, C.; Ouada, H. B.; Cosnier, S., Impedimetric immunosensor using avidin-biotin for antibody immobilization. *Bioelectrochemistry* **2002,** 56, (1-2), 131-133.

140. Kaushik, A.; Solanki, P. R.; Ansari, A. A.; Ahmad, S.; Malhotra, B. D., Chitosan-iron oxide nanobiocomposite based immunosensor for ochratoxin-A. *Electrochemistry Communications* **2008,** 10, (9), 1364-1368.

141. Tully, E.; Higson, S. P.; O'Kennedy, R., The development of a 'labeless' immunosensor for the detection of Listeria monocytogenes cell surface protein, Internalin B. *Biosensors and Bioelectronics* **2008,** 23, (6), 906-912.

142. Muchindu, M.; Iwuoha, E.; Pool, E.; West, N.; Jahed, N.; Baker, P.; Waryo, T.; Williams, A., Electrochemical ochratoxin A immunosensor developed on sulphonated polyaniline. *Electronalysis* **2011,** 23, (1), 122-128.

143.   Owino, J.; Ignaszak, A.; Al-Ahmed, A.; Baker, P.; Alemu, H.; Ngila, J.; Iwuoha, E., Modelling of the impedimetric responses of an aflatoxin B1 immunosensor prepared on an electrosynthetic polyaniline platform. *Analytical and Bioanalytical Chemistry* **2007,** 388, (5), 1069-1074.

144.   Foulds, N. C.; Lowe, C. R., Enzyme entrapment in electrically conducting polymers. Immobilisation of glucose oxidase in polypyrrole and its application in amperometric glucose sensors. *Journal of the Chemical Society, Faraday Transactions 1: Physical Chemistry in Condensed Phases* **1986,** 82, (4), 1259-1264.

145.   Sadik, O. A.; Wallace, G. G., Pulsed amperometric detection of proteins using antibody containing conducting polymers. *Analytica Chimica Acta* **1993,** 279, (2), 209-212.

146.   Schuhmann, W.; Lehn, C.; Schmidt, H. L.; Gründig, B., Comparison of native and chemically stabilized enzymes in amperometric enzyme electrodes. *Sensors and Actuators: B. Chemical* **1992,** 7, (1-3), 393-398.

147.   Gun, J.; Lev, O., Sol-gel derived, ferrocenyl-modified silicate-graphite composite electrode: Wiring of glucose oxidase. *Analytica Chimica Acta* **1996,** 336, (1-3), 95-106.

148.   Trojanowicz, M.; vel Krawczyk, K. T.; Electrochemical biosensors based on enzymes immobilized in electropolymerized films. *Mikrochimica Acta* **1995,** 121, (1-4), 167-181.

149.   Padoa, C. J.; Crowther, N. J., Engineered antibodies: A new tool for use in diabetes research. *Diabetes Research and Clinical Practice* **2006,** 74, (2 SUPPL.).

150. Conroy, P. J.; Hearty, S.; Leonard, P.; O'Kennedy, R. J., Antibody production, design and use for biosensor-based applications. *Seminars in Cell & Developmental Biology* **2009,** 20, (1), 10-26.

151. Rodi, D. J.; Soares, A. S.; Makowski, L., Quantitative Assessment of Peptide Sequence Diversity in M13 Combinatorial Peptide Phage Display Libraries. *Journal of Molecular Biology* **2002,** 322, (5), 1039-1052.

152. Luppa, P. B.; Sokoll, L. J.; Chan, D. W., Immunosensors--principles and applications to clinical chemistry. *Clinica Chimica Acta* **2001,** 314, (1-2), 1-26.

153. Sadik, O. A.; Wallace, G. G., Effect of polymer composition on the detection of electroinactive species using conductive polymers. *Electroanalysis* **1993,** 5, (7), 555-563.

154. Pournaras, A. V.; Koraki, T.; Prodromidis, M. I., Development of an impedimetric immunosensor based on electropolymerized polytyramine films for the direct detection of Salmonella typhimurium in pure cultures of type strains and inoculated real samples. *Analytica Chimica Acta* **2008,** 624, (2), 301-307.

155. Pejcic, B.; De Marco, R., Impedance spectroscopy: Over 35 years of electrochemical sensor optimization. *Electrochimica Acta* **2006,** 51, (28), 6217-6229.

156. Guilbault, G. G.; Pravda, M.; Kreuzer, M.; O'Sullivan, C. K., Biosensors - 42 Years and counting. *Analytical Letters* **2004,** 37, (8), 1481-1496.

157. Meadows, D., Recent developments with biosensing technology and applications in the pharmaceutical industry. *Advanced Drug Delivery Reviews* **1996,** 21, (3), 179-189.

158. Warsinke, A.; Benkert, A.; Scheller, F. W., Electrochemical immunoassays. *Fresenius' Journal of Analytical Chemistry* **2000,** 366, (6-7), 622-634.

159. Alfonta, L.; Bardea, A.; Khersonsky, O.; Katz, E.; Willner, I., Chronopotentiometry and Faradaic impedance spectroscopy as signal transduction methods for the biocatalytic precipitation of an insoluble product on electrode supports: Routes for enzyme sensors, immunosensors and DNA sensors. *Biosensors and Bioelectronics* **2001,** 16, (9-12), 675-687.

160. Guan, J. G.; Miao, Y. Q.; Zhang, Q. J., Impedimetric biosensors. *Journal of Bioscience and Bioengineering* **2004,** 97, (4), 219-226.

161. Katz, E.; Willner, I., Probing biomolecular interactions at conductive and semiconductive surfaces by impedance spectroscopy: Routes to impedimetric immunosensors, DNA-sensors, and enzyme biosensors. *Electroanalysis* **2003,** 15, (11), 913-947.

162. Bordi, F.; Cametti, C.; Gliozzi, A., Impedance measurements of self-assembled lipid bilayer membranes on the tip of an electrode. *Bioelectrochemistry* **2002,** 57, (1), 39-46.

163. Chaki, N. K.; Vijayamohanan, K., Self-assembled monolayers as a tunable platform for biosensor applications. *Biosensors and Bioelectronics* **2002,** 17, (1-2), 1-12.

164. Chou, H. A.; Zavitz, D. H.; Ovadia, M., In vivo $CH_3(CH_2)_{11}SAu$ SAM electrodes in the beating heart: In situ analytical studies relevant to pacemakers and interstitial biosensors. *Biosensors and Bioelectronics* **2003,** 18, (1), 11-21.

165.   Yin, P.; Burns, C. J.; Osman, P. D. J.; Cornell, B. A., A tethered bilayer sensor containing alamethicin channels and its detection of amiloride based inhibitors. *Biosensors and Bioelectronics* **2003,** 18, (4), 389-397.

166.   Cheng, T. J.; Lin, T. M.; Chang, H. C., Physical adsorption of protamine for heparin assay using a quartz crystal microbalance and electrochemical impedance spectroscopy. *Analytica Chimica Acta* **2002,** 462, (2), 261-273.

167.   Mimica, D.; Ringuedé, A.; Agurto, C.; Bedioui, F.; Zagal, J., Biomimetic electroreduction of O_2 by hemoglobin in a surfactant film: Preliminary electrochemical impedance spectroscopy insight. *Electroanalysis* **2004,** 16, (19), 1632-1636.

168.   Zhao, G. C.; Zhang, L.; Wei, X. W.; Yang, Z. S., Myoglobin on multi-walled carbon nanotubes modified electrode: Direct electrochemistry and electrocatalysis. *Electrochemistry Communications* **2003,** 5, (9), 825-829.

169.   Marco, M. P.; Gee, S.; Hammock, B. D., Immunochemical techniques for environmental analysis I. Immunosensors. *Trends in Analytical Chemistry* **1995,** 14, (7), 341-350.

170.   Patel, P. D., (Bio)sensors for measurement of analytes implicated in food safety: a review. *TrAC Trends in Analytical Chemistry* **2002,** 21, (2), 96-115.

171.   Prodromidis, M. I., Impedimetric immunosensors-A review. *Electrochimica Acta* **2010,** 55, (14), 4227-4233.

172.   Bataillard, P.; Gardies, F.; Jaffrezic-Renault, N.; Martelet, C.; Colin, B.; Mandrand, B., Direct detection of immunospecies by capacitance measurements. *Analytical Chemistry* **1988,** 60, (21), 2374-2379.

173. Gehring, A. G.; Patterson, D. L.; Tu, S. I., Use of a light-addressable potentiometric sensor for the detection of Escherichia coli O157:H7. *Analytical Biochemistry* **1998,** 258, (2), 293-298.

174. Ahuja, T.; Mir, I. A.; Kumar, D.; Rajesh, Biomolecular immobilization on conducting polymers for biosensing applications. *Biomaterials* **2007,** 28, (5), 791-805.

175. Dicks, J. M.; Cardosi, M. F.; Turner, A. P. F.; Karube, I., The application of ferrocene-modified n-type silicon in glucose biosensors. *Electroanalysis* **1993,** 5, (1), 1-9.

176. Rajesh; Bisht, V.;Takashima, W.; Kaneto, K., An amperometric urea biosensor based on covalent immobilization of urease onto an electrochemically prepared copolymer poly (N-3-aminopropyl pyrrole-co-pyrrole) film. *Biomaterials* **2005,** 26, (17), 3683-3690.

177. Gooding, J. J., Electrochemical DNA hybridization biosensors. *Electroanalysis* **2002,** 14, (17), 1149-1156.

178. Palecek, E., Past, present and future of nucleic acids electrochemistry. *Talanta* **2002,** 56, (5), 809-819.

179. Wang, J., Electrochemical nucleic acid biosensors. *Analytica Chimica Acta* **2002,** 469, (1), 63-71.

180. Brett, C. M. A.; Oliveira Brett, A. M.; Serrano, S. H. P., EIS study of DNA-modified electrodes. *Electrochimica Acta* **1999,** 44, (24), 4233-4239.

181. Filipe, O. M. S.; Brett, C. M. A., Characterization of carbon film electrodes for electroanalysis by electrochemical impedance. *Electroanalysis* **2004,** 16, (12), 994-1001.

182. Krishna, G.; Schulte, J.; Cornell, B. A.; Pace, R.; Wieczorekt, L.; Osman, P. D., Tethered bilayer membranes containing ionic reservoirs: The interfacial capacitance. *Langmuir* **2001,** 17, (16), 4858-4866.

183. Cornell, B. A.; Braach-Maksvytis, V. L. B.; King, L. G.; Osman, P. D. J.; Raguse, B.; Wieczorek, L.; Pace, R. J., A biosensor that uses ion-channel switches. *Nature* **1997,** 387, (6633), 580-583.

CHAPTER 3

EXPERIMENTAL

This chapter consists of materials and experimental procedures for the electrochemical synthesis of polyaniline doped with poly(vinylsulphonate), layer-by-layer desoption of amine- and sulphate-modified polystyrene latex beads, ultraviolet-visible spectroscopy and scanning electron microscopy characterization and application of the modified polyaniline nano-composites in detection of nitrites and Ochratoxin A.

3.1 Reagents

Aniline (99%), purchased from Aldrich was vacuum distilled and stored frozen under nitrogen. Two types of polystyrene nanoparticles (PS_{NP}) surface functionalized with amine ($PS_{NP}-NH_2$) and sulphate ($PS_{NP}-OSO_3^-$) groups, respectively, with mean particles sizes of 100 nm were obtained as 2.5% (w/v) aqueous suspensions from Sigma. Poly(sodium-4-styrene-sulfonate) ($PS-SO_3^-Na^+$, M_w ca.70000), poly(diallyldimethyl-ammonium chloride) (PDDA, low molecular weight, 20% weight in water) and poly(vinylsulfonic acid sodium salt) ($PV-SO_3^-$, 25 wt% in water) were purchased from Aldrich. Standard nitrite aqueous solutions were prepared daily in 0.1 M Na_2SO_4. Ochratoxin A (OTA) from *Aspergillus ochraceus* received from Sigma-aldrich, USA (product code 01877-5MG) was dissolved in ethanol at 1 mg/mL and stored as aliquots in tightly sealed vials at -20 ºC. A polyclonal antibody of ochratoxin A from *Aspergillus ochraceus* conjugated to Bovine serum albumin (BSA) was supplied by Acris antibodies, Germany (catalog number BP666). The antibody contained 5 mg of total protein per

millilitre and was quoted as specific to OTA having cross-reactivity with OTA (100%), OTB (1%) and BSA-absorbed (< 0.1%) in 0.1 M phosphate buffered saline (PBS) solution containing 0.09% NaN_3 as a preservative. The antibody was also aliquoted and stored at −20 °C until use. ELISA kit and certified corn, wheat and coffee reference material were purchased from RIDASCREEN[®]. All electrochemical measurements for OTA were carried out in 0.1 M phosphate-buffered saline. Basic salts including, NaH_2PO_4, Na_2HPO_4 and KCl used in the preparation of 0.1 M PBS containing 0.1 M KCl at pH 7.2 were received from Sigma (SA). All other chemicals were of analytical grade, and Milli-Q water (resistance over 18 MΩ cm) from a Millipore Q water purification system was used throughout.

3.2 Instrumentation

Voltammetric and amperometric experiments were recorded with BASi 100B electrochemical work station (LG Fayette) using the conventional three-electrode system. For electropolymerization of aniline, the working electrodes used were screen printed carbon (SPCE) (diameter 3.0 mm), glassy carbon (GCE) (diameter 3.0 mm) electrodes and platinum (diameter 1.0 mm) while a platinum mesh or wire and a silver/silver chloride (3 M NaCl type) electrode (Bioanalytical Systems Ltd., UK) were used as counter electrode and reference electrode, respectively. Electrochemical impedance spectroscopy of the PANI modified electrodes was measured with a Voltalab instrument (Radiometer Analytical, France). Impedance measurements were performed in the frequency range from 100 kHz to 50 mHz at 0 V, which was found to have the least

impedance after potential step from 0 to 800 mV. The AC amplitude was 5 mV. The ultraviolet-visible spectra of the PANI and PANI|PS$_{NP}$ films were determined using a GBC UV-visible 920 spectrometer. The modified SPCEs were used for scanning electron microscopy (SEM) studies while the modified GCEs were used for the detection of NO$_2^-$, using the same reference electrode and counter electrode. SEM images were taken with a Hitachi S3000N scanning electron microscope. An acceleration voltage of 20 kV was employed at various magnifications. Gold sputtering of the SEM samples was done using a SC7640 Auto/Manual high resolution super coater (Quorum Technology Ltd., England) at a voltage of 2 kV and plasma current of 25 mA for one minute. Surface morphology of the SPCE in buffer was studied with atomic force spectroscopy (AFM) tapping mode Veeco NanoMan V model with silicon tip using spring constant of 1-5 N/m and resonance frequency of 60-100 kHz. Alumina micro-polish (1.0, 0.3 and 0.05 mm alumina slurries) and polishing pads (Buehler, IL, USA) were used for polishing the electrode.

3.3 Preparation of electrodes

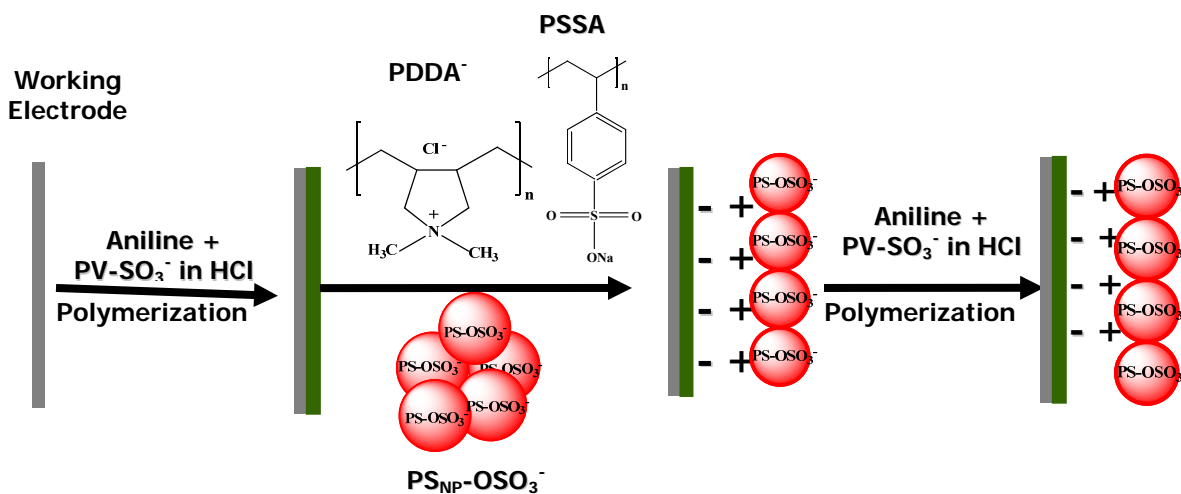### 3.3.1 Polyaniline-poly(vinylsulphonate) (PANI-PV-SO$_3^-$)

Before the electro-synthesis of PANI-PV-SO$_3^-$ on the working electrode surfaces (GCE, SPCE or Pt), electrodes were preconditioned as follows: the Pt WE and GCE were first polished using 0.3 and 0.05 mm alumina slurries and then rinsed with distilled water. Hydrophilic sites on the GCE and SPCE were electrochemically activated in 0.2 M

H_2SO_4 using two cycles of cyclic voltammetry (CV) between -1200 and +1500 mV at a scan rate of 100 mV/s after briefly rinsing with water[1, 2]. The electropolymerization solution was prepared by mixing 1.0 M HCl (3.9 mL), 0. 2 M distilled aniline (93 µL) and PV-SO_3^- (1.0 mL); and the mixture was degassed with nitrogen for 10 min before electropolymerization. Doped aniline was polymerized on the surfaces of the Pt, GCE and SPCE by scanning the working electrode potential between -200 and +1100 mV for 10 cycles at a scan rate of 100 mV/s. The PANI-modified Pt, GCE and SPCE thus prepared are hence denoted as Pt|PANI, GCE|PANI and SPCE|PANI, respectively.

3.3.2 Electrostatic layer by layer preparation of PANI-PV-SO_3^- electrodes templated with sulphate modified polystyrene (PS_{NP}-SO_3^-)

Polyaniline-polystyrene nanocomposites were fabricated via the layer-by-layer electrostatic adsorption strategy according a procedure described by Luo, et al.[3] A PANI film-modified electrode was first dipped into a solution of the PS-$SO_3^-$$Na^+$ (5.0 mg mL^{-1}), then into a solution of the PDDA (5.0 mg mL^{-1}), and finally into an aqueous suspension of the PS_{NP}-OSO_3^- (0.1% (w/v) for 30 min, 30 min and 1 h, respectively. Each step was followed by a thorough rinse of the resulting layer with water in order to remove any excess polyelectrolyte that had not been adsorbed. Scheme 3.1 shows a proposed mechanism for polymerisation of aniline on PS_{NP}- SO_3^- template.

Scheme 3.1: Electropolymerisation of 0.2 M aniline and layer by layer self-assembly of negatively charged PS_{NP}-OSO_3^-.

3.3.3 Electrostatic layer by layer preparation of PANI-PV-SO_3^- electrodes templated with amine modified polystyrene (PS_{NP}-NH_2)
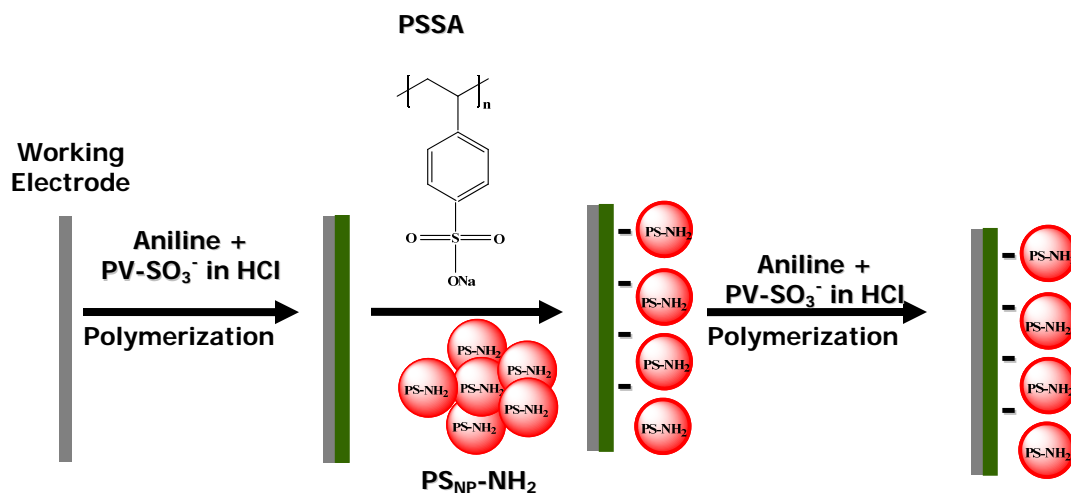
Similarly, a separate PANI-modified electrode was coated with amine-functionalized polystyrene beads (PS_{NP}-NH_2) used without the PDDA adsorption step discussed in Section 3.3.2 and replacing the PS_{NP}-OSO_3^- suspension with a suspension of the PS_{NP}-NH_2. Scheme 3.2 shows a proposed mechanism for polymerisation of aniline on PS_{NP}-NH_2 template.

Scheme 3.2 Proposed electropolymerisation of 0.2 M aniline and layer by layer self assembly of PS_{NP}-NH_2 template.

The assumption behind this strategy was that, the first steps would convert the PANI surface into a robust polyanionic composite platform and the nanoparticles would electrostatically self-assemble on the preceding oppositely charged layer of PS-SO_3^- or PDDA. The resulting layer-by-layer constructed nanocomposite systems on the working electrodes, (SPCE, GCE and Pt), at this stage was represented as PANI|PS_{NP}-OSO_3^- and PANI|PS_{NP}-NH_2 (omitting the electrodes and interceding polyionic interlinks). A final layer (1 CV) of PANI was electropolymerised onto the PANI|PS_{NP}-SO_3^- and PANI|PS_{NP}-NH_2 at a scan rate of 50 mV/s. The intention of this final step was to cover the outer most surface of the modified electrode with a thin layer of nanostructured PANI. Henceforth, we shall denote the resulting nanocomposite systems as PANI|PS_{NP}-OSO_3^-|PANI and PANI|PS_{NP}-NH_2|PANI. Electrochemical behaviour of PANI and PANI|PS_{NP}-OSO_3^-|PANI

and PANI|PS$_{NP}$-NH$_2$|PANI nanocomposite structures were studied in 0.1 M HCl and 0.1 M PBS solutions by cyclic voltammetry at 100 mV/s from -200 to 1100 mV.

3.3.4 Application of polyaniline-polystyrene nanocomposite electrodes as amperometric nitrite nanosensor

The three different electrodes, GCE|PANI, GCE|PANI|PS$_{NP}$-SO$_3$$^-$|PANI and GCE|PANI|PS$_{NP}$-NH$_2$|PANI were tested for amperometric sensing of nitrite. Amperometric determination of nitrite was carried out at an applied potential of +50 mV under magnetic stirring in aqueous 0.1 M HCl solution as the supporting electrolyte. Nitrite standards were prepared daily from sodium nitrite stock solutions by appropriate dilutions in 0.1 M Na$_2$SO$_4$ as nitrites are unstable at low pH[4]. The background current was allowed to reach steady value before aliquots of standard nitrite solutions were spiked successively into the supporting electrolyte. The steady-state current values were recorded as the response. All experiments were carried out at room temperature.

3.3.5 pH, interference studies and application in rainwater

The pH range of the nitrite test solutions were adjusted with 1 M HCl. For the interference studies; K$^+$, Mg^{2+}, Na$^+$, NH$_4$$^+$, Cl$^-$, SO$_4$$^{2-}$ and NO$_3$$^-$ ions were dissolved in distilled water and each was added to 50 μM NO$_2$$^-$ acidic solution. The applicability of these nanosensors in determining NO$_2$$^-$ in a natural sample was demonstrated in rainwater collected in an open space outside the chemistry department, UWC. The pH of the

rainwater samples was on average found to be 6.0. It was adjusted to pH 1 by adding a few drops of concentrated HCl. Different standard concentrations of NO_2^- were added to 5 ml aliquots of rain water. The water was then analysed without any further pre-treatment by amperometry at 50 mV.

3.4 Procedure for the 2-D gel protein electrophoresis

BioRad strip (7 cm) immobilized pH gradient (IPG) strip (pH 4-7) was rehydrated passively overnight at room temperature with a total sample volume of 125 μL; containing 150 μg equivalent polyclonal ochratoxin A antibody sample, 1.25 μL Ampholyte (pH 3-10) and made up to 125 μL with urea buffer (9M urea, 2M thiourea, 4% 3-[(3-cholamidopropyl)dimethylammonio]-1-propanesulfonate (CHAPS), 0.002% bromophenol blue, 0.08% dithiothreitol (DTT)). The IPG strip was covered with mineral oil to prevent dehydration. The resultant hydrated strip was run on Amersham Biosciences Ettan IPGphor II in a three stepwise programmed run; step 1: 250 V for 0.15 hr, Step 2: 3500 V for 3800 Vhr, Step 3: 4200 V for 4600 Vhr. The IPG strip was then equilibrated, reduced and alkylated with urea equilibration buffer (50 nM Tris-HCl pH 8.8, 6 M Urea, 30% glycerol, 2% SDS, 0.002% bromophenol blue), in the first instance with 2% DTT added, and secondly with 2.5% iodoacetic acid, with shaking for 10mins each respectively, after which the strip was transferred to 12% SDS polyacrylamide gel and run in the second dimension. The strip was initially run at 50 V until the dye from the agarose sealing gel had migrated into the resolving gel. The voltage was then changed to 100 V until the dye front just runs out of the base of the gel.

3.5 Ochratoxin A antibody immobilization

The three different modified electrodes, PANI, PANI|PS$_{NP}$-OSO$_3^-$|PANI and PANI|PS$_{NP}$-NH$_2$|PANI were transferred to a 2 mL cell. The surface of the polymer nanocomposite was reduced in 2 mL PBS at -500 mV versus Ag/AgCl for 600 s. The polyclonal OTA antibody was diluted to 10 µg/mL in PBS prior to use. After reduction was complete, PBS was removed from the cell and replaced with the negatively charged OTA antibody solution. Oxidation was performed at 700 mV versus Ag/AgCl for 600 s. During oxidation, the antibody was electrostatically attached to the polymer surface. The antibody solution was then carefully removed from the cell and the immobilized electrode denoted as Pt|PANI|anti-OTA, Pt|PANI|PS$_{NP}$-OSO$_3^-$|PANI|anti-OTA and Pt|PANI|PS$_{NP}$-NH$_2$|PANI|anti-OTA were left for 15 min in blank buffer solution, standard buffer solution of OTA or buffer solution of the extracts of certified reference materials, before making electrochemical measurements.

3.6 Extraction of OTA from certified corn, wheat and coffee reference material

Preparation of ground certified corn, wheat and coffee reference material involved the weighing out of 1 g of the sample which was then added to 50 mL centrifuge screw cap vials with 20 mL of 0.13 M sodium hydrogen carbonate buffer. The solution was shaken vigorously for 15 min and centrifuged for 15 min at 3500 rpm and the supernatant was extracted through a filter paper. 4 µL of the filtrate was diluted with 2 mL PBS solution in the electrochemical cell for EIS measurements of OTA.
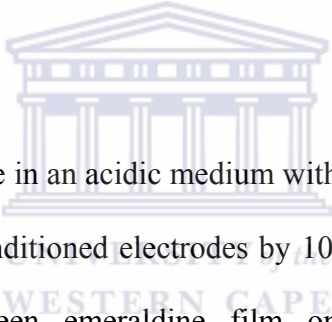
References

1. Grennan, K.; Killard, A. J.; Smyth, M. R., Physical characterizations of a screen-printed electrode for use in an amperometric biosensor system. *Electroanalysis* **2001,** 13, (8-9), 745-750.

2. Maruyama, J.; Abe, I., Influence of anodic oxidation of glassy carbon surface on voltammetric behavior of Nafion®-coated glassy carbon electrodes. *Electrochimica Acta* **2001,** 46, (22), 3381-3386.

3. Luo, X.; Vidal, G.; Killard, A.; Morrin, A.; Smyth, M., Nanocauliflowers: A Nanostructured Polyaniline-Modified Screen-Printed Electrode with a Self-Assembled Polystyrene Template and Its Application in an Amperometric Enzyme Biosensor. *Electroanalysis* **2007,** 19, (7-8), 876-883.

4. Malone, M. M.; Doherty, A. P.; Smyth, M. R.; Vos, J. G., Flow injection amperometric determination of nitrite at a carbon fibre electrode modified with the polymer [Os(bipy)$_2$(PVP)$_{20}$Cl]Cl. *Analyst* **1992,** 117, (8), 1259-1263.

CHAPTER 4

PART 1-RESULTS AND DISCUSSION: FABRICATION OF CHEMOSENSORS FOR NITRITE

This chapter presents results and discussion on the electrochemical synthesis, characterization and application in nitrite determination in rainwater on polyaniline and its amine- and sulphate- modified polystyrene nanocomposites. Ultraviolet-visible spectroscopy, scanning electron microscope morphology and electrochemistry of the poly(vinylsulphonate) doped PANI nanocomposites are discussed.

4.1 Polymerisation of aniline

Electropolymerisation of aniline in an acidic medium with $PV-SO_3^-$ as dopant was carried out at 100 mV/s on the pre-conditioned electrodes by 10 cyclic voltammograms (Figure 4.1). This resulted in a green emeraldine film on the electrode surface. The polymerisation reaction was initiated by the formation of resonance-stabilised aniline radical cations from the protonated aniline monomer[1].The polymerisation current increased as the number of cyclic voltamograms increased confirming that the polymer was conducting. The polymer thickness increased with successive potential cycles[2]. A homogenous film was produced after the 10 cyclic voltamograms[1]. There anodic peaks and cathodic peaks were observed as shown in Figure 4.1. Similar voltamograms have been reported by other researchers for the polymer in acid media[1, 3-7]. The peak characteristics depend on the type and concentration of the acid. The first redox peak is leucoemeraldine/leucoemeraldine radical cation (A/A')[5, 7]. Peaks B/B' are emeraldine

radical cation/emeraldine and the final redox peak is the pernigraniline radical cation/pernigraniline (C/C'). From the experimental design, voltammograms represent the electrochemical behaviour of the PANI composite at a high potential scan rate, 100 mV/s in this case. Studies carried out by Iwouha, *et al.*,[2] at varying scan rates proved that the polymer was electroactive and the diffusion of electrons took place along the polymer chain.
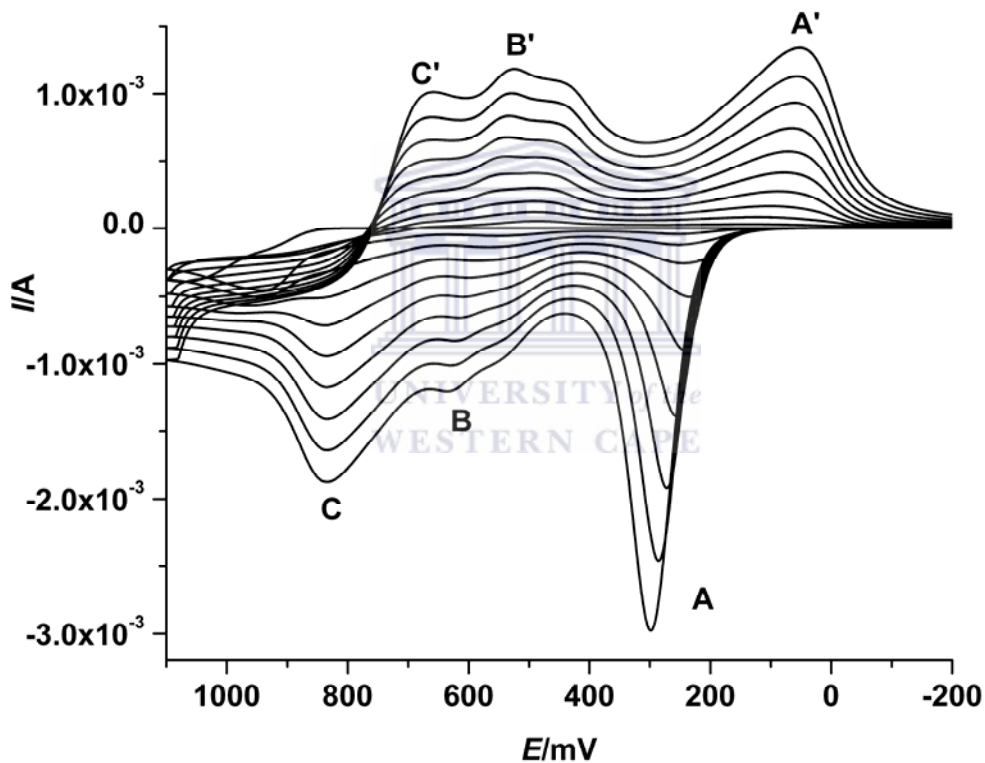

Figure 4.1: Electropolymerisation of aniline by cyclic voltammetry.

Other researchers[8] showed that the first anodic peak was a one electron transfer process in which leucoemaraldine is oxidised to leucoemeraldine radical. The prominence of the leucoemaraldine cation radical at the anodic peak and emeraldine at the cathodic peak

indicated that the growth of PANI film and its reversible electrochemistry. It has been reported[1] that polymer films grown at other scan rates exhibit slower electron transfer rates than films grown at 100mV/s.

4.2 Layer-by-layer assembly and scanning electron microscope (SEM) characterisation of PANI, PANI|PS$_{NP}$-NH$_2$ and PANI|PS$_{NP}$-SO$_3^-$ electrodes

Figure 4.2 shows SEM images of the bare and PANI modified electrodes. Clusters of the carbon paste for the bare SPCE were evident in Figure 4.2(a). Aggregates of sponge-like, nodular porous-structured PANI on the surface of the SPCE|PANI electrode were observed under SEM at 50000X magnification as shown in Figure 4.2 (b). These PANI clusters varied in size, from 100-500 nm.
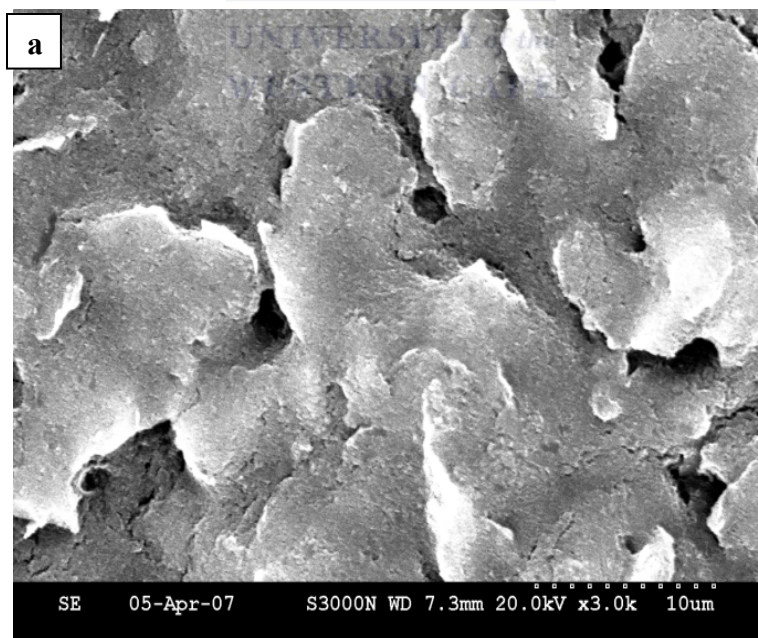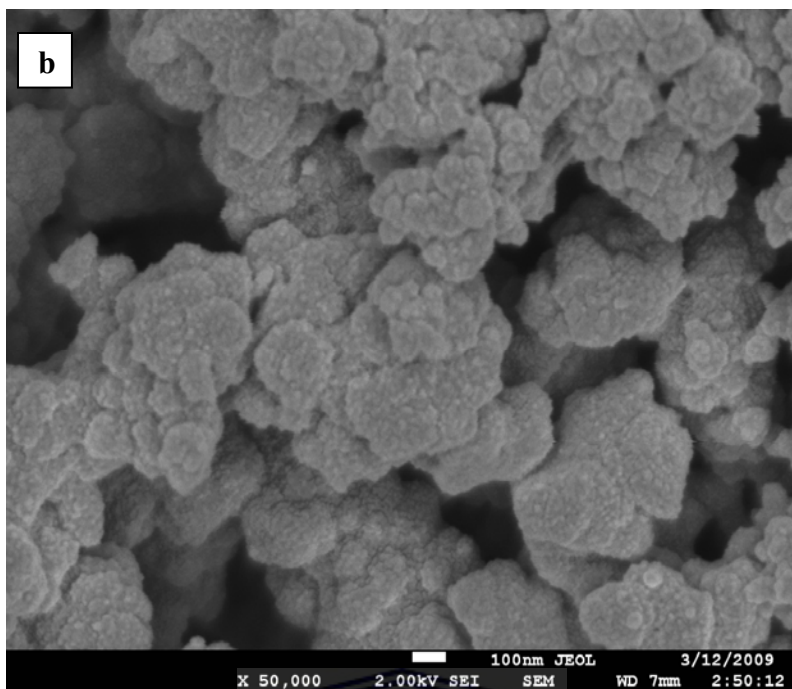

Figure 4.2: (a) SEM images of SPCE at 3000X.

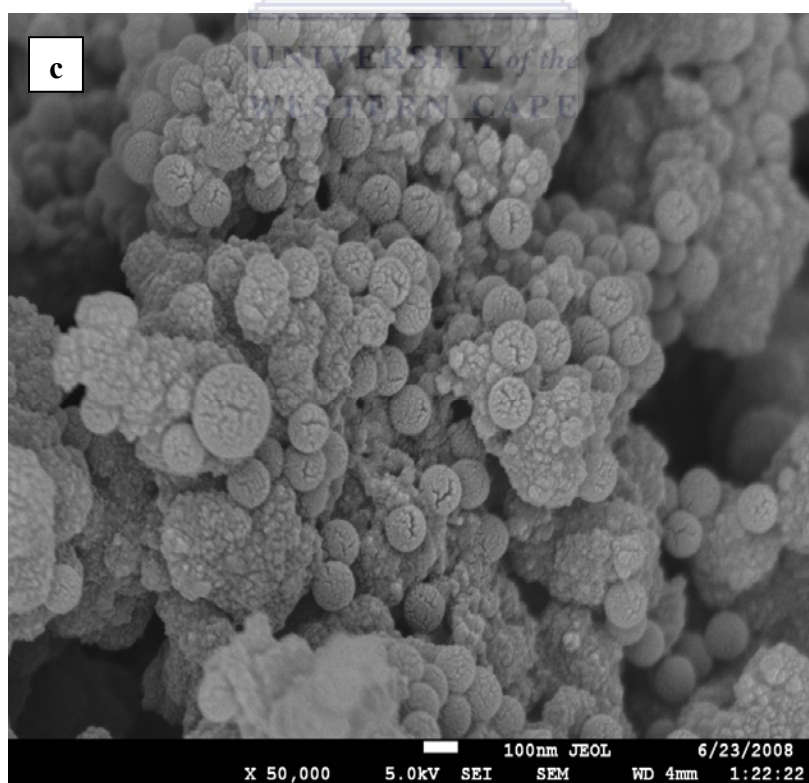Figure 4.2: (b) SPCE|PANI at 50000X.
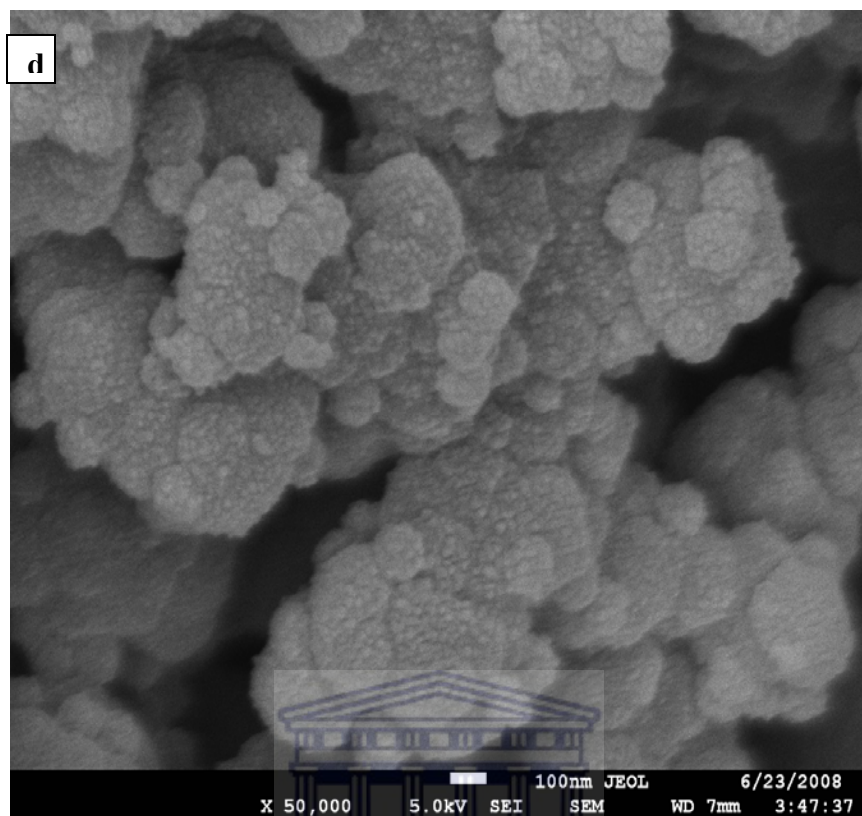

Figure 4.2: (c) SPCE|PANI| PS$_{NP}$-NH$_2$| at 50000X.

91

Figure 4.2: (d) SPCE|PANI| PS_{NP}-OSO_3^- |PANI at 50000X.

Addition of polyelectrolytes, poly(sodium 4-styrene-sulfonate) (PS-SO_3^-) and poly(diallydiminethylammonium chloride) (PDDA), adsorbed on the poly(vinylsulphonate) (PV-SO_3^-) doped PANI film did not show any difference when compared to the images of SPCE|PANI in Figure 4.2(b). Positively charged, amine-modified polystyrene (PS_{NP}-NH_2) latex beads of 100 nm were self-assembled onto the prepared PANI film followed by a final layer of PANI incorporated by CV as depicted in Scheme 3.2. This LbL composite, SPCE|PANI|PS_{NP}-NH_2^-|PANI, resulted in a cauliflower like nano-composite structure of about 100 nm in size as shown in Figure 4.2(c). For the negatively charged sulphate-modified polystyrene beads (PS_{NP}-OSO_3^-) self assembly on SPCE|PANI surface adsorbed with PS-SO_3^- and PDDA polyelectrolytes and a final layer

92

of PANI on the negatively charged PS_{NP} beads (Scheme 3.1), a well defined nanocauliflower structure in the SEM images in Figure 4.2(d) can also be observed. The 100 nm beads are visible in Figure 4.2(b), (c) and (d) at 50 000 magnification within the PANI clusters. A similar LbL approach has also been reported[9, 10].

4.3 Characterisation of PANI, PANI|PS_{NP}-NH_2 and PANI|PS_{NP}-SO_3^-

In Figure 4.3 at scan rates above 50 mV/s in 1 M HCl, the distinct emeraldine and leucoemeraldine peaks could not be seen, but rather a single broad anodic and cathodic peak due to the incorporation of the dopant and PS_{NP} templates was observed. The redox couple in Figure 4.3 has a formal potential of approximitely 500 mV. The couple can be explained as resulting from the merging of the emeraldine and leucoemeraldine peaks. Using this couple, the surface concentration, Γ^* of PANI, PANI|PS_{NP}-NH_2 and PANI|PS_{NP}-OSO_3^- films were estimated from a plot of peak current, I_p against scan rate, υ in accordance with Brown-Anson equation[11]:

$$\frac{I_p}{\upsilon} = \frac{n^2 F^2 A \Gamma^*}{4RT} \qquad \text{Equation 4.1}$$

where n is the number of electrons transferred F, is the Faraday constant (96500 C/mol), A is the area of the electrode (0.071 cm^2), R, is the gas constant (8.314 J/mol/K) and T (K) is the absolute temperature of the system.

The surface concentration of PANI, PANI|PS_{NP}-NH_2 and PANI|PS_{NP}-OSO_3^- films was estimated to be 2.66 x 10^{-8}, 3.07 x 10^{-8} and 2.36 x 10^{-8} mol cm^{-2}, respectively.
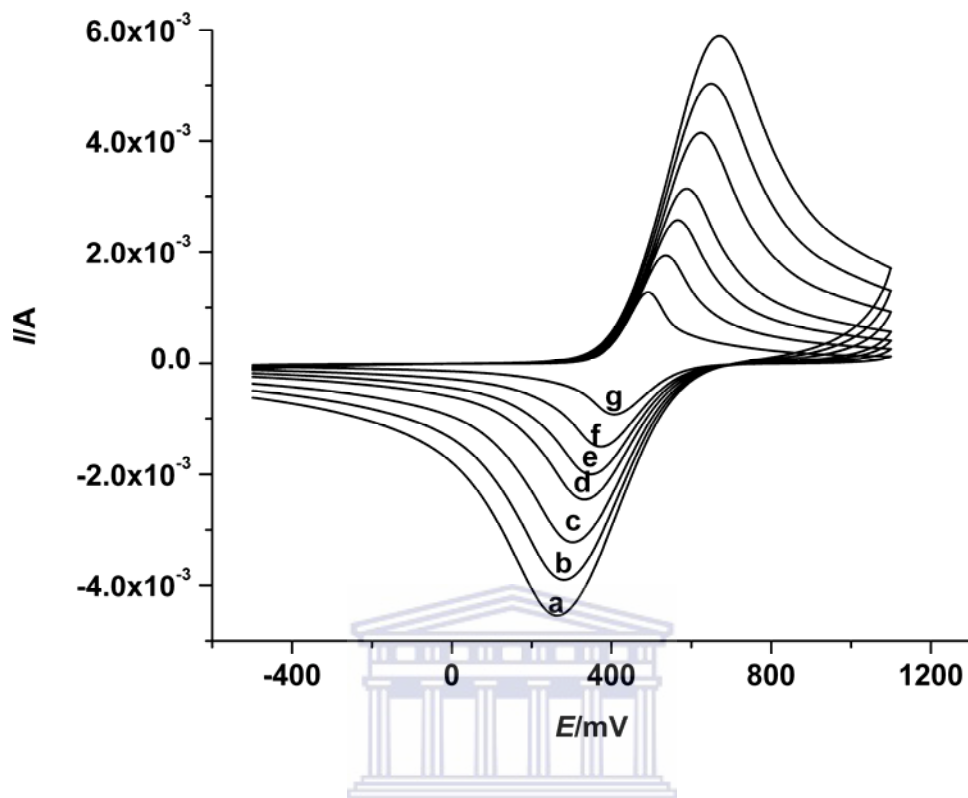
Figure 4.3: Cyclic voltammograms of PANI|PS$_{NP}$-NH$_2$ in 1 M HCl in the potential range -500 to +1100 mV at scan rates 500-50 mV/s for a-g, respectively.

In order to compare the conductivity of the three modified electrodes, cyclic voltammetry of PANI, PANI|PS$_{NP}$-NH$_2$ and PANI|PS$_{NP}$-SO$_3$$^-$ nanocomposite films were performed in 0.1 M HCl solution at 20 mV/s as presented in Figure 4.4. The typical PANI redox peaks (emeraldine and leucoemeraldine) of PANI were observed for all three electrode surfaces that is, PANI (a), PANI|PS$_{NP}$-NH$_2$ (b) and PANI|PS$_{NP}$-OSO$_3$$^-$ (c). Peak currents of the two redox couple for PANI were higher than that of both amine- and sulphate- modified PANI|PS$_{NP}$ because the PS$_{NP}$ latex bead templates in the nano-composites are insulating.
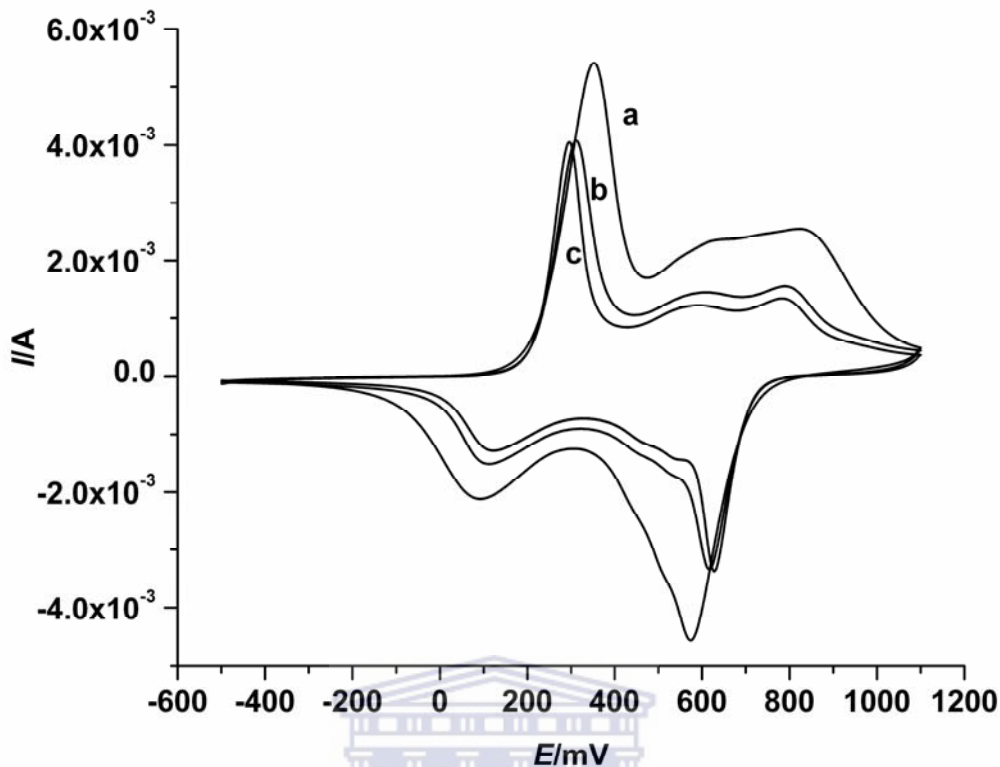
Figure 4.4: Cyclic voltammograms of PANI (a), PANI|PS$_{NP}$-NH$_2$ (b) and PANI|PS$_{NP}$-SO$_3^-$(c) in 0.1 M HCl scanned at 20 mV/s.

4.4 Spectroscopic characterisation of PANI, PANI|PS$_{NP}$-NH$_2$ and PANI|PS$_{NP}$-SO$_3^-$

UV-visible spectroscopy has been widely adopted in studying the electronic structure of conducting polymers including PANI[12]. The UV-visible spectra of PANI, PANI|PS$_{NP}$-NH$_2$ and PANI|PS$_{NP}$-OSO$_3^-$ films in DMSO are shown in Figure 4.5. The green coloured films showed two absorption peaks at 480 nm due to π-π* transition within the benzenoid segment and a broad peak in the visible region at 740 nm was ascribed to exciton formation in the quinoid rings[12, 13]. The fact that there was no shift in the wavelength of PANI at 480 nm in the nanocomposite suggests that the chemical structure of PANI was

not altered in the modified electrode preparation. Rather the composites were incorporated by physical bonding which is characteristic of self assembly.
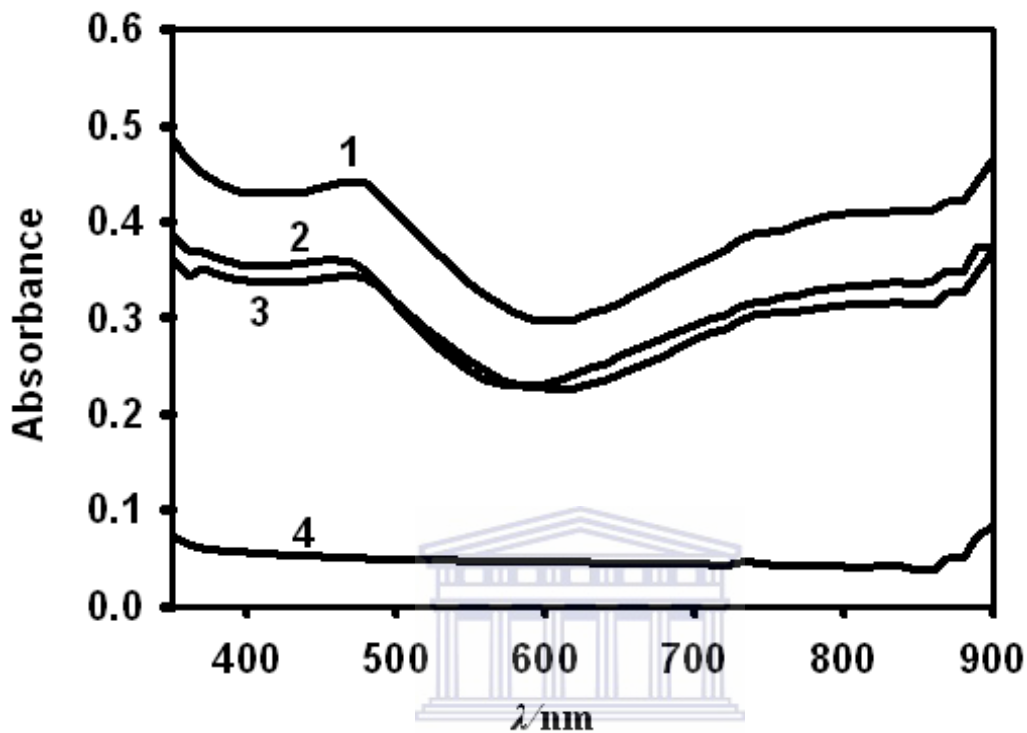

Figure 4.5: UV-visible spectra of PANI (1), PANI|PS_{NP}-NH_2 (2) and PANI|PS_{NP}-SO_3^- (3) films in DMSO (4).

4.5 Reduction of nitrite at the PANI modified electrodes

Reduction of nitrite was carried out using steady state amperometry at a potential of 50 mV as shown in Figure 4.6.
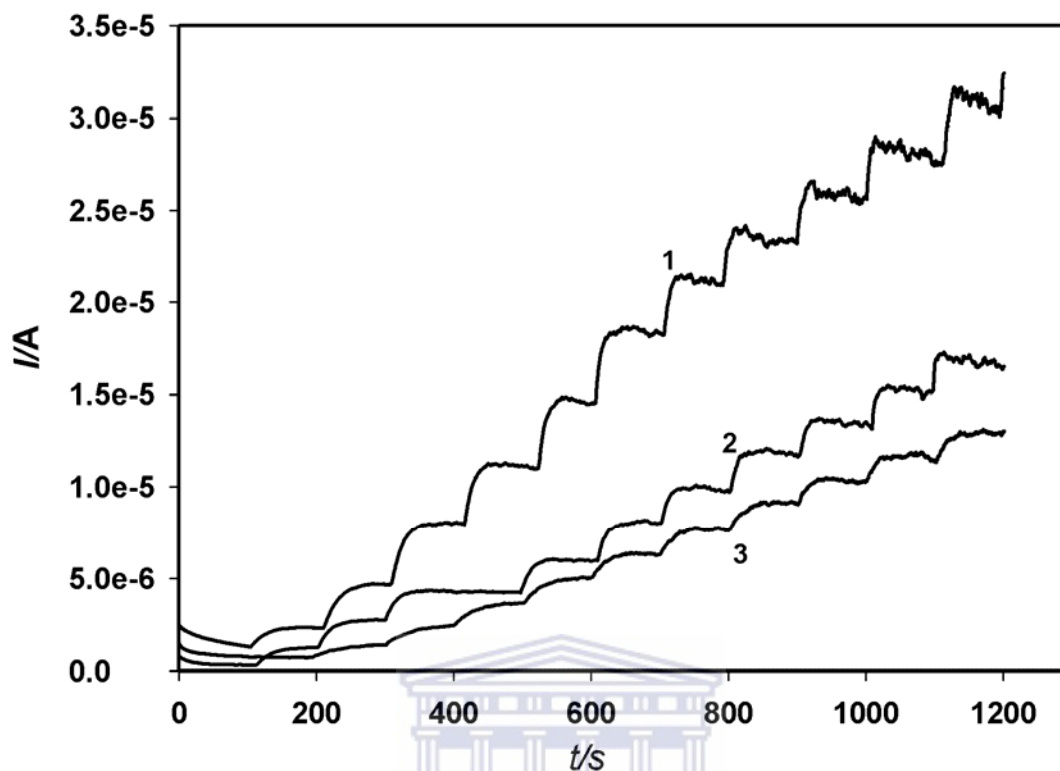
Figure 4.6: Amperometric response of PANI|PS$_{NP}$-NH$_2$ (1), PANI (2) and PANI|PS$_{NP}$-SO$_3^-$ (3) modified electrodes at +50 mV after successive addition of 50 μM nitrite.

The electrocatalytic mechanism for the reduction of NO$_2^-$ is shown in Scheme 4.1. The reduction potential of 50 mV converted emeraldine to leucoemeraldine. Leucoemeraldine irreversibly reduces nitrite (which is at equilibrium with HNO$_2$) to nitric oxide (NO)[14]. This results in the oxidation of leucoemeraldine back to emeraldine.

Scheme 4.1: Electrocatalytic reduction mechanism of NO_2^- on PANI modified electrodes.

From Figure 4.7, the highest current response was at -200 and 50 mV. However, 50 mV was chosen as the optimised potential because the negative potentials could interfere with the reduction of nitrite due to high background current because of dissolved oxygen in solution[15].
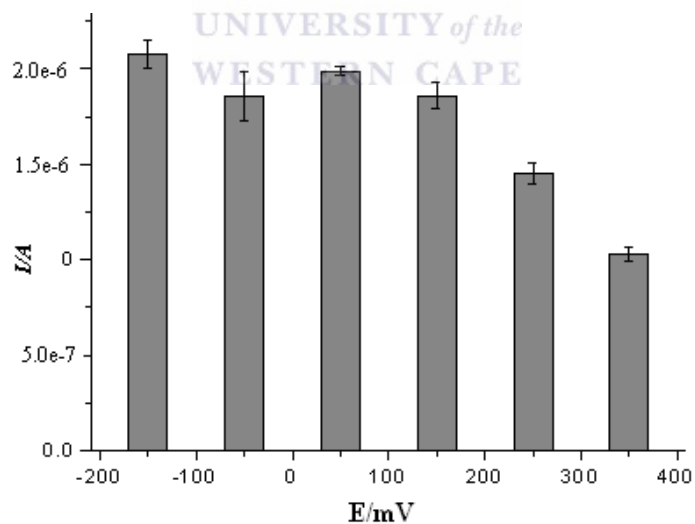

Figure 4.7: Influence of applied potential (vs. Ag/AgCl) on the response of PANI to 100 μM $NaNO_2$ in 0.1 M HCl.

Modified electrodes of PANI, PANI|PS$_{NP}$-NH$_2$ and PANI|PS$_{NP}$-OSO$_3^-$ were catalytic towards nitrite ions. Interestingly as seen in Figure 4.8, response due to PANI|PS$_{NP}$-NH$_2$ nanocomposite had the highest reduction current of the three electrodes.

Figure 4.8: Nitrite ion responses of GCE|PANI|PS$_{NP}$-NH$_2$|PANI (1), GCE|PANI (2) and GCE|PANI|PS$_{NP}$-OSO$_3^-$|PANI (3) nanosensors.

This can be explained by the electrostatic attraction between the positively charged PANI|PS$_{NP}$-NH$_2$ and negatively charged nitrite ion. PANI|PS$_{NP}$-OSO$_3^-$ electrode had the lowest response due to the repulsion of like negative charges of the nanocomposite electrode and nitrite ion. It should be noted that the effect of this repulsion was reduced by convection mass transport during stirring at 150 rpm. PANI electrode response to nitrite was lower than PANI|PS$_{NP}$-NH$_2$ but less than PANI|PS$_{NP}$-OSO$_3^-$. Though a similar

response is expected due to charge similarities between PANI|PS$_{NP}$-NH$_2$ and PANI (polyaniline is a cationic polymer), the smaller size of the PANI|PS$_{NP}$-NH$_2$ nanocomposite resulted in the higher response. From the response curve in Figure 4.8, saturation was attained at concentrations greater than 600 µM. As concentration of nitrite detected increased (over 800 µM), the noise to signal level also increased with each addition (Figure 4.6). This made it difficult to quantify the current response at these higher concentrations.

A linear plot of the reduction of nitrite on the different electrodes is shown in Figure 4.9. The correlation coefficient of the linear plots were all greater than 0.992 and the sensitivity was obtained from the slope of each plot. Sensitivity was 60, 40 and 30 µA/ mM for PANI|PS$_{NP}$-NH$_2$, PANI and PANI| PS$_{NP}$-OSO$_3^-$, respectively. The reason for this trend has been explained above. A correlation between surface concentration in mol cm^{-2} of PANI (2.66 x 10^{-8}), PANI|PS$_{NP}$-NH$_2$ (3.07 x 10^{-8}) and PANI|PS$_{NP}$-SO$_3^-$ (2.36 x 10^{-8}) with the calculated sensitivity was also observed. The sensitivity for the electrodes was higher than that reported by Luo et al.[16] for PANI|PS$_{NP}$ nanocomposite electrodes. The limit of detection was calculated and found to be 7.4, 9.2 and 38.2 µM for PANI|PS$_{NP}$-NH$_2$, PANI and PANI|PS$_{NP}$-OSO$_3^-$, respectively. These values are lower than that reported by Ojani, et al.[17]
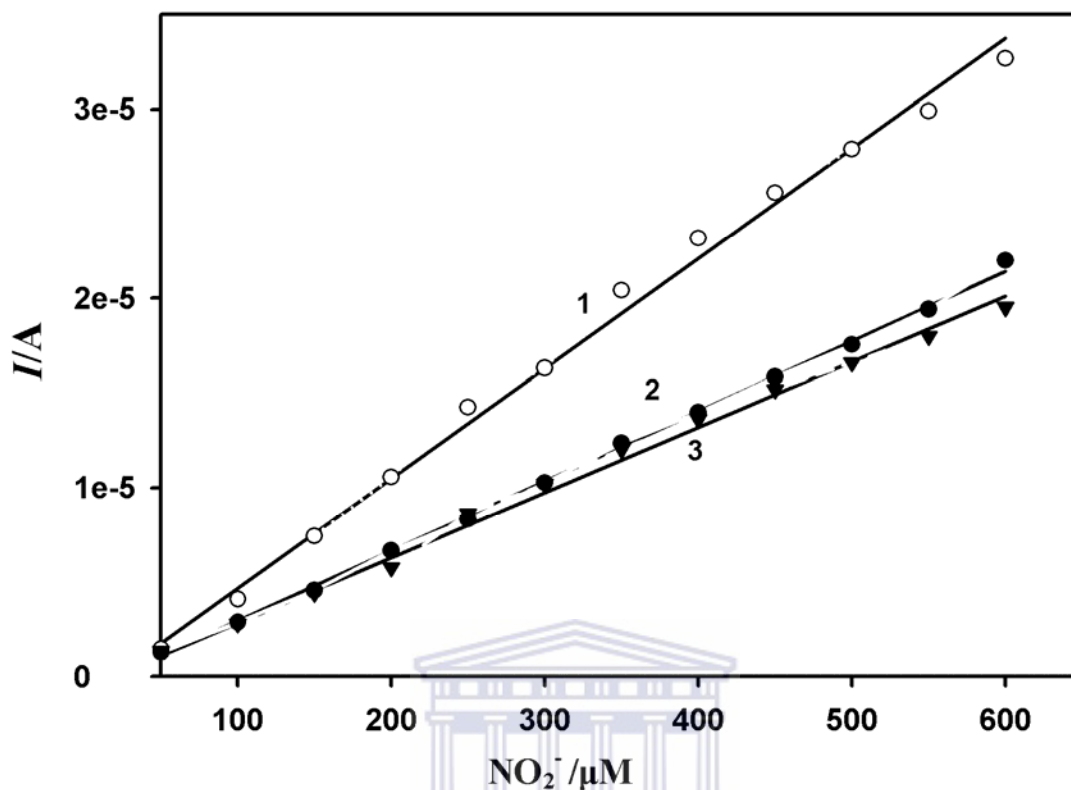
Figure 4.9: Linear plot of the amperometric reduction of nitrite on PANI|PS$_{NP}$-NH$_2$ (1), PANI (2) and PANI|PS$_{NP}$-OSO$_3^-$ (3) electrodes.

4.6 Effect of pH on nitrite ion determination

The determination of nitrite on PANI, PANI|PS$_{NP}$-NH$_2$ and PANI|PS$_{NP}$-OSO$_3^-$ modified electrodes was carried out at different pH values of the test using cyclic voltammetry at a potential of about 200 mV. A pH of about 1 was chosen as the optimum pH current response due to nitrite reduction (Figure 4.10). PANI is highly conducting at this low pH and due to the pKa value for HNO$_2$ of 3.3, nitrite ions are fully protonated[14, 17].

Figure 4.10: Anodic peak currents of PANI|PS$_{NP}$-NH$_2$ (1) and PANI (2), PANI|PS$_{NP}$-OSO$_3^-$ (3) at different pH values of HCl in 0.2 mM nitrite ion.

4.7 Interferences on nitrite ion determination

Possible interferences, such as, K^+, Mg^{2+}, Na^+, NH_4^+, Cl^-, SO_4^{2-} and NO_3^- were investigated on PANI, PANI|PS$_{NP}$-NH$_2$ and PANI|PS$_{NP}$-OSO$_3^-$ [14, 18-20]. No interference was observed in the presence of 800-fold excess of all ions at 50 mV. This is an advantage for the determination of nitrite on PANI, PANI|PS$_{NP}$-NH$_2$ and PANI|PS$_{NP}$-OSO$_3^-$ nanosensors.

4.8 Application of PANI nanosensors on rainwater

The applicability of these nanosensors in determining NO_2^- was demonstrated in rainwater. Concentrations of NO_2^- determined on PANI|PS$_{NP}$-NH$_2$, PANI and PANI|PS$_{NP}$-OSO$_3^-$ in rainwater was estimated to be 107.2, 63.2 and 67.0 µM, respectively. These results indicate that the method is applicable to rainwater and can also be applied to other natural waters, including lake and river water.

References

1. Iwuoha, E. I.; de Villaverde, D. S.; Garcia, N. P.; Smyth, M. R.; Pingarron, J. M., Reactivities of organic phase biosensors. 2. The amperometric behaviour of horseradish peroxidase immobilised on a platinum electrode modified with an electrosynthetic polyaniline film. *Biosensors and Bioelectronics* **1997,** 12, (8), 749-761.

2. Grennan, K.; Killard, A. J.; Hanson, C. J.; Cafolla, A. A.; Smyth, M. R., Optimisation and characterisation of biosensors based on polyaniline. *Talanta* **2006,** 68, (5), 1591-1600.

3. Benyoucef, A.; Boussalem, S.; Ferrahi, M. I.; Belbachir, M., Electrochemical polymerization and in situ FTIRS study of conducting polymers obtained from o-aminobenzoic with aniline at platinum electrodes. *Synthetic Metals* **2010,** 160, (15-16), 1591-1597.

4. Mathebe, N. G. R.; Morrin, A.; Iwuoha, E. I., Electrochemistry and scanning electron microscopy of polyaniline/peroxidase-based biosensor. *Talanta* **2004,** 64, (1), 115-120.

5. Ndangili, P. M.; Waryo, T. T.; Muchindu, M.; Baker, P. G. L.; Ngila, C. J.; Iwuoha, E. I., Ferrocenium hexafluorophosphate-induced nanofibrillarity of polyaniline-polyvinyl sulfonate electropolymer and application in an amperometric enzyme biosensor. *Electrochimica Acta* **2010,** 55, (14), 4267-4273.

6. Raj, J. A.; Mathiyarasu, J.; Vedhi, C.; Manisankar, P., Electrochemical synthesis of nanosize polyaniline from aqueous surfactant solutions. *Materials Letters* **2010,** 64, (8), 895-897.
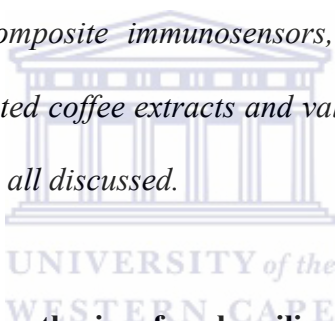
7. Iwuoha, E. I.; Mavundla, S. E.; Somerset, V. S.; Petrik, L. F.; Klink, M. J.; Sekota, M.; Bakers, P., Electrochemical and Spectroscopic Properties of Fly Ash–Polyaniline Matrix Nanorod Composites. *Microchimica Acta* **2006,** 155, (3), 453-458.

8. Pekmez, N.; Pekmez, K.; Yıldız, A., Electrochemical behavior of polyaniline films in acetonitrile. *Journal of Electroanalytical Chemistry* **1994,** 370, (1-2), 223-229.

9. Kazimierska, E.; Muchindu, M.; Morrin, A.; Iwuoha, E.; Smyth, M. R.; Killard, A. J., The fabrication of structurally multiordered polyaniline films and their application in electrochemical sensing and biosensing. *Electroanalysis* **2009,** 21, (3-5), 595-603.

10. Luo, X.; Morrin, A.; Killard, A.; Smyth, M., Application of Nanoparticles in Electrochemical Sensors and Biosensors. *Electroanalysis* **2006,** 18, (4), 319-326.

11. Mathebe, N. G. R.; Morrin, A.; Iwuoha, E. I., Electrochemistry and scanning electron microscopy of polyaniline/ peroxidase-based biosensor. *Talanta* **2004,** 64, (1), 115-120.

12. Wang, Y.; Jing, X., Effect of solution concentration on the UV-vis spectroscopy measured oxidation state of polyaniline base. *Polymer Testing* **2005,** 24, (2), 153-156.

13. Gaikwad, P. D.; Shirale, D.J.; Savale, P. A.; Datta, K.; Ghosh, P.; Pathan, A.J.; Rabbani G.; Shirsat, M.D., Development of PANI-PVS-GOD electrode by potentiometric method for determination of glucose. *International Journal of Electrochemical Science* **2007,** 2, 488 - 497.

14. Guo, M.; Diao, P.; Cai, S., Hydrothermal growth of perpendicularly oriented ZnO nanorod array film and its photoelectrochemical properties. *Applied Surface Science* **2005,** 249, (1-4), 71-75.

15. Antoine, O.; Durand, R., In situ electrochemical deposition of Pt nanoparticles on carbon and inside Nafion. *Electrochemical and Solid-State Letters* **2001,** 4, (5), A55-A58.

16. Luo, X.; Killard, A. J.; Smyth, M. R., Nanocomposite and Nanoporous Polyaniline Conducting Polymers Exhibit Enhanced Catalysis of Nitrite Reduction. *Chemistry - A European Journal* **2007,** 13, 2138-2143.

17. Ojani, R.; Raoof, J. B.; Zarei, E., Electrocatalytic reduction of nitrite using ferricyanide; Application for its simple and selective determination. *Electrochimica Acta* **2006,** 52, (3), 753-759.

18. Kamyabi, M. A.; Aghajanloo, F., Electrocatalytic oxidation and determination of nitrite on carbon paste electrode modified with oxovanadium(IV)-4-methyl salophen. *Journal of Electroanalytical Chemistry* **2008,** 614, (1-2), 157-165.

19. Malone, M. M.; Doherty, A. P.; Smyth, M. R.; Vos, J. G., Flow injection amperometric determination of nitrite at a carbon fibre electrode modified with the polymer [Os(bipy)$_2$(PVP)$_{20}$Cl]Cl. *Analyst* **1992,** 117, (8), 1259-1263.

20. Radojević, M.; Bashkin., V.N., Practical Environmental Analysis **2006**. In edition, 2nd. Ed. RSC Publishing: Cambridge, UK.

CHAPTER 5

PART 2-RESULTS AND DISCUSSION: FABRICATION OF IMMUNOSENSORS
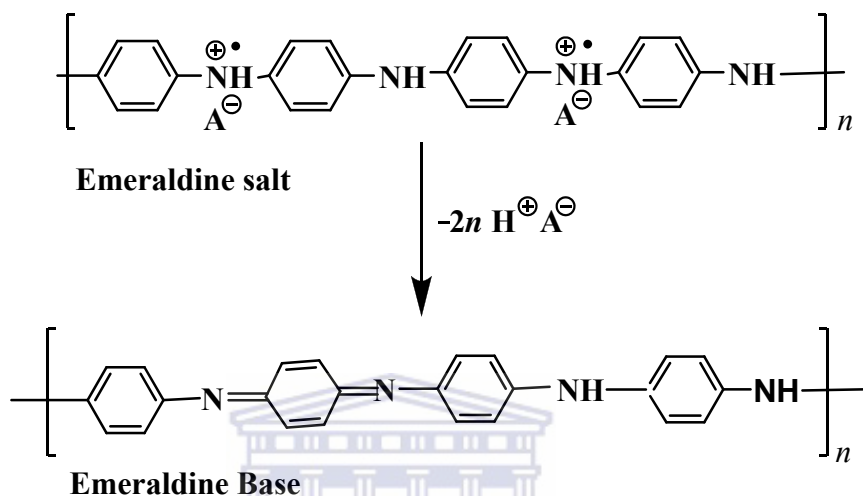
FOR OCHRATOXIN A

This chapter presents results obtained after the conditioning of polyaniline and its amine- and sulphate-modified polystyrene nanocomposites in phosphate buffer saline (PBS) at pH 7.2. The immobilization of ochratoxin A antibody onto the modified electrode surfaces, their SEM and AFM morphological characterization, electrochemistry of the polyaniline-polystyrene nanocomposite immunosensors, their application in certified reference corn, wheat and roasted coffee extracts and validation of these latter (certified materials) results by ELISA are all discussed.

5.1 Optimisation of electrosynthesis of polyaniline and polyaniline-polystyrene nanocomposites

Aniline doped with $PV-SO_3^-$ was polymerized on Pt electrode in 1 M HCl as explained in Section 4.1. Acidic medium is required to produce polyaniline emeraldine salt which is the polymer's most conducting state[1-5]. It must be noted that in this discussion, the outer surface on the polyaniline-polystyrene nanocomposites, $PANI|PS_{NP}-OSO_3^-|PANI$ and $PANI|PS_{NP}-NH_2|PANI$ and PANI-modified electrodes will all be referred to as $PANI-PV-SO_3^-$. The acidic $PANI-PV-SO_3^-$ was conditioned in 0.1 M PBS to lower the effects of hysteresis[6]. The electronic structure in the protonated ES metal is similar to that of a

metal and its conductivity is due to the formation of a polaron band resulting from the proton-induced spin-unpairing mechanism[7]. Treatment of the emeraldine salt with a neutral solution such as PBS at pH 7.2 converted it into its semiconducting emeraldine base (EB) as shown in Scheme 5.1.

Emeraldine salt

$-2n\ H^{\oplus}A^{\ominus}$

Emeraldine Base

Scheme 5.1: Protonated PANI-PV-SO$_3^-$ emeraldine salt (ES) is de-protonated by conditioning in PBS to emeraldine base (EB).

A high current was observed in the first CV (Figure 5.1 (i)) performed in PBS because the polymer was still in its emeraldine salt state and its internal microscopic environment was still acidic. In subsequent CVs, as shown in Figure 5.1 (ii), a decrease in current was observed as the emeraldine salt was converted to an emeraldine base as shown in Scheme 5.1. The emeraldine base is an *n*-type semiconductor in PBS at pH 7.2. The presence of PV-SO$_3^-$ dopant modulated the distribution of electrons within the polyaniline film. The conductivity of emeraldine salt has been reported to be 1 Scm^{-1} while that of emeraldine base (EB) is between 10^{-8} to 10^{-10} Scm^{-1} [8]. The Fermi level now lies below the conduction band in this semiconductor[9]. The electrochemical potential of the buffer solution

108

determined by the redox potential of the electrolyte solution and the semiconductor is determined by the Fermi level. The charge transfer abilities of the PANI- PV-SO$_3^-$ doped semiconductor electrode depends on the availability of excess charge in the accumulation layer or a depletion layer. This excess charge on the semiconductor does not lie at the surface, as it would for a metallic electrode. This region referred to as the space charge region, has an associated electrical field. Therefore, the interfacial equilibrium between the semiconductor PANI-PV-SO$_3^-$ electrode and PBS electrolyte solution was attained when the electrochemical potential of the two phases (PANI-PV-SO$_3^-$|PBS) became equal.
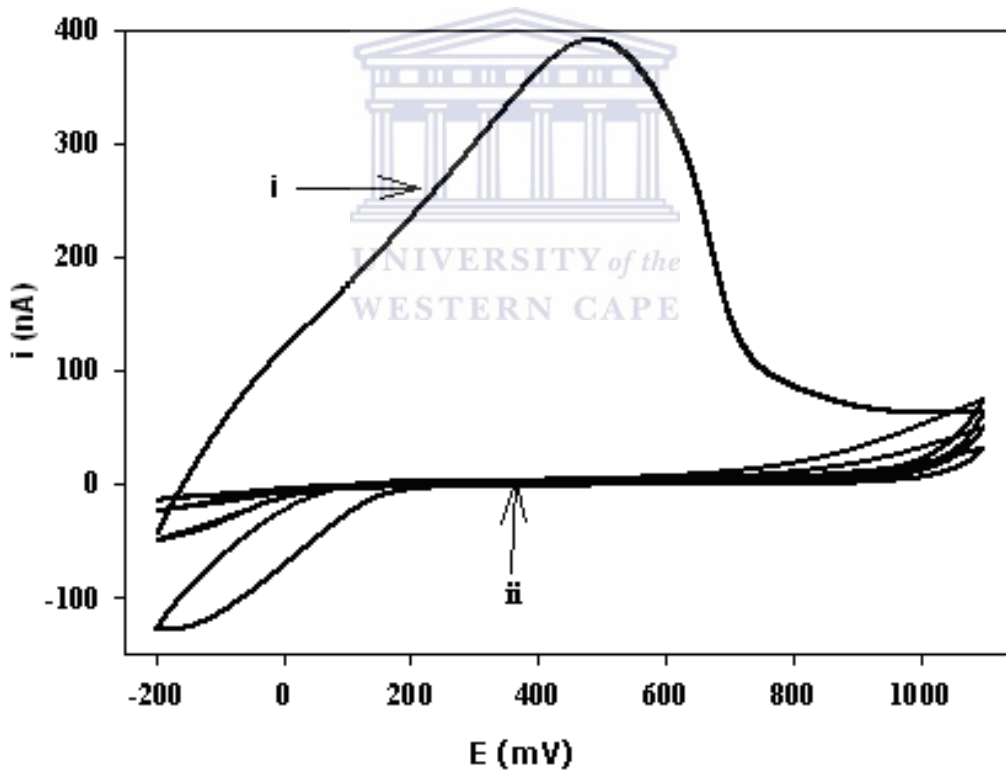

Figure 5.1: Cyclic voltammograms of PANI-PV-SO$_3^-$ in PBS: (i) immediately after electrosynthesis and (ii) after conditioning (cycling until equilibration of voltammetric current).

Figure 5.1(ii) voltammograms showed that within a potential window of 0 to +800 mV the conditioned polymer had zero current which meant that it could be used as a catalytic surface without interferences from the background current of the polymer.

5.2 Scanning electron microscope (SEM) characterisation of PANI, PANI|PS$_{NP}$-NH$_2$|PANI and PANI|PS$_{NP}$-OSO$_3^-$|PANI electrodes

Aggregates of PANI and its polystyrene nanocomposites, PANI|PS$_{NP}$ were observed at 50000X magnification on the surface of a SPCE under a scanning electron microscope (SEM) as shown in Figures 5.2. The PANI clusters in Figure 5.2 (a) appeared more amorphous in texture and varied in size, from 25-100 nm. The polyaniline-polystyrene nanocomposites in Figures 5.2(b) and (c) of PANI|PS$_{NP}$-NH$_2$|PANI and PANI|PS$_{NP}$-OSO$_3^-$|PANI, respectively, provided a highly controlled charge and size (approximately 100 nm) polystyrene (PS$_{NP}$) template nano-aggregates. The benefit of using self-assembled PS$_{NP}$ scaffolds is that they allowed fabricating structures such as the observed nano-cauliflower that was otherwise not possible[4, 10-12]. It has been explained that the final layer of PANI electropolymerized on the positively charged PS$_{NP}$-NH$_2$ template grew from the surface of the electrode into the interstitial spaces between the latex beads whereas the negatively charged PS$_{NP}$-OSO$_3^-$ nanoparticles enforced growth of PANI around the template particles to form PS$_{NP}$-OSO$_3^-$|PANI core-shell nanostructures[10].
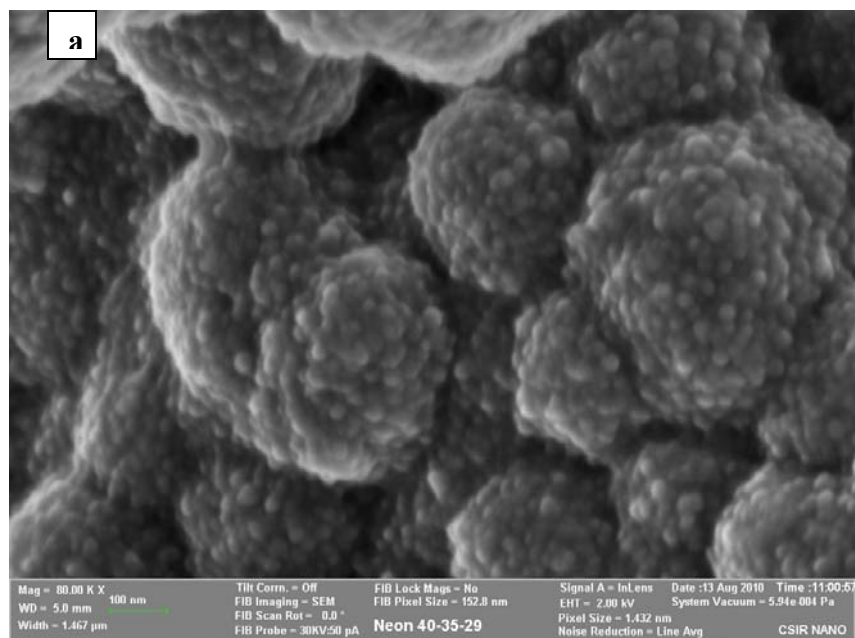
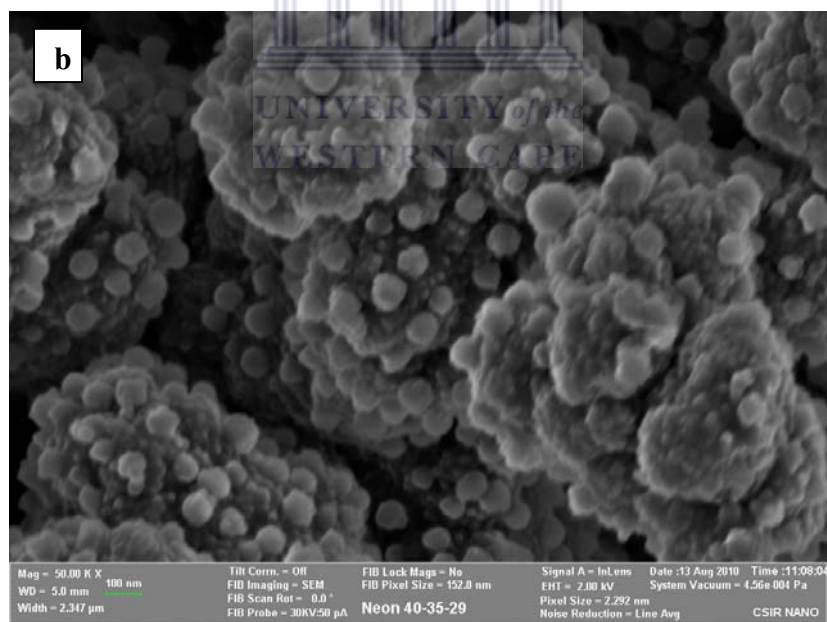Figure 5.2: (a) SPCE|PANI at 50000X after conditioning in 0.1 M PBS at pH 7.2.

Figure 5.2: (b) SPCE|PANI|PS$_{NP}$-NH$_2$|PANI at 50000X after conditioning in 0.1 M PBS at pH 7.2.
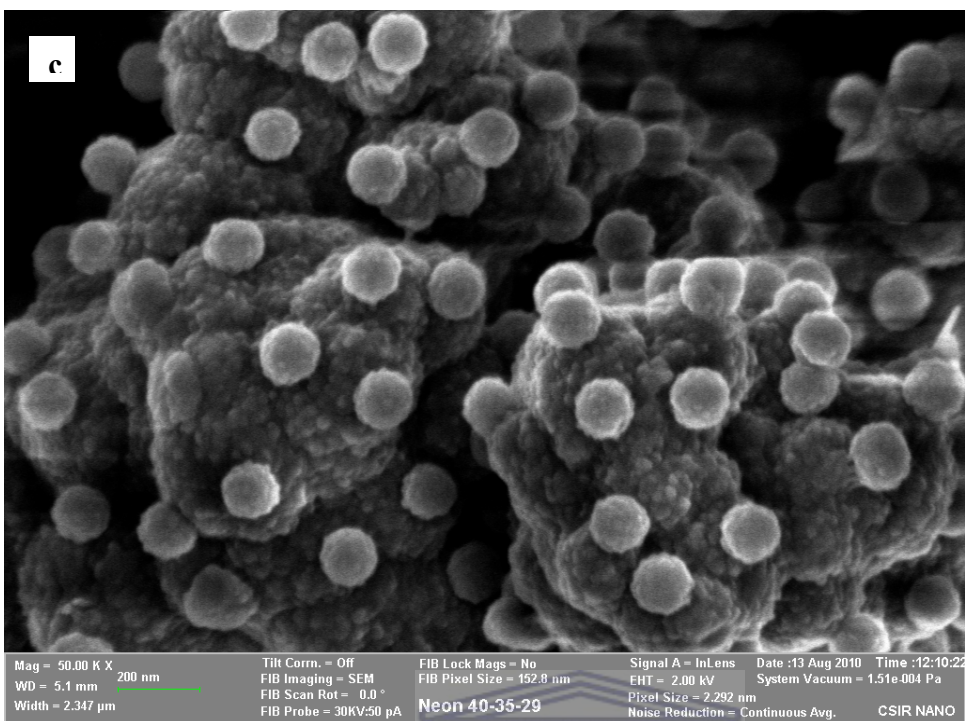
Figure 5.2: (c) SPCE|PANI| PS_{NP}-OSO_3^-|PANI observed at 50000X after conditioning of the modified electrode in 0.1 M PBS at pH 7.2.

5.3 Electrochemical impedance spectroscopy (EIS) characterization of Pt|PANI PANI|PS_{NP}-NH_2|PANI and PANI|PS_{NP}-OSO_3^-|PANI electrodes

The EIS of buffer-conditioned Pt|PANI, Pt|PANI|PS_{NP}-NH_2|PANI and Pt|PANI|PS_{NP}-OSO_3^-|PANI electrodes were studied over a potential range of 0 to +800 mV. A similar trend shown by Nyquist plots in Figure 5.3 was observed for all three Pt|PANI platforms. The Nyquist plot shows the magnitude of impedance, $|Z|$, given by Real, Z' and Imaginary, Z'' impedance.

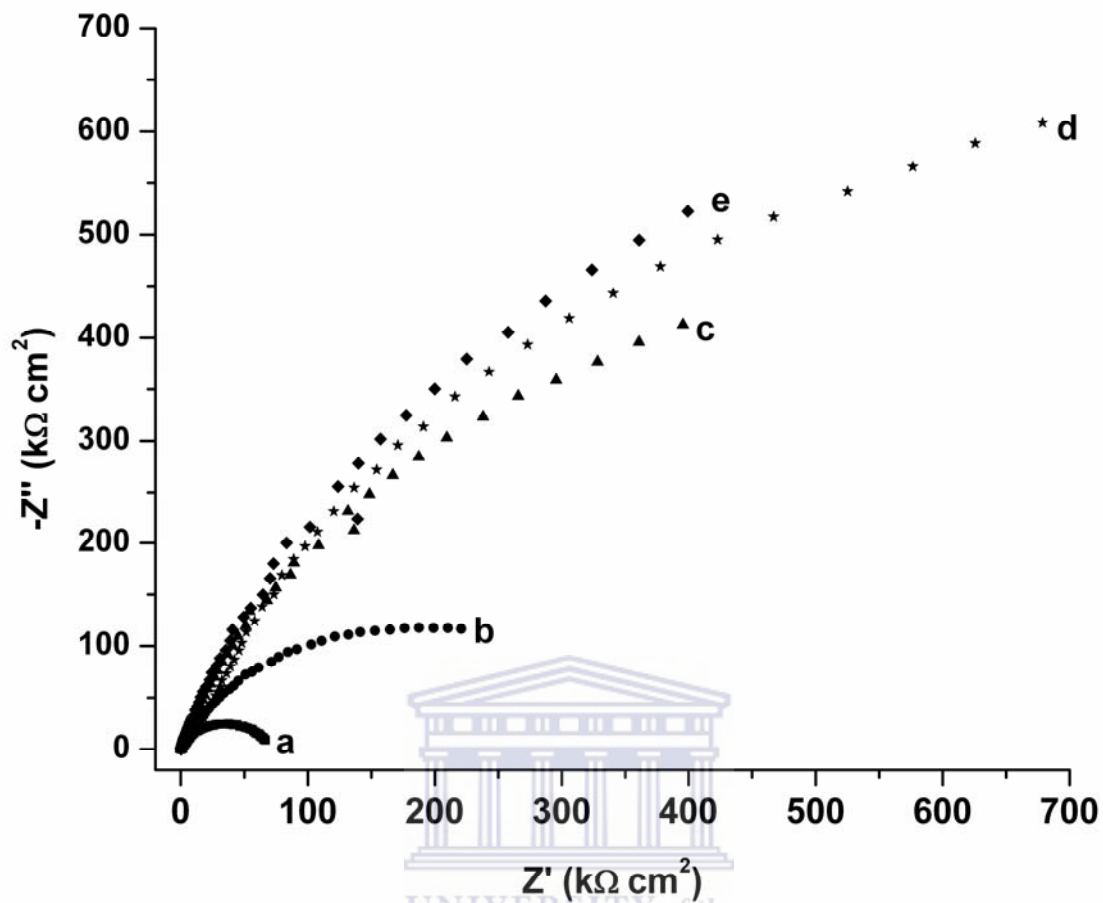$$|Z| = \sqrt{Z'^2 + Z''^2}$$ Equation 5.1

112

Figure 5.3: Nyquist plots of Pt|PANI at different bias potentials (a, b, c, d and e are 0, 100, 400, 600 and 800 mV, respectively).

Based on an equivalent circuit (Figure 5.4) in which the solution resistance, R_s, precedes a constant phase element, CPE, which is in parallel with charge transfer resistance, R_{ct}; the optimal AC potential was found to be 0 mV. A similar potential was reported by Owino *et al.*, for PANI doped with polystyrene sulphonic acid[13].

A zero bias potential is ideal for the EIS studies as it leads to electronic circuit simplicity and low induced diffusion current. It may also be noted that this electrical circuit (Figure 5.4) is a simplified representation of an amorphous semiconductor in which charge

transport occurs through hopping as reported by Dyre,1998 [14] . The hopping contribution is included in the real part of the impedance while the capacitor collects unrelated purely imaginary contributions from the atomic polarizability given by the high frequency dielectric constant[15].
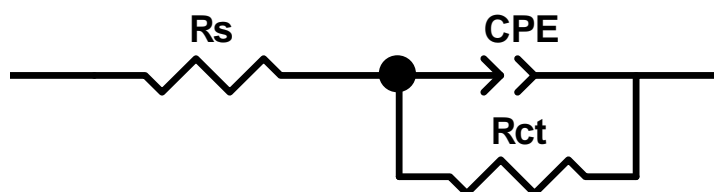

Figure 5.4: Equivalent circuit of Pt|PANI, PANI|PS_{NP}-NH_2|PANI and PANI|PS_{NP}-OSO_3^-|PANI (R_s = solution resistance, CPE = constant phase element; R_{ct} = charge transfer resistance).

The Nyquist plots of the bare Pt and Pt|PANI-PV-SO_3^- electrode systems at 0 mV are shown in Figure 5.5. The frequency of maximum imaginary impedance of PANI-PV-SO_3^- and Pt electrodes were calculated to be 1.0 and 0.794 kHz, respectively. The surface coverage of the Pt by the semiconductor PANI|PV-SO_3^- film was calculated to be 64%. A comparison of the impedimetric parameters of Pt (R_s = 445.9 Ω; R_{ct} = 181.500 kΩ) and Pt|PANI-PV-SO_3^- (R_s = 176.5 Ω; R_{ct} = 65.591 kΩ) electrodes in PBS shows that the R_s and R_{ct} values of the polymer-modified Pt were lower than those of unmodified Pt. The difference in R_s values of Pt and Pt|PANI-PV-SO_3^- electrodes has been attributed to a change in the proximity of the working electrode to the reference electrode[16]. These R_s values represent the property of the bulk solution and make up for uncompensated Ohmic resistance via a non-Faradaic process[17]. On the other hand, the drastic drop in the R_{ct}

value of Pt when modified with PANI-PV-SO$_3^-$ is as a result of the charge delocalization along the conducting polymer film, which makes the polymer electrode very suitable for charge transfer applications and electrostatic deposition of charged biomolecules.
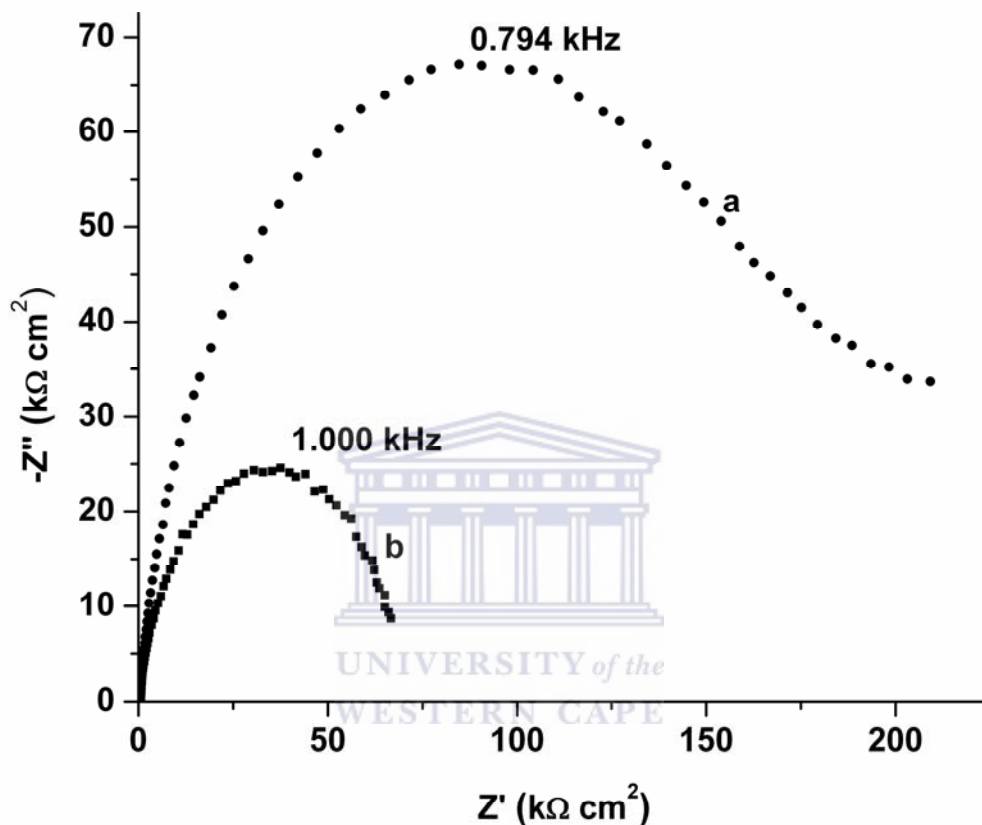

Figure 5.5: Nyquist plots of bare Pt (a) and Pt|PANI-PV-SO$_3^-$ (b) in PBS at 0 mV.

The frequency dependence of both the impedance and the phase angle of the electrodes are shown in Figure 5.6. The figure shows a decrease in the impedance of the electrodes as frequency increases. However, the impedance of PANI-PV-SO$_3^-$ modified electrodes was generally lower than that of unmodified Pt electrode over the frequency range studied, which is an indication of improved conductivity of the PANI-containing system. At low frequencies, the phase shift was below 10º for both electrodes. This is expected

for a simple equivalent circuit (Figure 5.4) that has a capacitor in parallel with a resistor[15]. The phase shift increased with frequency until a characteristic frequency, f_c, where the phase shift has a maximum value of 71º for Pt electrode and 75º for Pt|PANI-PV-SO$_3^-$ electrode. For frequencies higher than f_c, the phase shift of Pt|PANI-PV-SO$_3^-$ was greater than that of Pt until a frequency is reached where both materials had the same phase shift value of 10º. The kinetic analysis of the two electrode systems showed that the exchange current, i_o

$$i_0 = \frac{RT}{nFR_{ct}}$$ Equation 5.2

and heterogeneous rate constant, k_{et}:

$$i_o = nFAK_{et}C^*$$ Equation 5.3

of Pt|PANI-PV-SO$_3^-$ (i_o = 3.92 x10^{-7} A; k_{et} = 2.02 x 10^{-3} cm/s) were 3 times the values for bare Pt (i_o = 1.42 x10^{-7} A; k_{et} = 7.32 x 10^{-4} cm/s). The implication is that the modification of the Pt electrode with PANI-PV-SO$_3^-$ improved the kinetics at the electrode surface.
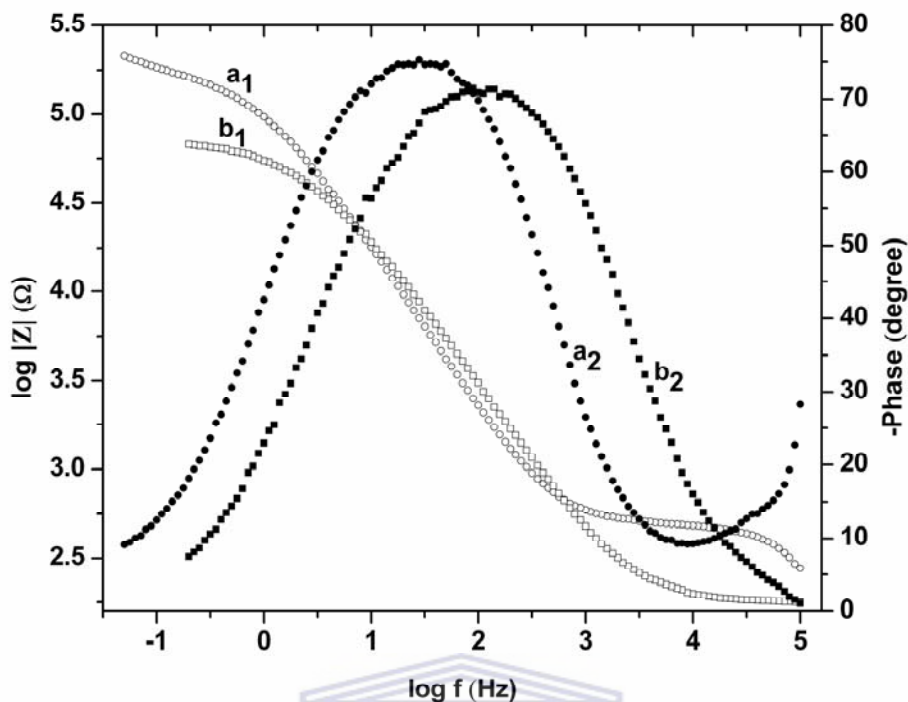
Figure 5.6: Frequency dependences of the impedance (a_1 and b_1) and phase shift (a_2 and b_2) in the Bode plots for bare Pt (a_1 and a_2) and Pt|PANI-PV-SO_3^- (b_1 and b_2) in PBS at 0 mV.

5.4 Electrochemical impedance spectroscopy (EIS) characterization of Pt|PANI PANI|PS$_{NP}$-NH$_2$|PANI and PANI|PS$_{NP}$-OSO$_3^-$|PANI immunosensors in PBS

Electro-deposition of the antibody onto the Pt|PANI, PANI|PS$_{NP}$-NH$_2$|PANI and PANI|PS$_{NP}$-OSO$_3^-$|PANI platforms by chrono-potentiometry shown in Figure 5.7 was carried out by a method adapted from Owino et $al.$[13]
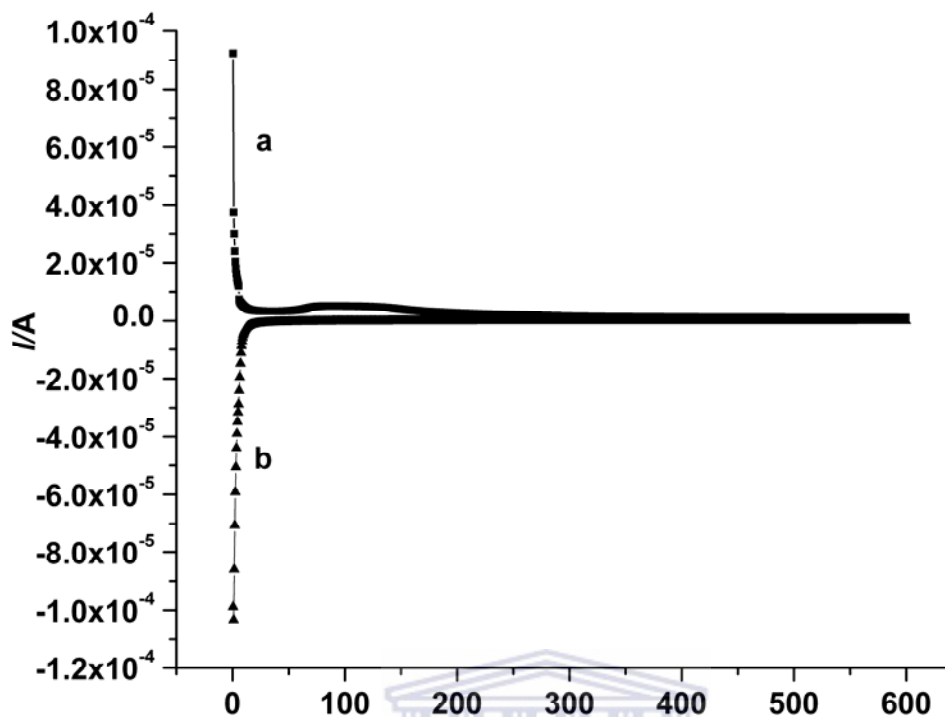
Figure 5.7: Oxidation (a) and reduction (b) of PANI, PANI|PS$_{NP}$-OSO$_3$⁻|PANI and PANI|PS$_{NP}$-NH$_2$|PANI in 0.1 M PBS and 10 µg/mL polyclonal OTA antibody in 0.1 M PBS, respectively.

The mechanism of the antibody-antigen reaction at the electrodes involved a variation in the capacitive properties of the polymer [17, 18]. At neutral pH, the antibody give a negative charge and the interactions between the immobilized negatively charged antibody at neutral pH and the polymer chain of the semiconductor induced changes in the capacitance of the PANI modified electrode. A comparison of the Nyquist and Bode plots for the templated PANI|PS$_{NP}$ nanocomposites and PANI immunosensors are shown in Figures 5.8 and 5.9.
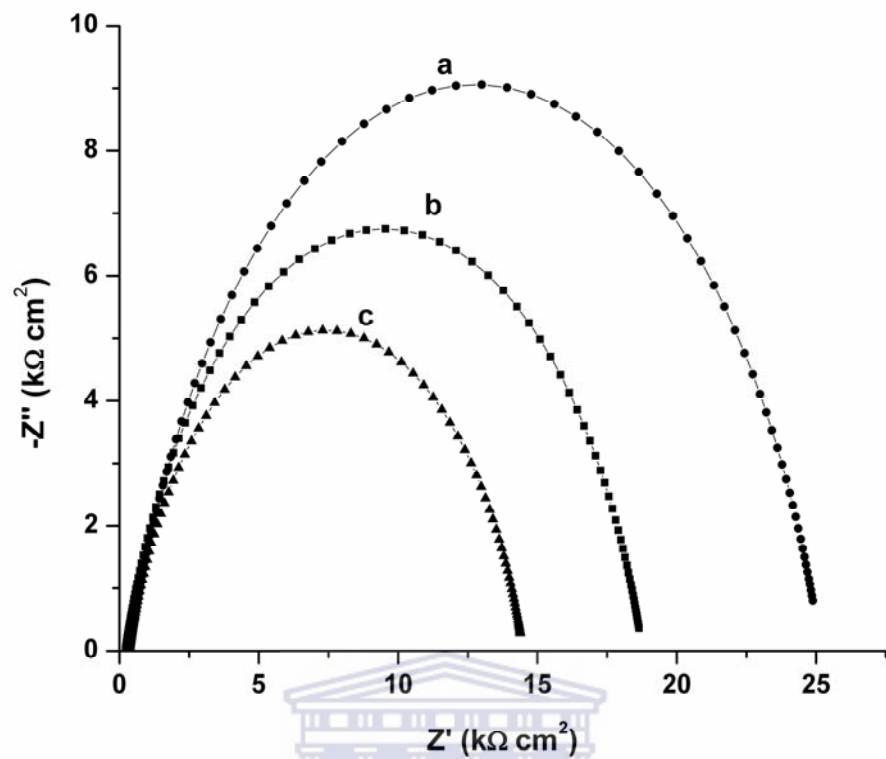
Figure 5.8: Nyquist plots of PANI|PS$_{NP}$-NH$_2$|PANI|anti-OTA (a), PANI|anti-OTA (b) and

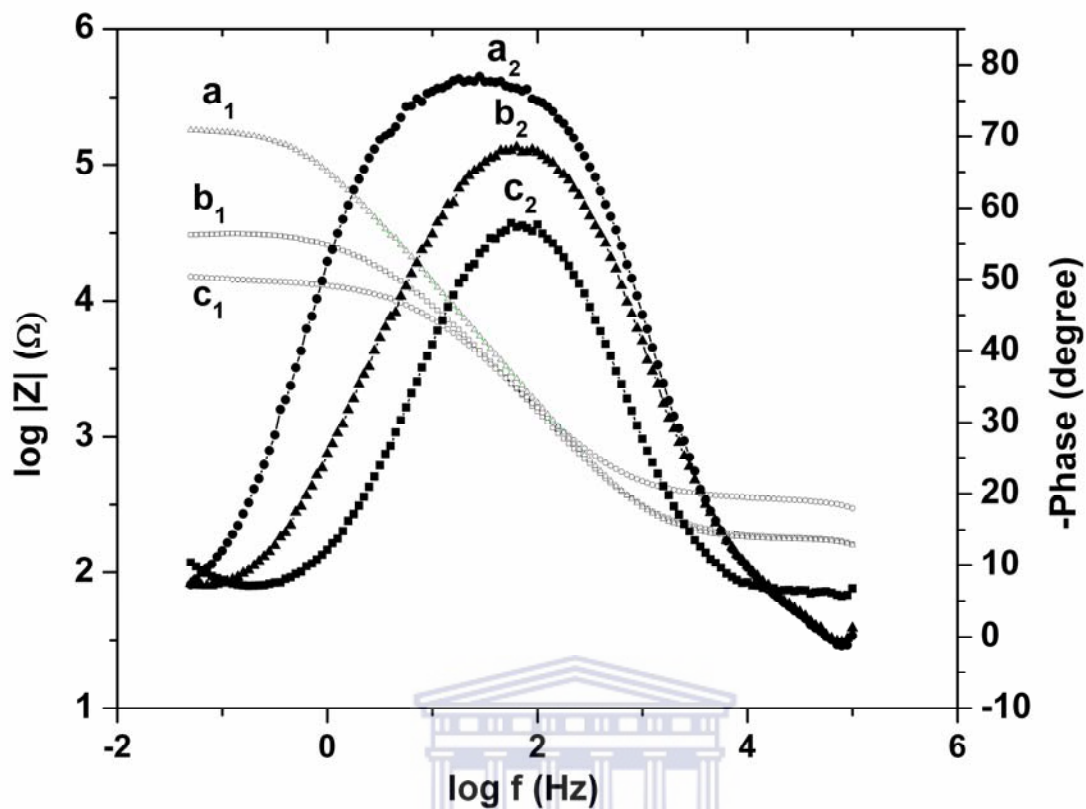PANI|PS$_{NP}$-OSO$_3^-$|PANI|anti-OTA (c) immunosensors in PBS

Figure 5.9: Bode plots of PANI|PS$_{NP}$-NH$_2$|PANI|anti-OTA (a), Pt| PANI|anti-OTA (b) and PANI|PS$_{NP}$-OSO$_3^-$| PANI|anti-OTA (c) immunosensors in 0.1 M PBS.

The electrochemical impedance spectroscopy (EIS) parameters are summarized in Table 5.1. PANI|PS$_{NP}$-NH$_2$|PANI|anti-OTA immunosensor showed higher resistance, constant phase element and phase shift values as compared to PANI|anti-OTA and PANI|PS$_{NP}$-OSO$_3^-$|PANI|anti-OTA immunosensors.

Table 5.1: EIS parameters of Pt|PANI-PS$_{NP}$|anti-OTA immunosensors in PBS at 0 mV

Circuit Element	Pt|PANI|anti-OTA	Pt|PANI-PS$_{NP}$-NH$_2$|anti-OTA	Pt|PANI-PS$_{NP}$-OSO$_3^-$|anti-OTA
R$_s$ (Ω)	215.7	379.2	333
R$_{ct}$ (Ω)	18556	24788	14155
CPE (F)	2.80 e-6	3.56 e-6	3.82 e-6
Phase shift |φ|	2.66	17.6	6.77

5.5 Ultraviolet-visible spectroscopic characterization of ochratoxin A antigen and antibody

Ultra violet-visible (UV-vis) spectroscopy was used to study the electronic structure of ochratoxin A antigen and antibody as shown in Figure 5.10. Absorbance was observed at 330 and 390 nm for spectra of OTA antigen (a) and OTA antibody-antigen (b) due to the phenolic species of the OTA antigen. Protonated phenol has been reported to absorb at 332 nm[19, 20]. At a buffer pH of 7.2, deprotonation of the phenolic species resulted in absorbance at 390 nm. A lower absorbance was observed in the presence of OTA antibody (Figure 5.9 (b)) due to binding of the antigen to the antibody. A spectrum of OTA antibody (Figure 5.10 (c)) did not show any absorbance.
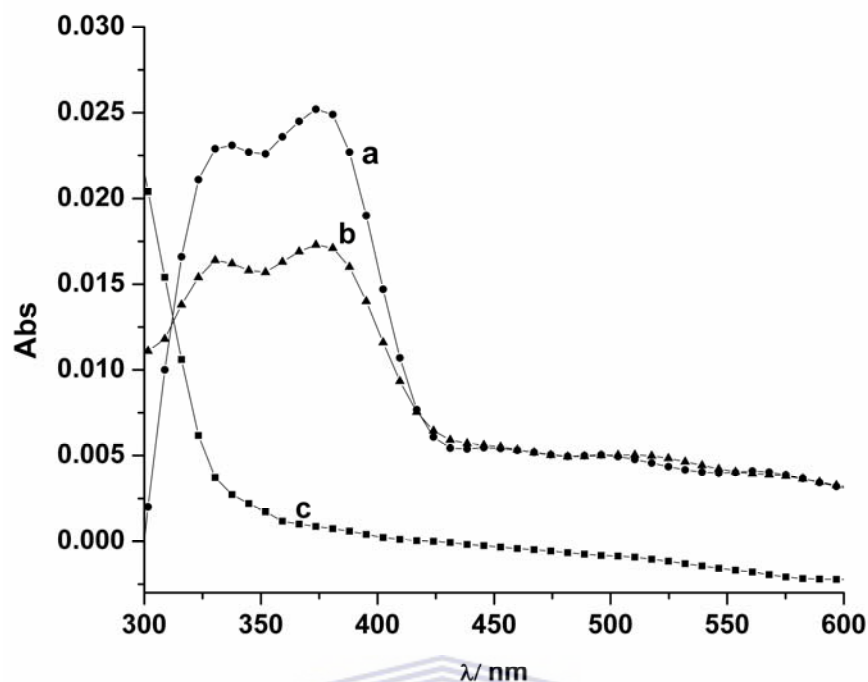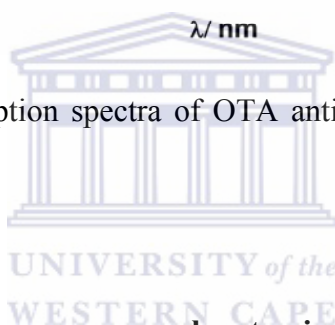
Figure 5.10: UV-visible absorption spectra of OTA antigen (a), OTA antibody-antigen (b) and OTA antibody (c).

5.6 Characterization of the immunosensors by atomic force microscope (AFM)

Atomic force microscope (AFM) analysis was carried out on PANI and PANI|PS$_{NP}$ immunosensors to investigate the difference in surface morphology. Screen printed carbon electrodes (Figure 5.11a) were used as substrate on which AFM analysis of the immunosensors was to be carried out. Carbon ink clusters were observed in 3-D providing an in-depth profile of the morphology. The globular, cauliflower nanostructured images observed in SEM images in Figure 5.11 were observed after immoblization of antibody onto their surfaces on both the 1-D and 3-D profiles of PANI|anti-OTA (b and c) PANI|PS$_{NP}$-NH$_2$|PANI|anti-OTA (d and e) and PANI|PS$_{NP}$-OSO$_3^-$|PANI|anti-OTA (f and g), respectively.
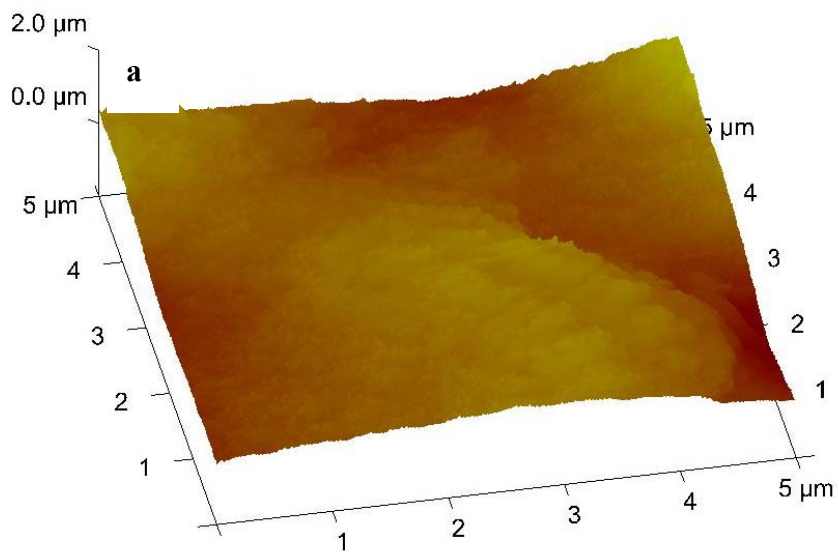
Figure 5.11(a): AFM image of SPCE
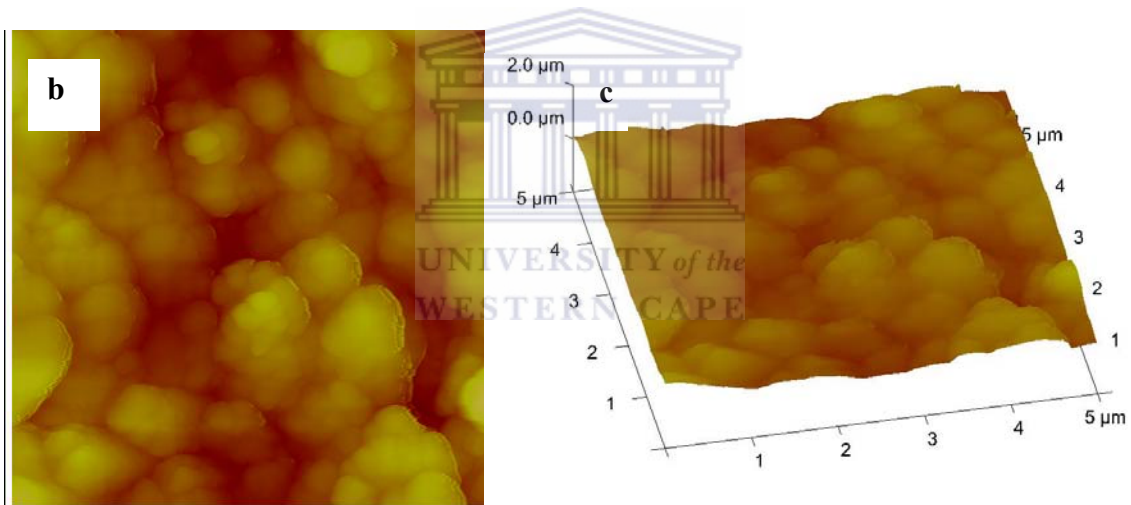
Figure 5.11: AFM images of SPCE|PANI|anti-OTA (b and c)
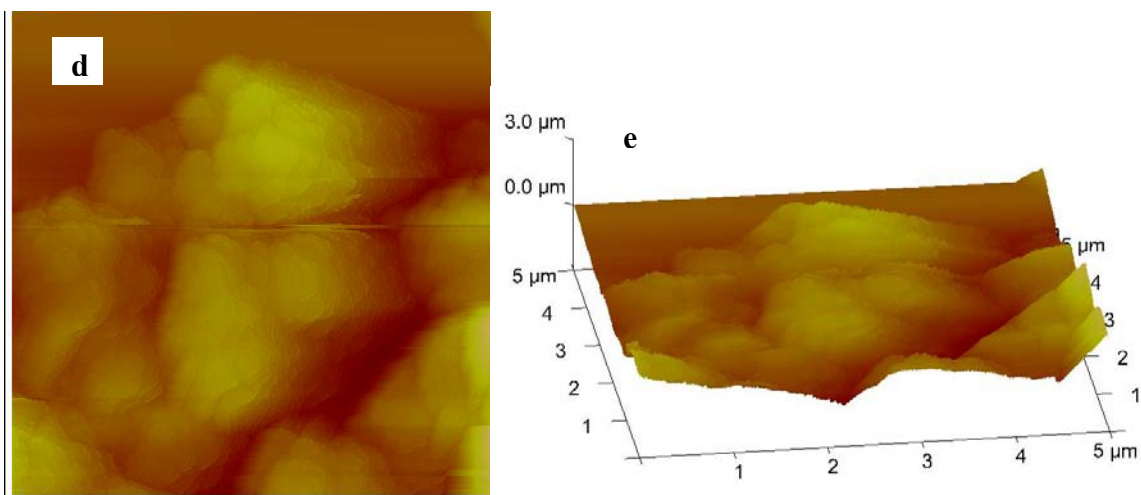
Figure 5.11: SPCE|PANI|PS$_{NP}$-NH$_2$|PANI|anti-OTA (d and e)
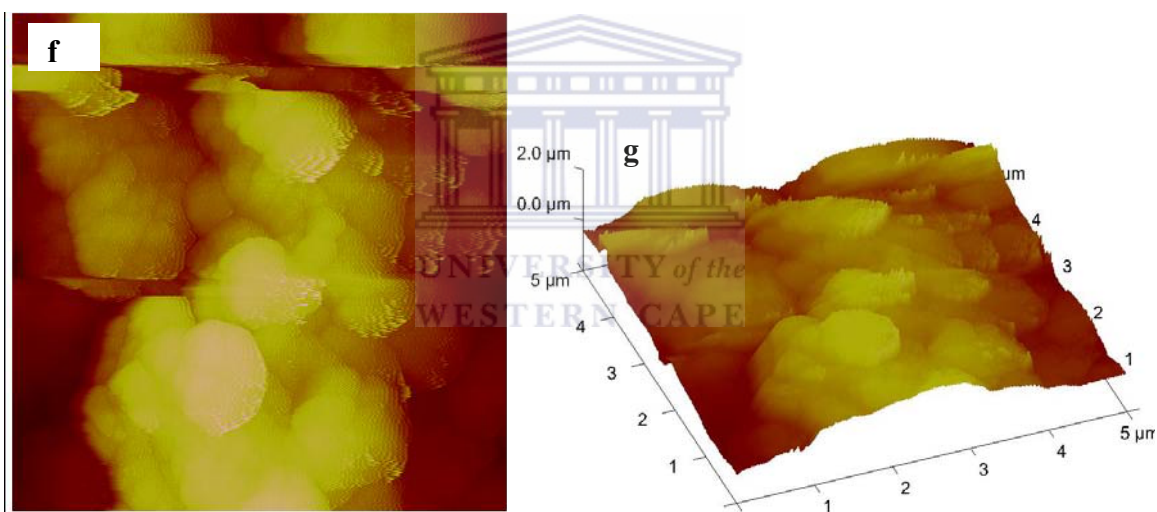
Figure 5.11: AFM images of SPCE|PANI|PS$_{NP}$-OSO$_3^-$ |PANI|anti-OTA (f and g)

5.7 Isoelectric point (pI) studies ochratoxin A polyclonal antibody by 2-D gel electrophoresis

The pI of ochratoxin A antibody was found to be 6.2 as shown in Figure 5.12. At a buffer pH of 7.2, this meant that the antibody had more negative charges on its surface. Hence,

the determination of the antibody's pI was important on deciding on reduction or oxidisation of the antibody onto the PANI nanocomposites during electrostatic deposition (immobilisation). In this instance, electrodeposition in buffer solution at pH 7.2 was by oxidation.
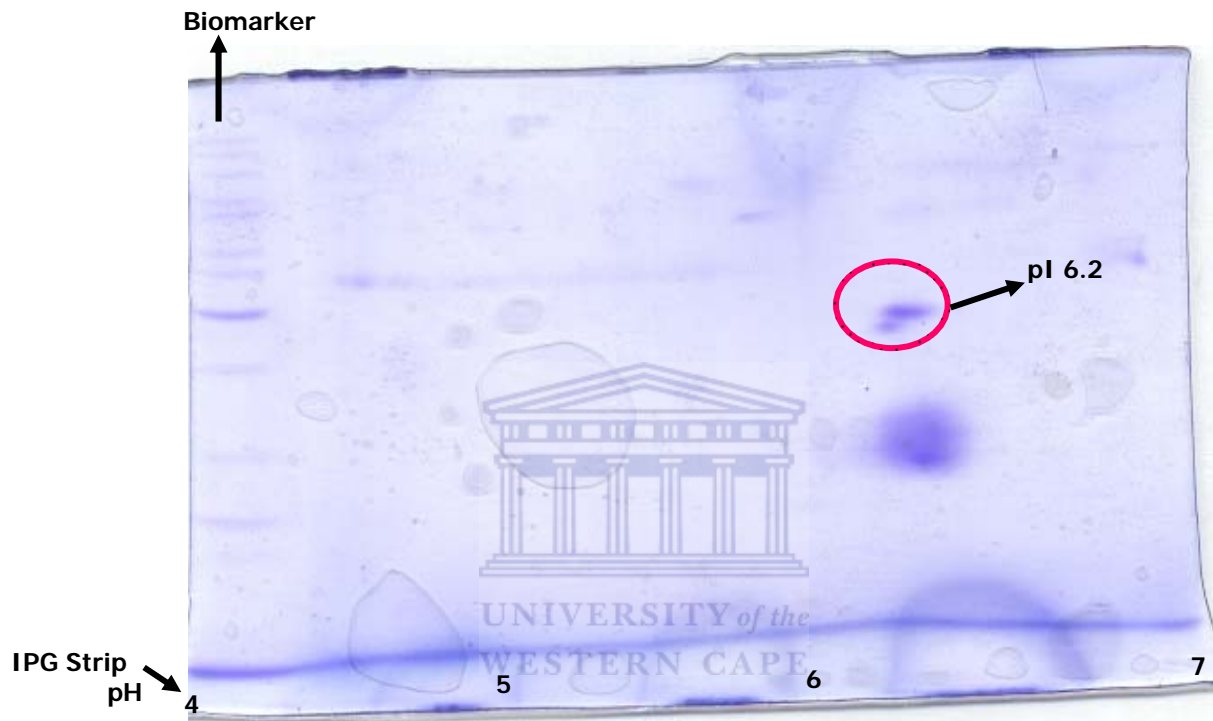

Figure 5.12: SDS-PAGE gel in determination of OTA polyclonal antibody pI by electrophoresis.

5.8 OTA responses to PANI|anti-OTA, PANI|PS$_{NP}$-NH$_2$|PANI|anti-OTA and PANI|PS$_{NP}$-OSO$_3$⁻|PANI|anti-OTA immunosensors

The impedimetric responses on PANI|anti-OTA, PANI|PS$_{NP}$-NH$_2$|PANI|anti-OTA and PANI|PS$_{NP}$-OSO$_3$⁻|PANI|anti-OTA immunosensors to ochratoxin A were studied in the frequency range of 100 kHz-50 mHz as shown in Figures 5.13 (i), ii and (iii),

respectively. Artefacts were observed at lower frequencies due to inductance as has been reported for PANI[21]. The antigen exists as a di-anion (OTA^{2-}) at neutral pH due to the ionization of carboxyl and phenol groups[22]. Binding of this charged antigen to the OTA immunosensors reduced the charge transfer resistance in both imaginary and real impedance as shown in Figures 5.13.
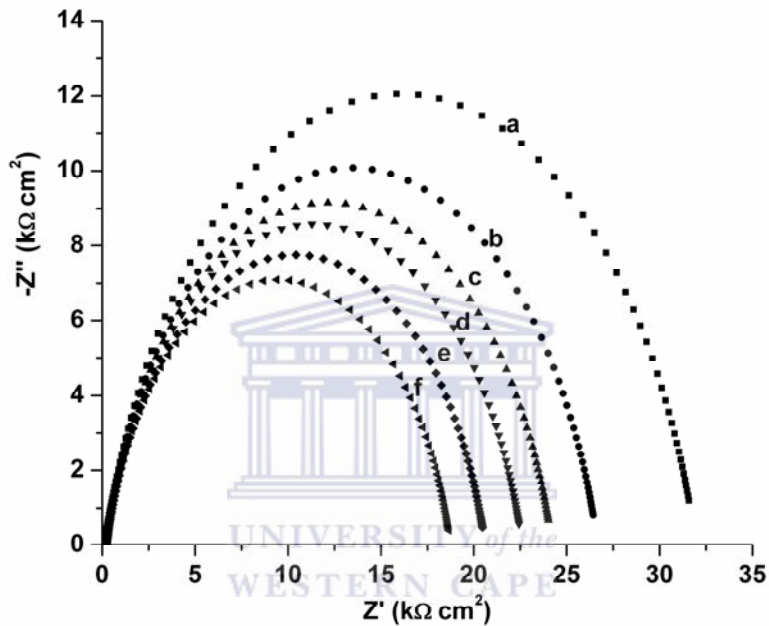
Figure 5.13 (i): EIS responses of Pt|PANI|anti-OTA immunosensor to standard OTA solutions in PBS (a, b, c, d, e and f are 0, 2, 4, 6, 8 and 10 ng/mL OTA antigen, respectively).
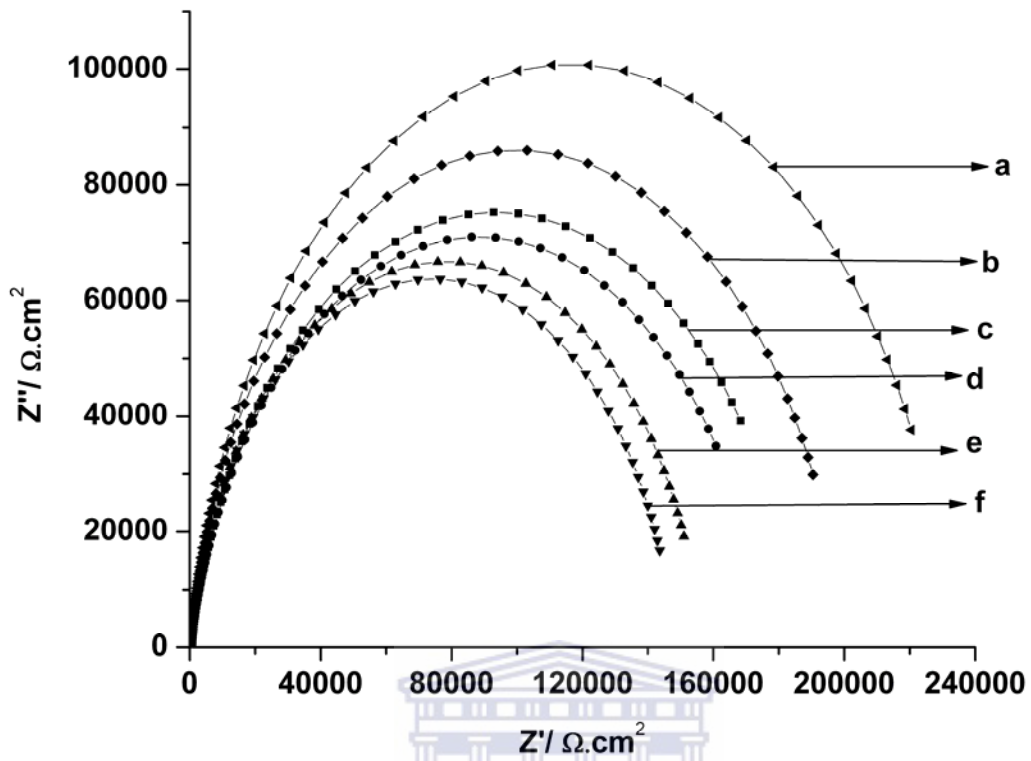
Figure 5.13 (ii): EIS responses of Pt|PANI-PS$_{NP}$-NH$_2$|anti-OTA immunosensor to standard OTA solutions in PBS (a, b, c, d, e and f are 0, 2, 4, 6, 8 and 10 ng/mL OTA antigen, respectively).
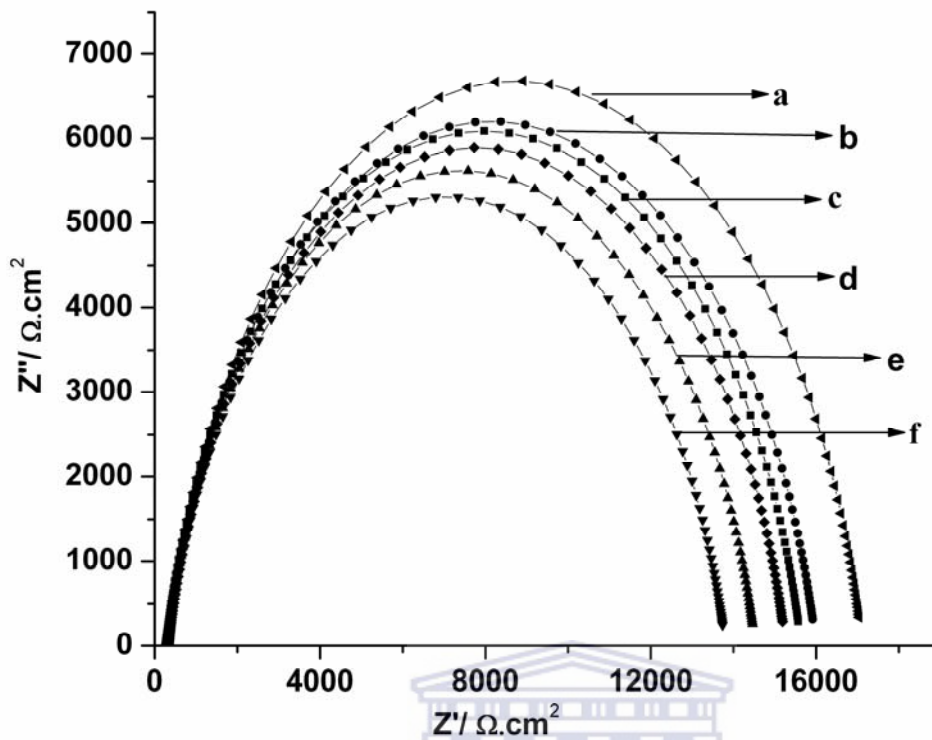
Figure 5.13 (iii): EIS responses of Pt|PANI-PS$_{NP}$-OSO$_3^-$|anti-OTA immunosensor to standard OTA solutions in PBS (a, b, c, d, e and f are 0, 2, 4, 6, 8 and 10 ng/mL OTA antigen, respectively).

The equivalent circuit in Figure 5.4 was used to fit the responses of the immunosensor to standard OTA solutions. The R_{ct} values were subtracted from those of the blank PBS (i.e. response at 0 ng/mL OTA) to obtain the normalized values that were plotted in Figure 5.13. An automated solution handling and delivery system along with real-time sensing measurements could improve the accuracy[23] of the results.
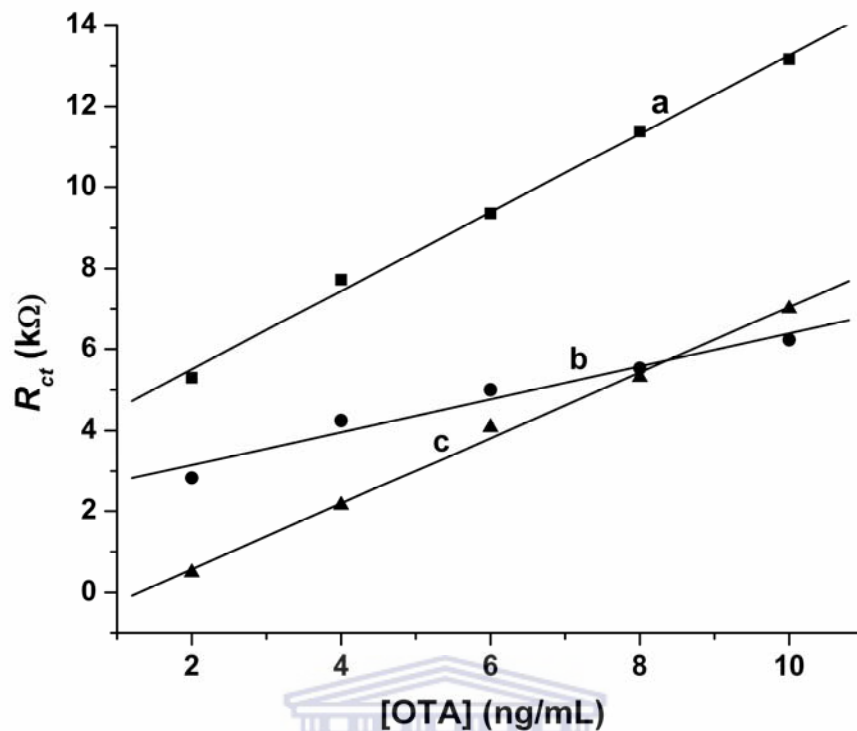
Figure 5.14: Linear calibration plot of Pt|PANI|anti-OTA (a), Pt|PANI|PS$_{NP}$-OSO$_3^-$| PANI|anti-OTA (b) and Pt|PANI|PS$_{NP}$-NH$_2$|PANI|anti-OTA (c) immunosensors to various OTA concentrations.

The detection limit of the sensors (s/n = 3) were calculated as shown in Table 5.2. Pt|PANI|PS$_{NP}$-NH$_2$|anti-OTA immunosensor had the lowest limit of detection of 7 pg/kg with a sensitivity of 819 kΩ L/ng. The positive charge of the polystyrene nano-beads increased the affinity of the Pt|PANI|PS$_{NP}$-NH$_2$|anti-OTA immunosensor for the negatively charged OTA^{2-}.

Table 5.2: Sensitivity and detection limits (LOD) of Pt|PANI-anti OTA, Pt|PANI-PS$_{NP}$-NH$_2$-anti OTA and Pt|PANI-PS$_{NP}$- OSO$_3^-$-anti OTA

Immunosensor	Sensitivity (kΩ.L/ng)	LOD (ppt)
Pt|PANI-anti-OTA	563	10
Pt|PANI|PS$_{NP}$-NH$_2$|PANI|anti-OTA	819	7
Pt|PANI|PS$_{NP}$-OSO$_3^-$| PANI|anti-OTA	400	12

5.9 Detection of ochratoxin A standards and certified reference materials by RIDASCREEN® enzyme-linked immunosorbent assay (ELISA) test kit

Ochratoxin A standards and certified reference materials of corn, wheat and roasted coffee were also detected by ELISA for validation of the immunosensors. The concentration range of OTA standard in the ELISA test was 50-1800 ppt. A standard calibration curve was obtained by plotting [OTA] against absorbance as shown in Figure 5.15. The sensitivity of the slope from the initial linear part of the graph was calculated to be 5.0 pg/kg and the limit of detection was 2.0 ppt. These values represent a better feedback in detecting ochratoxin A, making the use of ELISA appropriate in validating the fabricated PANI ochratoxin A immunosensors.
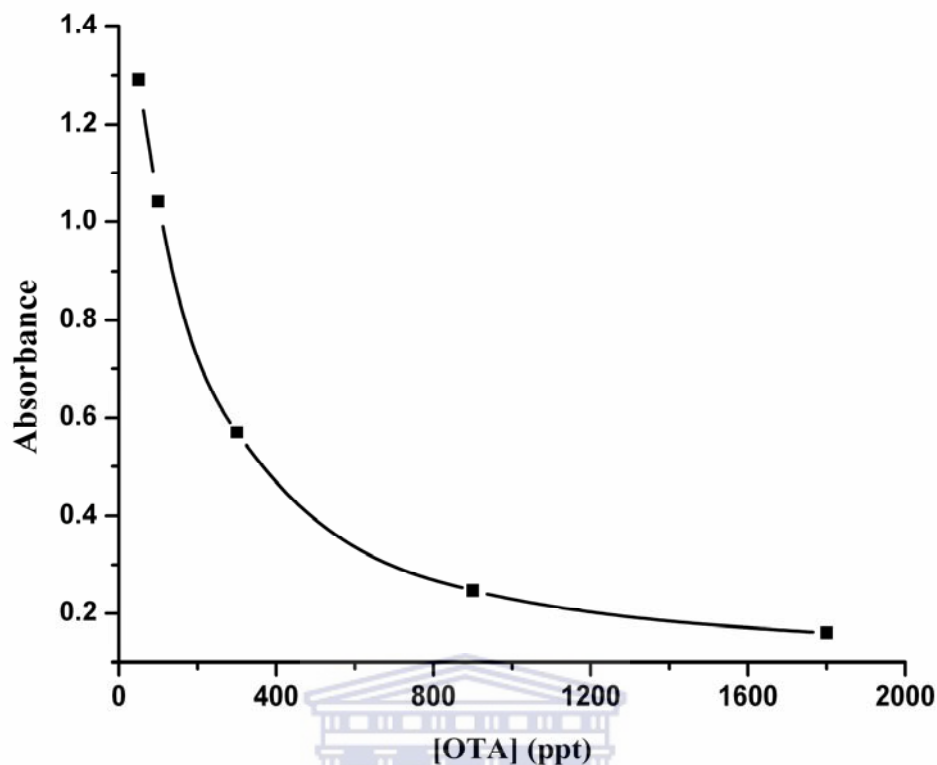
Figure 5.15: Detection of ochratoxin A standards by ELISA

The OTA was extracted from certified reference material of wheat, corn and roasted coffee using the RIDASCREEN® rapid extraction procedure. The OTA extract was analyzed on Pt|PANI|anti-OTA, Pt|PANI|PS$_{NP}$-NH$_2$|PANI|anti-OTA and Pt| PANI|PS$_{NP}$-OSO$_3^-$| PANI|anti-OTA immunosensors and results are shown in Table 5.3. The Pt| PANI|PS$_{NP}$-NH$_2$|PANI|anti-OTA had a higher sensitivity to all the certified samples. The OTA values of the immunosensors to certified reference material were comparable to those obtained with ELISA technique as well as the quantity advertised by the vendor. This was not the case for wheat and roasted coffee. It is not clear whether the differences in the ELISA, immunosensors and vendor values for OTA in certified roasted coffee and wheat are due to incomplete extraction or matrix effects.

Table 5.3. Ochratoxin A content of wheat, corn and roasted coffee certified reference materials

| Certified reference material	Pt|PANI-anti OTA (µg/kg)	Pt|PANI|PS$_{NP}$-NH$_2$|PANI|anti-OTA (µg/kg)	Pt|PANI|PS$_{NP}$-OSO$_3^-$|PANI|anti-OTA (µg/kg)	Vendor (µg/kg)	ELISA (µg/kg)
Roasted Coffee	2.5	3.2	2.3	7.7	1.2
Wheat	8.6	7.8	7.2	7.1	13.8
Corn	21.5	22	19.1	18.8	19

UNIVERSITY of the
WESTERN CAPE

References

1. Iwuoha, E. I.; de Villaverde, D. S.; Garcia, N. P.; Smyth, M. R.; Pingarron, J. M., Reactivities of organic phase biosensors. 2. The amperometric behaviour of horseradish peroxidase immobilised on a platinum electrode modified with an electrosynthetic polyaniline film. *Biosensors and Bioelectronics* **1997,** 12, (8), 749-761.

2. Killard, A. J.; Zhang, S.; Zhao, H.; John, R.; Iwuoha, E. I.; Smyth, M. R., Development of an electrochemical flow injection immunoassay (FIIA) for the real-time monitoring of biospecific interactions. *Analytica Chimica Acta* **1999,** 400, (1-3), 109-119.

3. Mathebe, N. G. R.; Morrin, A.; Iwuoha, E. I., Electrochemistry and scanning electron microscopy of polyaniline/peroxidase-based biosensor. *Talanta* **2004,** 64, (1), 115-120.

4. Muchindu, M.; Waryo, T.; Arotiba, O.; Kazimierska, E.; Morrin, A.; Killard, A. J.; Smyth, M. R.; Jahed, N.; Kgarebe, B.; Baker, P. G. L.; Iwuoha, E. I., Electrochemical nitrite nanosensor developed with amine- and sulphate-functionalised polystyrene latex beads self-assembled on polyaniline. *Electrochimica Acta* **2010,** 55, (14), 4274-4280.

5. Ndangili, P. M.; Waryo, T. T.; Muchindu, M.; Baker, P. G. L.; Ngila, C. J.; Iwuoha, E. I., Ferrocenium hexafluorophosphate-induced nanofibrillarity of polyaniline-polyvinyl sulfonate electropolymer and application in an amperometric enzyme biosensor. *Electrochimica Acta* **2010,** 55, (14), 4267-4273.

6.   Kogan, I. L.; Gedrovich, G. V.; Fokeeva, L. S.; Shunina, I. G., Electrochemical and conducting properties of polyaniline in the neutral aqueous solutions of potassium acetate and zinc salts. *Electrochimica Acta* **1996,** 41, (11-12), 1833-1837.

7.   Ayad, M. M.; Salahuddin, N. A.; Alghaysh, M. O.; Issa, R. M., Phosphoric acid and pH sensors based on polyaniline films. *Current Applied Physics* **2010,** 10, (1), 235-240.

8.   Gospodinova, N.; Mokreva, P.; Terlemezyan, L., Alternative concept of the transition emeraldine base-emeraldine salt. *Polymer* **1993,** 34, (6), 1330-1332.

9.   Bott, A. W., Electrochemistry of Semiconductors. *Current Separations* **1998,** 3, (17), 87- 91.

10.   Kazimierska, E.; Muchindu, M.; Morrin, A.; Iwuoha, E.; Smyth, M. R.; Killard, A. J., The fabrication of structurally multiordered polyaniline films and their application in electrochemical sensing and biosensing. *Electroanalysis* **2009,** 21, (3-5), 595-603.

11.   Luo, X.; Killard, A. J.; Smyth, M. R., Nanocomposite and Nanoporous Polyaniline Conducting Polymers Exhibit Enhanced Catalysis of Nitrite Reduction. *Chemistry - A European Journal* **2007,** 13, 2138-2143.

12.   Luo, X.; Vidal, G.; Killard, A.; Morrin, A.; Smyth, M., Nanocauliflowers: A Nanostructured Polyaniline-Modified Screen-Printed Electrode with a Self-Assembled Polystyrene Template and Its Application in an Amperometric Enzyme Biosensor. *Electroanalysis* **2007,** 19, (7-8), 876-883.

13. Owino, J.; Ignaszak, A.; Al-Ahmed, A.; Baker, P.; Alemu, H.; Ngila, J.; Iwuoha, E., Modelling of the impedimetric responses of an aflatoxin B1 immunosensor prepared on an electrosynthetic polyaniline platform. *Analytical and Bioanalytical Chemistry* **2007,** 388, (5), 1069-1074.

14. Dyre, J. C., The random free-energy barrier model for ac conduction in disordered solids. *Journal of Applied Physics* **1988,** 64, 2456-2469.

15. Hui, D.; Alexandrescua, R.; Chiparab,M.; Morjana, I.; Aldicac, Gh.; Chipara, M. D.; Laud, K. T., Impedance spectroscopy studies on doped polyanilines. *Journal of Optoelectronics and Advanced Materials* **2004,** 6, (3), 817 - 824.

16. Owino, J. H. O.; Arotiba, O. A.; Baker, P. G . L.; Guiseppi - Elie, A.; Iwuoha, E. I., Synthesis and characterization of poly (2-hydroxyethyl methacrylate)-polyaniline based hydrogel composites. *Reactive and Functional Polymers* **2008,** 68, (8), 1239-1244.

17. Sargent, A.; Sadik, O. A., Monitoring antibody-antigen reactions at conducting polymer-based immunosensors using impedance spectroscopy. *Electrochimica Acta* **1999,** 44, (26), 4667-4675.

18. Sargent, A.; Loi, T.; Gal, S.; Sadik, O. A., The electrochemistry of antibody-modified conducting polymer electrodes. *Journal of Electroanalytical Chemistry* **1999,** 470, (2), 144-156.

19. Frenette, C.; Paugh, R. J.; Tozlovanu, M.; Juzio, M.; Pfohl-Leszkowicz, A.; Manderville, R. A., Structure-activity relationships for the fluorescence of ochratoxin A: Insight for detection of ochratoxin A metabolites. *Analytica Chimica Acta* **2008,** 617, (1-2), 153-161.

20. Ringot, D.; Chango, A.; Schneider, Y.-J.; Larondelle, Y., Toxicokinetics and toxicodynamics of ochratoxin A, an update. *Chemico-Biological Interactions* **2006,** 159, (1), 18-46.

21. Chen, W.-C.; Wen, T.-C.; Hu, C.-C.; Gopalan, A., Identification of inductive behavior for polyaniline via electrochemical impedance spectroscopy. *Electrochimica Acta* **2002,** 47, (8), 1305-1315.

22. Valenta, H., Chromatographic methods for the determination of ochratoxin A in animal and human tissues and fluids. *Journal of Chromatography A* **1998,** 815, (1), 75-92.

23. Park, M.; Cella, L. N.; Chen, W.; Myung, N. V.; Mulchandani, A., Carbon nanotubes-based chemiresistive immunosensor for small molecules: Detection of nitroaromatic explosives. *Biosensors and Bioelectronics* **2010**, 26, 1297-1301.
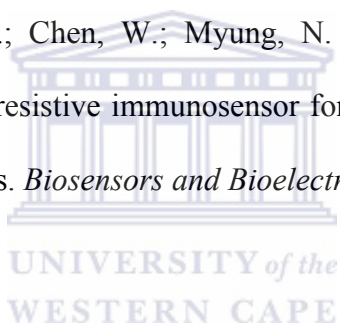
CHAPTER 6

CONCLUSIONS AND RECOMMENDATIONS

6.1 Conclusions

Polyaniline plays an important role in sensors, either in the sensing mechanism of nitrite ions or as a platform to immobilise ochratoxin A antibodies responsible for sensing ochratoxin A antigen. Nanocomposites of PANI with functionalized polystyrene latex beads, PANI|PS_{NP}-NH_2|PANI or PANI|PS_{NP}-OSO_3^-|PANI were successfully prepared. These nano-sized cauliflower-like polymeric films were applied as amperometric chemosensors for nitrite ion in acidic solution (pH<1) at +50 mV/Ag-AgCl, based on the electro-catalytic reduction of nitrite ion on PANI. The sensitivity of the nanosensors for nitrite followed the order: PANI|PS_{NP}-NH_2|PANI > PANI > PANI|PS_{NP}-OSO_3^-|PANI. The sensor containing positively charged PS_{NP}-NH_2 exhibited the highest sensitivity and lowest detection limit compared to that containing negatively charged PS_{NP}-OSO_3^- and the PANI that did not contain any functionalised polystyrene nanoparticles. Operated at a low potential of +50 mV, the sensor systems showed high selectivity for nitrite ion in the presence of interferences. With very little sample preparation (adjusting pH), the novelty of the three PANI modified chemosensor nano-systems was displayed when they were successfully applied in the detection of nitrite in rainwater. PANI|PS_{NP}-NH_2 was found to be twice as sensitive as compared to the other two sensors. PANI|PS_{NP}-NH_2|PANI and PANI sensors can be used to detect nitrites in drinking water (permissible limit of 46 μM).

In order to fabricate more specific sensors, an antibody for ochratoxin A (anti-OTA) was immobilised on PANI and the nanocomposites, $PANI|PS_{NP}-NH_2|PANI$ and $PANI|PS_{NP}-OSO_3^-|PANI$. For the first time, studies on PANI and PANI-PS$_{NP}$ nanocomposites conditioned in buffer as biocompatible platforms for attaching polyclonal antibodies in impedimetric immunosensors were successfully carried out. Theses polyclonal antibodies were opted for as they have been reported to be easier to produce, were commercially available, cheaper and more stable as compared to monoclonal or recombinant antibodies[1]. Affinity of OTA antigen to the immunosensors was observed in the following order: $Pt|PANI|PS_{NP}-NH_2|PANI$-anti OTA > Pt|PANI-anti OTA > $Pt|PANI|PS_{NP}-OSO_3^-|PANI$-anti OTA. This detection of ochratoxin antigen was a positive feedback that can be put to use for trace detection of OTA. The $Pt|PANI|PS_{NP}-NH_2$-anti OTA immunosensor had the lowest limit of detection of (7 pg/kg) with a high sensitivity of (819 kΩ.L/ng) for OTA. Apart from increase in surface area due to nanostructure of the modified electrodes, charge of the latex beads played a major role in the affinity of the charged analytes to the electrochemical nanocomposite sensors. These detection limits of OTA by label-free immunosensors in pg/kg range are the lowest reported to date and are lower than the European Commission limit of 5 µg/kg OTA in roasted coffee and cereals. This work has demonstrated its applicability on certified reference materials of wheat, roasted coffee and corn. The limit of detection of the immunosensors agreed with both ELISA and vendor data. This confirmed that PANI immunosensors can be successfully applied in detecting ochratoxin A in real samples.

6.2 Future work and recommendations

Great interest has been generated in polyaniline (PANI) because it is inexpensive, easy to process and dope, has high conductivity and the raw materials for its synthesis are readily available. Miniaturisation of these chemosensors would make it possible to use in remote operations hence making them ideal for rapid on-site analysis. Electro-catalysis of other environmental pollutants such as persistent organic pollutants can also be studied on these PANI nanocomposite transducers. In the long-run, these transducers can be for multi-array detection. Other polymer nanocomposites may also be developed and used in the detection of nitrite. Research into functional substrates of PANI electrodeposited nanostructures for the development of molecularly imprinted polymer based sensors may also be carried out[2-4]. These imprinted sensors would couple the intrinsic advantages of the nano-structured PANI transducer and the robustness and stability of molecular imprinted polymers. More research may be done to improve specificity of the immunosensors in order to discriminate more efficiently between closely related forms of ochratoxin A. Recombinants are the product of genetic manipulation of antibody genes and have the capability of engineering affinity and monoclonal antibodies. These recombinants can be raised as they are more specific to the different forms of ochratoxin A. Novel antibody fragments aid in immobilisation, high throughput screening and this facilitates improvements in sensitivity due to the ability to screen much larger recombinant libraries[1]. Possible interferences on the ochratoxin A immunosensors should also be studied. This would shed more light on possible sample matrix effects. Other pH values can be used to study the behaviour of the immunosensors. This will optimise the

pH value of the immunosensors and enable the detection of OTA in different environments other than the human physiological pH of 7.2.

References

1. Conroy, P. J.; Hearty, S.; Leonard, P.; O'Kennedy, R. J., Antibody production, design and use for biosensor-based applications. *Seminars in Cell & Developmental Biology* **2009,** 20, (1), 10-26.

2. Mayes, A. G.; Whitcombe, M. J., Synthetic strategies for the generation of molecularly imprinted organic polymers. *Advanced Drug Delivery Reviews* **2005,** 57, (12), 1742-1778.

3. Pardieu, E.; Cheap, H.; Vedrine, C.; Lazerges, M.; Lattach, Y.; Garnier, F.; Remita, S.; Pernelle, C., Molecularly imprinted conducting polymer based electrochemical sensor for detection of atrazine. *Analytica Chimica Acta* **2009,** 649, (2), 236-245.

4. Mäkelä, T.; Haatainen, T.; Majander, P.; Ahopelto, J., Continuous roll to roll nanoimprinting of inherently conducting polyaniline. *Microelectronic Engineering* **2010,** 84, (5-8), 877-879.